UNIVERSITY OF CALIFORNIA

Santa Barbara

Nutrient and Organic Matter Cycling in the Nearshore Ocean and Marine Sediment of the Santa Barbara Channel

A dissertation submitted in partial satisfaction of the requirements for the degree of

Doctor of Philosophy in Ecology, Evolution, and Marine Biology

by

Heili Eileen Lowman

Committee in charge:

Professor John M. Melack, Chair

Professor Mark A. Brzezinski

Professor Sally MacIntyre

Professor Deron E. Burkepile

June 2020

The dissertation of Heili Eileen Lowman is approved.

_____

Deron E. Burkepile

_____

Sally MacIntyre

_____

Mark A. Brzezinski

_____

John M. Melack, Committee Chair

May 2020

Nutrient and Organic Matter Cycling in the Nearshore Ocean and Marine Sediment of the Santa Barbara Channel

ACKNOWLEDGEMENTS

I would like to thank John Melack, who provided me with this incredible opportunity. He encouraged me to become an independent, self-sufficient scientist but was always available whenever I needed his help. He made sure I kept track of every detail without losing sight of the bigger picture. And most importantly, throughout it all, he was consistently my advocate and my mentor. It has been a privilege to be his graduate student, and I feel incredibly lucky to have had him as my advisor. Thank you, John.

I would like to thank each of my committee members – Sally MacIntyre, Mark Brzezinski, and Deron Burkepile – who provided valuable feedback on the work included here and encouraged me to approach my research from their multidisciplinary perspectives. I would like to extend a special thank you to Bob Miller, Jenny Dugan, and Mark Page for encouraging my ideas and providing me with the opportunity to collaborate with them on some fantastic projects. I would also like to thank Allison Horst for inspiring me to give data science a second chance and whose support transformed my graduate school experience.

Kyle Emery and Mark Hirsch were the best collaborators I could have asked for; their field and technical expertise was irreplaceable. Katherine Le was the most fantastic undergraduate mentee, and I was so happy to have been able to work alongside her for all these years. Thank you also to Chloe Smith, Lila Kubler-Dudgeon, and Tyler Daniel for their hard work and enthusiasm during long days in the field and in the laboratory.

I would like to thank all of the folks at the Santa Barbara Coastal Long Term Ecological Research (SBC LTER) Project, namely Clint Nelson, Sarah Sampson, and Shannon Harrer for sample collection and field coordination and Ken Marchus, Georges Paradis, Bill Clinton, Keri Opalk, Janice Jones, and Matthew Meyerhof for their help with

sample analyses. I would also like to extend a huge thank you to my collaborators Matthieu Moingt and Marc Lucotte at the Université du Québec à Montréal. I am deeply appreciative of the administrative, teaching, and research support I received from the departments of Ecology, Evolution, and Marine Biology, the Marine Science Institute, and the Bren School of Environmental Science and Management. Funding for this work was provided by the National Science Foundation, the SBC LTER, the Associated Students Coastal Fund, and the University of California Office of the President's Dissertation Year Fellowship.

Throughout my degree, I had the support of a tremendous group of friends and family in Santa Barbara and all over the country. I found an incredible community at UCSB, and I am so grateful for all of the friendships and adventures I could not have even begun to envision just five years ago. Thank you everyone!

I would like to thank Isa, Ema, Evi, and Mommom for encouraging me, being my constant cheerleaders, and providing me with love and support during this long journey. I would also like to thank Susan, Richard, Jake, and Kieran for all of their love and encouragement. This dissertation is dedicated to my family, past and present, who have recognized education as the gateway to opportunity and the means to a better life.

And, finally, I would like to thank Sam, who has encouraged my every dream and been at my side every step of the way. Without his support, none of this would have been possible. Sam, I love you, and I cannot wait to see what the next chapter has in store for us.

In closing, this dissertation was prepared and presented during the coronavirus pandemic in the spring of 2020. I would like to acknowledge the many lives that have been lost due to this virus, and I am grateful to every person working and volunteering to keep our communities fed, housed, safe, and healthy through this crisis.

VITA OF HEILI EILEEN LOWMAN
May 2020

Education

Ph.D.	Ecology, Evolution, and Marine Biology (EEMB) University of California, Santa Barbara (UCSB) Santa Barbara, California	June 2020
B.A.	Chemistry, French & Francophone Studies Vassar College Poughkeepsie, New York	May 2012

Professional and Research Experience

Graduate Researcher Santa Barbara Coastal Long Term Ecological Research Project Santa Barbara, California	2015-2020
Teaching Assistant UCSB Bren School of Environmental Science and Management Santa Barbara, California	2017-2019
Teaching Assistant UCSB Department of EEMB Santa Barbara, California	2016-2018
Research Assistant University of Iowa Department of Biology Iowa City, Iowa	2013-2015
Research Assistant University of Iowa Department of Engineering Iowa City, Iowa	2014
Senior Associate Berkeley Research Group Springfield, Missouri and New Haven, Connecticut	2012-2014
Communications Coordinator National Marine Sanctuary Foundation Silver Spring, Maryland	2012

Peer-Reviewed Publications

Lowman, H.E., K.A. Emery, J.E. Dugan, R.J. Miller. Nutritional Quality of Giant Kelp Declines Due to Warming Ocean Temperatures. *Limnology and Oceanography Letters* (in review).

Lowman, H.E., K.A. Emery, L. Kubler-Dudgeon, J.E. Dugan, and J.M. Melack. 2019. Contribution of Macroalgal Wrack Consumers to Dissolved Inorganic Nitrogen Concentrations in Intertidal Pore Waters of Sandy Beaches. *Estuarine, Coastal and Shelf Science*. 219: 363-371. https://doi.org/10.1016/j. ecss.2019.02.004.

Schroer, A.L., **H.E. Lowman**, and C.L. Just. 2015. Educating the Aware, Informed, and Action-oriented Sustainable Citizen. *Sustainability.* 7(2): 1985-1999. https://doi.org/10.3390/su7021985.

Aldeborgh, H., K. George, M. Howe, **H. Lowman,** H. Moustakas, N. Strunsky, and J.M. Tanski. 2014. Analysis of Small Molecule X-Ray Crystal Structures: Chemical Crystallography with Undergraduate Students in a Teaching Laboratory. *Journal of Chemical Crystallography*. 44(2): 70-81. https://doi.org/ 10.1007/s10870-013-0485-z.

Conference Presentations

Lowman, H.E. and T. Treude. 2020. Marine Sediments: Fluxes, Fauna, and Forecasting. Session Chair. Ocean Sciences Meeting. San Diego, California.

Lowman, H.E., J.M. Melack, M. Moingt, and A. Zimmerman. 2019. Distribution of Terrestrial Organic Material in Nearshore Marine Ecosystems due to Debris Flow Emergency Response. Coastal and Estuarine Research Federation Conference. Mobile, Alabama.

Lowman, H.E., J.M. Melack, and H.M. Page. 2018. Lignin Phenols as Biomarkers of Terrestrial Organic Matter in the Santa Barbara Channel. Association for the Sciences of Limnology and Oceanography Summer Meeting. Victoria, British Columbia.

Just, C., and **H.E. Lowman**. 2014. Sustainability Education and Community Conversation Training. Just Sustainability Conference. Seattle, Washington.

Fellowships, Scholarships, and Research Grants

University of California President's Dissertation Year Fellowship	2019-2020
Santa Barbara Coastal Long Term Ecological Research Fellowship	2016-2019
Worster Summer Research Award	2018
UCSB Associated Students Coastal Fund Research Grant	2018
UCSB Department of EEMB Block Grant	2018
UCSB Department of EEMB Fellowship	2015
Vassar College Environmental Research Institute Scholarship	2012

ABSTRACT

Nutrient and Organic Matter Cycling in the Nearshore Ocean and Marine Sediment of the Santa Barbara Channel

by

Heili Eileen Lowman

Coastal regions lie along a dual ecotone: the boundary of terrestrial and marine ecosystems and at the convergence of fresh and saltwater aquatic ecosystems. These ecotones are biogeochemically active regions that are stimulated by the supply and transport of organic material by way of their aquatic linkages. My dissertation addresses questions of organic matter and nutrient supply, retention, and transformation in the coastal regions of the Santa Barbara Channel with a focus on maintaining sufficiently high nitrogen concentrations to support primary production of kelp forests during low nutrient periods. To examine fluctuations of nitrogen concentrations in nearshore marine waters, and their relationships with physical and biological factors, I conducted intensive sampling for ammonium concentrations during the summer season and found a distinct periodicity in concentrations throughout the full water column in relationship to the tidal cycle. To determine if permeable marine sediment is a source of dissolved inorganic nitrogen to the overlying water column, I conducted a multi-year series of nutrient flux measurements using flow-through sediment bioreactors containing sediment collected near kelp forests and found that they are a source of ammonium and total dissolved nitrogen during the summer season. To investigate organic

matter supply to marine sediment, I analyzed coastal sediment samples for evidence of terrestrial organic matter input before, during, and after a period with considerable rainfall that followed a 5 year drought, and I found evidence in both stream and marine sediment of terrestrial organic matter inputs becoming increasingly varied and less degraded over time. Using a Santa Barbara Coastal LTER dataset, I examined carbon and nitrogen in giant kelp tissue to evaluate patterns in nutritional content as they relate to changes in seawater temperature and larger oceanographic indices. I found that the nutritional content of giant kelp tissue collected in the Santa Barbara Channel has declined over the past 17 years, and this decline is correlated with increasing seawater temperatures and fluctuations of the North Pacific Gyre Oscillation index.

TABLE OF CONTENTS

CHAPTER 1:

INTRODUCTION

Coastal regions lie along a dual ecotone, the boundary of terrestrial and marine ecosystems as well as at the convergence of fresh and saltwater aquatic ecosystems. Recent advances in the field of biogeochemistry suggest that research should focus on the linkages, rather than the borders, between these environments (Xenopoulos et al., 2017). The "land-ocean aquatic continuum" is recognized as a region where organic matter and nutrients undergo significant transformation and processing (Billen et al., 1991). In particular, nutrient transformations performed by microbes and dependent on redox conditions reach high rates at the aquatic-terrestrial interface (Grimm et al., 2003). Additional information regarding nutrient limitation, retention, and transformation in coastal regions is needed as these areas may respond rapidly to global change, such as increasing atmospheric temperatures, CO_2 concentrations (Gruber, 2008), and land use changes (Glibert et al., 2016).

Overall, my dissertation improves knowledge of coastal nitrogen and organic matter cycling in the nearshore ocean and marine sediment surrounding giant kelp forests and addresses questions of organic matter and nutrient availability, retention, and transformation in the coastal regions of the Santa Barbara Channel located in central California. This area experiences three distinct oceanographic seasons with different nitrogen availability in each season – spring upwelling establishes high NO_3^- conditions from March through June, warm, stratified waters are associated with low nutrient conditions from July through November, and winter storms deliver dissolved inorganic nitrogen (DIN) via runoff from December through February (McPhee-Shaw et al., 2007; Brzezinski et al., 2013). Storms are episodic in

nature, and precipitation can occur in such a strong pulse that half of the annual suspended sediment loading to the ocean can be discharged over the course of less than two days, or a single storm event (Warrick et al., 2015). Wildfires increase sediment and DIN fluxes from the watersheds of the Santa Ynez Mountains into the Santa Barbara Channel (Aguilera and Melack, 2018). The second and fourth chapters of this dissertation aim to further our understanding of nutrient and organic matter concentrations in nearshore water and sediments, respectively, and consider how this supply might support primary production in the context of the oceanographic and climate conditions. The third and fifth chapters explore sources and sinks of nutrients and organic matter in sediments and kelp forests, respectively, with a particular focus on maintaining sufficiently high nitrogen concentrations to support primary production during otherwise low nutrient periods.

Chapter Overviews

Chapter 2 examines diel fluctuations of nitrogen concentrations in nearshore marine waters and their relationships with physical and biological factors such as tides and phytoplankton. In coastal regions, external sources of nitrogen include upwelling of deep ocean water, runoff from groundwater, storm water, or wastewater sources, atmospheric deposition, and fixation (Jickells et al., 2017). The majority of nitrogen cycling in the ocean is mediated by microbes which transform compounds between forms of dissolved inorganic nitrogen and dissolved and particulate organic nitrogen (DON and PON) (Zehr and Ward, 2002). Although nitrate (NO_3^-) is the most common form of DIN measured in marine environments (Capone et al., 2008), most marine phytoplankton prefer to uptake ammonium (NH_4^+) (Glibert et al., 1982). Due to reduced standing stocks and rapid uptake, NH_4^+ must be

detected using extremely sensitive methods (Brzezinski, 1988) in conjunction with frequent sampling (Wheeler et al., 1989). Combining a recently refined detection method (Holmes et al., 1999; Taylor et al., 2007) with frequent measurement, I present the results of an intensive nearshore sampling campaign for NH_4^+ concentrations during the summer season in the Santa Barbara Channel.

Chapter 3 presents DIN and DON efflux rates from permeable marine sediment sampled at several nearshore locations over multiple years. Due to their low organic matter content, permeable sands were often assumed to be areas of low biogeochemical activity until recent studies suggested they are active sites of organic matter remineralization and sequestration in coastal ecosystems (Huettel et al., 2014). In estuarine and coastal marine ecosystems, sediment supplies an average of 15-32% of the nitrogen demand required by the overlying water column, with larger percentages reported for temperate latitudes (Boynton et al., 2018). The quantity and quality of organic matter deposited in these sediments is the main factor regulating benthic biogeochemistry and metabolic rates (Herbert, 1999; Boynton et al., 2018), although changes in permeability (Marchant et al., 2016) and oscillations in oxygen and other terminal electron acceptor concentrations (Rocha, 2008; Middelburg and Levin, 2009) may also impact organic matter breakdown and nutrient regeneration rates. In oxygenated surface sediments, remineralization rates can be up to 25 times greater than in deeper, anoxic sediment (Laverman et al., 2012). While microbial populations in permeable sediment may resemble those found in muddy sediments, they have been demonstrated to take better advantage of pulses of organic matter input (Woulds et al., 2016). Measuring rapid rates of remineralization prior to uptake by primary producers requires experimental approaches designed for hourly timescales (Boynton et al., 2018). Using a series of flow-

through sediment bioreactors, I present the findings from a multi-year series of nutrient flux experiments conducted on permeable sediment surrounding giant kelp (*Macrocystis pyrifera*) forests.

To further investigate organic matter supply to marine sediment, Chapter 4 presents analyses of stream, estuarine, and marine sediment samples for evidence of terrestrial organic matter (TOM) input. Several decades ago, approximately 1% of terrestrial primary production was estimated to be exported to the ocean each year (Schlesinger and Melack, 1981). However, research since then suggests that the input of TOM to marine areas is greater than previously thought (Gordon and Goñi, 2003) and may serve as an important source of nutrients to support coastal primary production (Opsahl and Benner, 1997). Now, it is estimated that approximately one third of organic material in marine sediments is of terrestrial origin, with both greater remineralization and sequestration rates occurring in coastal sediments prior to reaching continental margins (Burdige, 2005). More research into coastal processing of TOM is required in order to better parameterize TOM export models, which, to date, often use a binary approach to suggest either all or none of the exported material and nutrients reach the open ocean and, consequently, deeper marine sediments (Sharples et al., 2017). In order to differentiate between terrestrial and marine sources of organic matter, lignin oxidation byproducts can serve as biomarkers of vascular, terrestrial plant material (Hedges and Parker, 1976; Louchouarn et al., 1999). Using this lignin oxidation method in conjunction with isotopic analyses, I present analyses of TOM content in coastal sediment before, during, and after a series of precipitation events associated with El Niño Seasonal Oscillation conditions.

While Chapters 2, 3, and 4 address coastal nutrient dynamics on hourly, diel, and seasonal scales, Chapter 5 examines yearly and decadal scale changes in macroalgal nutrient content. Long-term monitoring of nutrient dynamics in aquatic ecosystems (McCrackin et al., 2016), especially as these water bodies experience greater perturbation while simultaneously gaining socioeconomic value (Hampton et al., 2018), can be quite informative. Assimilation of nutrients is particularly important to quantify in coastal vegetated habitats, which account for over 10% of marine net primary production (Duarte, 2017). In high productivity temperate systems, nutrients have also been demonstrated to exert a stronger effect on primary producers than herbivory (Burkepile and Hay, 2006). Additional research is needed to determine if the nutritional demands of certain primary producers in coastal environments are being met and to consider the metabolic consequences for primary consumers and higher trophic levels. *Macrocystis pyrifera*, or giant kelp, is a macroalgae well-suited for nutritional studies; it cannot maintain nitrogen reserves in its tissues for longer than approximately two weeks (Gerard, 1982), so giant kelp's nutritional content tracks closely nutrient availability in the surrounding seawater. Giant kelp forests are among the most productive ecosystems (Mann, 2000), and ecosystem-level productivity in giant kelp forests is governed predominantly by oceanographic processes (Graham et al., 2007). Long-term *in situ* studies, such as those maintained by the Santa Barbara Coastal Long Term Ecological Research program, allow for ecological data collection that can be explored in the larger context of paired climate and oceanographic datasets. Using percent carbon and nitrogen measured in giant kelp tissue, I present patterns in nutritional content as they relate to changes in seawater temperature and larger oceanographic indices, i.e., the North Pacific Gyre Oscillation, and compare these results to globally reported values of kelp species' nutritional content.

References

Aguilera, R., Melack, J.M., 2018. Relationships among nutrient and sediment fluxes, hydrological variability, fire, and land cover in coastal California catchments. *Journal of Geophysical Research: Biogeosciences* 123, 2568–2589. https://doi.org/10.1029/2017JG004119

Billen, G.C., Lancelot, C., Meybeck, M., 1991. N, P, and Si retention along the aquatic continuum from land to ocean, in: Mantoura, R.F.C., Martin, J.-M., Wollast, R. (Eds.), *Ocean Margin Processes in Global Change*. Wiley, pp. 19–44.

Boynton, W.R., Ceballos, M.A.C., Bailey, E.M., Hodgkins, C.L.S., Humphrey, J.L., Testa, J.M., 2018. Oxygen and nutrient exchanges at the sediment-water interface: A global synthesis and critique of estuarine and coastal data. *Estuaries and Coasts* 41, 301–333. https://doi.org/10.1007/s12237-017-0275-5

Brzezinski, M., 1988. Vertical distribution of ammonium in stratified oligotrophic waters. *Limnology and Oceanography* 33, 1176–1182.

Brzezinski, M., Reed, D., Harrer, S., Rassweiler, A., Melack, J., Goodridge, B., Dugan, J., 2013. Multiple sources and forms of nitrogen sustain year-round kelp growth on the inner continental shelf of the Santa Barbara Channel. *Oceanography* 26, 114–123. https://doi.org/10.5670/oceanog.2013.53

Burdige, D.J., 2005. Burial of terrestrial organic matter in marine sediments: A re-assessment. *Global Biogeochemical Cycles* 19, GB4011. https://doi.org/10.1029/2004GB002368

Burkepile, D.E., Hay, M.E., 2006. Herbivore vs. nutrient control of marine primary producers: Context-dependent effects. *Ecology* 87, 3128–3139. https://doi.org/10.1890/0012-9658(2006)87[3128:HVNCOM]2.0.CO;2

Capone, D.G., Bronk, D.A., Mulholland, M.R., Carpenter, E.J., 2008. *Nitrogen in the Marine Environment*, 2nd ed. Academic Press, New York.

Duarte, C.M., 2017. Reviews and syntheses: Hidden forests, the role of vegetated coastal habitats on the ocean carbon budget. *Biogeosciences Discussions* 14, 301–310. https://doi.org/10.5194/bg-14-301-2017

Gerard, V.A., 1982. Growth and utilization of internal nitrogen reserves by the giant kelp Macrocystis pyrifera in a low-nitrogen environment. *Marine Biology* 66, 27–35.

Glibert, P.M., Lipschultz, F., McCarthy, J.J., Altabet, M.A., 1982. Isotope dilution models of uptake and remineralization of ammonium by marine plankton. *Limnology and Oceanography* 27, 639–650.

Glibert, P.M., Wilkerson, F.P., Dugdale, R.C., Raven, J.A., Dupont, C.L., Leavitt, P.R., Parker, A.E., Burkholder, J.M., Kana, T.M., 2016. Pluses and minuses of ammonium and nitrate uptake and assimilation by phytoplankton and implications for productivity and community composition, with emphasis on nitrogen-enriched conditions: Pluses and minuses of NH4+ *and* NO3−. *Limnology Oceanography* 61, 165–197. https://doi.org/10.1002/lno.10203

Gordon, E.S., Goñi, M.A., 2003. Sources and distribution of terrigenous organic matter delivered by the Atchafalaya River to sediments in the northern Gulf of Mexico. *Geochimica et Cosmochimica Acta* 67, 2359–2375. https://doi.org/10.1016/S0016-7037(02)01412-6

Graham, M.H., Vasquez, J.A., Buschmann, A.H., 2007. Global ecology of the giant kelp Macrocystis: from ecotypes to ecosystems. *Oceanography and Marine Biology* 45, 39-88.

Grimm, N.B., Gergel, S.E., McDowell, W.H., Boyer, E.W., Dent, C.L., Groffman, P., Hart, S.C., Harvey, J., Johnston, C., Mayorga, E., McClain, M.E., Pinay, G., 2003. Merging aquatic and terrestrial perspectives of nutrient biogeochemistry. *Oecologia* 137, 485–501. https://doi.org/10.1007/s00442-003-1382-5

Gruber, N., 2008. The marine nitrogen cycle: Overview and challenges, in: *Nitrogen in the Marine Environment*. Academic Press, New York, pp. 1–50.

Hampton, S.E., Scheuerell, M.D., Church, M.J., Melack, J.M., 2018. Long-term perspectives in aquatic research. *Limnology and Oceanography* 64, S2-S10. https://doi.org/10.1002/lno.11092

Hedges, J.I., Parker, P., 1976. Land-derived organic matter in surface sediments from the Gulf of Mexico. *Geochimica et Cosmochimica Acta* 40, 1019–1029.

Herbert, R.A., 1999. Nitrogen cycling in coastal marine ecosystems. *FEMS Microbiology Reviews* 23, 563–590.

Holmes, R.M., Aminot, A., Kérouel, R., Hooker, B.A., Peterson, B.J., 1999. A simple and precise method for measuring ammonium in marine and freshwater ecosystems. *Canadian Journal of Fisheries and Aquatic Sciences* 56, 1801–1808.

Huettel, M., Berg, P., Kostka, J.E., 2014. Benthic exchange and biogeochemical cycling in permeable sediments. *Annual Review of Marine Science* 6, 23–51. https://doi.org/10.1146/annurev-marine-051413-012706

Jickells, T.D., Buitenhuis, E., Altieri, K., Baker, A.R., Capone, D., Duce, R.A., Dentener, F., Fennel, K., Kanakidou, M., LaRoche, J., Lee, K., Liss, P., Middelburg, J.J., Moore, J.K., Okin, G., Oschlies, A., Sarin, M., Seitzinger, S., Sharples, J., Singh, A., Suntharalingam, P., Uematsu, M., Zamora, L.M., 2017. A re-evaluation of the magnitude and impacts of anthropogenic atmospheric nitrogen inputs on the ocean. *Global Biogeochemical Cycles* 31, 1–17. https://doi.org/10.1002/2016GB005586

Laverman, A.M., Pallud, C., Abell, J., Cappellen, P.V., 2012. Comparative survey of potential nitrate and sulfate reduction rates in aquatic sediments. *Geochimica et Cosmochimica Acta* 77, 474–488. https://doi.org/10.1016/j.gca.2011.10.033

Louchouarn, P., Lucotte, M., Farella, N., 1999. Historical and geographical variations of sources and transport of terrigenous organic matter within a large-scale coastal environment. *Organic Geochemistry* 30, 675–699.

Mann, K.H., 2000. *Ecology of Coastal Waters*. Blackwell Science, Maldin, MA.

Marchant, H.K., Holtappels, M., Lavik, G., Ahmerkamp, S., Winter, C., Kuypers, M.M.M., 2016. Coupled nitrification-denitrification leads to extensive N loss in subtidal permeable sediments. *Limnology and Oceanography* 61, 1033–1048. https://doi.org/10.1002/lno.10271

McCrackin, M.L., Jones, H.P., Jones, P.C., Moreno-Mateos, D., 2016. Recovery of lakes and coastal marine ecosystems from eutrophication: A global meta-analysis. *Limnology and Oceanography* 62, 507-518. https://doi.org/10.1002/lno.10441

McPhee-Shaw, E.E., Siegel, D.A., Washburn, L., Brzezinski, M.A., Jones, J.L., Leydecker, A., Melack, J., 2007. Mechanisms for nutrient delivery to the inner shelf:

Observations from the Santa Barbara Channel. *Limnology and Oceanography* 52, 1748–1766. https://doi.org/10.4319/lo.2007.52.5.1748

Middelburg, J.J., Levin, L.A., 2009. Coastal hypoxia and sediment biogeochemistry. *Biogeosciences* 6, 1273–1293. https://doi.org/10.5194/bg-6-1273-2009

Opsahl, S., Benner, R., 1997. Distribution and cycling of terrigenous dissolved organic matter in the ocean. *Nature* 386, 480–482.

Rocha, C., 2008. Sandy sediments as active biogeochemical reactors: compound cycling in the fast lane. *Aquatic Microbial Ecology* 53, 119–127. https://doi.org/10.3354/ame01221

Schlesinger, W.H., Melack, J.M., 1981. Transport of organic carbon in the world's rivers. *Tellus* 33, 172–187.

Sharples, J., Middelburg, J.J., Fennel, K., Jickells, T.D., 2017. What proportion of riverine nutrients reaches the open ocean?. *Global Biogeochemical Cycles* 31, 39–58. https://doi.org/10.1002/2016GB005483

Taylor, B.W., Keep, C.F., Hall Jr, R.O., Koch, B.J., Tronstad, L.M., Flecker, A.S., Ulseth, A.J., 2007. Improving the fluorometric ammonium method: matrix effects, background fluorescence, and standard additions. *Journal of the North American Benthological Society* 26, 167–177. https://doi.org/10.1899/0887-3593(2007)26[167:ITFAMM]2.0.CO;2

Warrick, J.A., Melack, J.M., Goodridge, B.M., 2015. Sediment yields from small, steep coastal watersheds of California. *Journal of Hydrology: Regional Studies* 4, 516–534. https://doi.org/10.1016/j.ejrh.2015.08.004

Wheeler, P.A., Kirchman, D.L., Landry, M.R., Kokkinakis, S.A., 1989. Diel periodicity in ammonium uptake and regeneration in the oceanic subarctic Pacific: Implications for interactions in microbial food webs. *Limnology and Oceanography* 34, 1025–1033.

Woulds, C., Bouillon, S., Cowie, G.L., Drake, E., Middelburg, J.J., Witte, U., 2016. Patterns of carbon processing at the seafloor: the role of faunal and microbial communities in moderating carbon flows. *Biogeosciences* 13, 4343–4357. https://doi.org/10.5194/bg-13-4343-2016

Xenopoulos, M.A., Downing, J.A., Kumar, M.D., Menden-Deuer, S., Voss, M., 2017. Headwaters to oceans: Ecological and biogeochemical contrasts across the aquatic continuum. *Limnology and Oceanography* 62, S3-S14. https://doi.org/10.1002/lno.10721

Zehr, J.P., Ward, B.B., 2002. Nitrogen Cycling in the Ocean: New Perspectives on Processes and Paradigms. *Applied and Environmental Microbiology* 68, 1015–1024. https://doi.org/10.1128/AEM.68.3.1015-1024.2002

CHAPTER 2:

PERIODICITY OF AMMONIUM CONCENTRATIONS IN TEMPERATE COASTAL WATERS DURING STRATIFIED CONDITIONS

Abstract:

Dissolved inorganic nitrogen is critical for supporting growth in productive marine ecosystems, such as giant kelp forests. Results from intensive water sampling in a nearshore region of the Santa Barbara Channel during the stratified summer season indicated a distinct periodicity in ammonium (NH_4^+) concentrations throughout the full water column in relation to the tidal cycle. We propose NH_4^+ concentrations increase at low tide due to export from beach and subtidal sediment pore waters and decrease at high tide due to the advection of low nutrient waters from offshore. A diel pattern in NH_4^+ concentrations, with lower concentrations measured during the day and higher concentrations measured at night also occurred. We propose these diel fluctuations are due to greater uptake by phytoplankton during the day and higher rates of remineralization and excretion at night.

Introduction

While both ammonium (NH_4^+) and nitrate (NO_3^-) support primary production in the world's oceans, concentrations of NH_4^+ tend to fluctuate more and accumulate less than NO_3^-. The processes that contribute to variations in NH_4^+ concentrations include microbial remineralization, excretion by zooplankton and larger organisms, and photochemical degradation of organic matter (Capone et al., 2008). Variable concentrations are also a result of rapid uptake, since NH_4^+ is the preferred form of nitrogen for phytoplankton, especially in

N limited conditions (Glibert et al., 2016). Microalgal cells use different transporters to uptake NH_4^+ and NO_3^- (Raven, 1980), and cells assimilating NO_3^- may expend significant energy first reducing it to NH_4^+ prior to using it for metabolic processes (Syrett, 1981). To examine the variability in NH_4^+ concentrations requires intense sampling (Wheeler et al., 1989; Cochlan et al., 1991) and detection of NH_4^+ at sub-micromolar (<1 μM) concentrations (Brzezinski, 1988; Holmes et al., 1999; Zhu et al., 2018).

Diel patterns in NH_4^+ concentrations and associated regeneration and uptake rates have been observed in several marine locations, including coastal waters of the Southern California Bight (Ward and Bronk, 2001; Bronk and Ward, 2005; Brzezinski et al., 2013), offshore surface waters in the northeast Pacific Ocean (Cochlan et al., 1991) and subarctic Pacific Ocean (Wheeler et al., 1989), and in shallow regions of the Baltic Sea (Mopper and Lindroth, 1982). In some cases, the source of the periodicity, such as zooplankton excretion (Harris and Malej, 1986), was identified. However, in other studies, it remains unclear if this periodicity is influenced more strongly by biological processes such as excretion and remineralization or physical processes such as advection of offshore or inshore waters to the study site.

During the stratified, summer months, dissolved inorganic nitrogen (DIN) concentrations in coastal waters of the Santa Barbara Channel (SBC) are low due to cessation of upwelling and storm runoff (Brzezinski et al., 2013). Despite consistently low nutrient conditions, high chlorophyll concentrations (Goodman et al., 2012) and high net primary production of nearby giant kelp (*Macrocystis pyrifera*) forests (Reed et al., 2015) persist. This suggests that there is a significant source of nitrogen to support primary production through the stratified period. A model of SBC giant kelp nitrogen uptake found that 50% of

nitrogen used by kelp during the stratified summer months is taken up in a form other than NO_3^- (Fram et al., 2008). NH_4^+ and urea may therefore serve a role in supporting primary production during an otherwise low nutrient period.

In addition to low concentrations of DIN, the SBC experiences the largest diel variation in temperature and wind during the summer (Dorman and Winant, 2000). However, existing long-term datasets of NH_4^+ concentrations provide only monthly measurements (Washburn et al., 2019). The following study is the first to combine DIN and chlorophyll concentrations from high-frequency water sampling and measurements of salinity and temperature in the nearshore region of the SBC. We investigate the periodicity of NH_4^+ concentrations, examine correlations with environmental conditions, and discuss how concentrations may fluctuate due to physical as well as biological processes.

Methods

Site Description

Sampling was performed from Goleta pier (Longitude 119.82858 W, Latitude 34.41417 N), Goleta, California, USA. The pier has moderate boating and fishing traffic and extends approximately 500 meters into Goleta Bay, bordered by the Goleta Slough and Goleta beach park to the north and the Santa Barbara Channel to the south. The sampling location was located approximately 300 m from shore, and water depth ranged from 5 to 8 m depending on the tidal cycle. The 20-m isobath in Goleta Bay is located approximately 1 km from shore. The nearshore (<15 m) current along the SBC mainland generally flows poleward (westward) at speeds up to 0.1 m s^{-1} (Harms and Winant, 1998; Fewings et al., 2015), while the nearshore cross-shelf current typically flows offshore (southward) at speeds

ranging from 0.01 to 0.02 m s^{-1} (Fewings et al., 2015). In nearshore areas (<15 m) of the SBC, seawater residence time is approximately 2 days (Fewings et al., 2015). However, time series measurements indicate alongshore flow in the nearshore area varies from 0.05 to 0.2 m s^{-1} and the flow within the region during summer is baroclinic, or influenced by stratification, such that at low tide, warmer water is replaced by cooler water (Fram et al., 2008).

Oceanographic conditions in the SBC are generally divided into three main seasons: upwelling conditions dominate from April through June, stratified conditions persist from July through November, and winter storms occur December through March (McPhee-Shaw et al., 2007; Brzezinski et al., 2013; Aguilera and Melack, 2018). Sampling was conducted during stratified conditions, when seawater was >15 ºC, and DIN concentrations were ≤1 μM (Brzezinski et al., 2013).

The sampling site was chosen due to ease of access and its proximity to kelp forests where monthly dissolved nutrient data are collected by the Santa Barbara Coastal Long Term Ecological Research (SBC LTER) Project (Washburn et al., 2019). Monthly sampling at five kelp forest sites occurs around midday at multiple depths throughout the water column (1, 5, and 10 m), depending on the depth at a given site, and seawater samples are processed for dissolved NH_4^+, NO_3^-, total dissolved nitrogen, and dissolved organic carbon. Meteorological data are collected every hour at the Santa Barbara Municipal Airport (Longitude 119.843 W, Latitude 34.426 N), located approximately 2 km inland from the Goleta Pier, by the National Oceanographic and Atmospheric Administration (NOAA National Centers for Environmental Information, 2020), and tidal height data are also collected by NOAA (National Oceanographic and Atmospheric Administration, 2020) at site 9411340 (Longitude 119.685 W, Latitude 34.401 N) in Santa Barbara, CA.

Sampling Design

Water sampling was performed over three 36-hour sampling periods in August of 2018 with samples collected every four hours, beginning at 06:00 the first morning and concluding at 18:00 the following day. The three campaigns took place over the course of approximately one week to incorporate neap, midway, and spring tide conditions on August 3, 7, and 10, respectively. Sampling was delayed ~20 minutes if a boat launch occurred to allow the water to disperse and stratification to re-establish. Prior to each water sampling, a vertical profile of the entire water column was obtained using a SBE 19plus V2 SeaCAT Profiler sampling at 4Hz (4 scans sec^{-1}). Temperature readings are accurate to 0.01ºC, and conductivity readings are accurate to 0.001 S m^{-1}. This instrument also maintains pump-controlled, ducted flow to match the time constants of temperature and conductivity sensors and reduce salinity spiking. Water samples were then collected using a 5L Okeanus GO-FLO Sampler at 1, 3, and 5 m depths, taking care not to disturb the underlying sediments. Seawater sample collection followed SBC LTER protocol, with HDPE sample vials acid washed (10% HCl) prior to use and several rinses of seawater performed prior to sample collection (Washburn et al., 2019).

Sample Processing

Immediately upon collection, water samples were placed on ice in coolers, transported back to the laboratory, and filtered through GF/F filters (0.7 µm, Whatman) for dissolved nutrients and MCE filters (0.45 µm, Millipore) for chlorophyll.

A subset of GF/F-filtered samples was analyzed immediately for NH_4^+ using the *ortho*-phthaldialdehyde method (Holmes et al., 1999; Taylor et al., 2007), and duplicates were measured using a Turner Trilogy Laboratory Fluorometer with a limit of detection of

0.05 µM. In order to best approximate potential matrix effects, standard curves were created using low nutrient seawater that was collected locally and incubated unfiltered for over 6 months.

Another subset of GF/F-filtered samples was stored frozen (-20 ºC) and measured later for combined nitrate (NO_3^-) and nitrite (NO_2^-) concentrations by flow injection analysis on a Lachat QuickChem 8500 Series 2 Analyzer (Hach Company) with a limit of detection of 0.2 µM. Samples below the limit of detection were reported and analyzed as equal to 0.2 µM. A third subset of the GF/F-filtered samples was acidified with 4N HCl and refrigerated (4 ºC) until analysis for dissolved organic carbon (DOC) by high temperature combustion on a Shimadzu TOC-V Analyzer with a limit of detection of 25 µM and a precision of 1-2 µM. One sample from August 4th was removed from the dataset due to concerns about contamination of the sample.

The MCE filters were folded into vials and stored frozen (-20 ºC) until they were analyzed for chlorophyll a and phaeopigments by extraction in 90% acetone (Strickland and Parsons, 1968; Smith et al., 1981) and measurement on a Turner 10AU Field and Laboratory Fluorometer with a limit of detection of 0.02 µg L^{-1}.

Data Analyses

Casts were processed and converted to mat file formats using SBE data processing software (v 7.26.7). Physical measurements were edited to remove the horizontal sections of each profile, suggesting spiking occurring in surficial or benthic waters. Data were collected approximately every 5 cm and was later binned and averaged to 10 cm intervals. Remaining data organization and analyses were performed using Excel (v 16.24), MATLAB (v R2018b 9.5), and R (v 3.4.3). All statistical analyses used an alpha (α) value of 0.05 unless otherwise

noted and were performed using the lm() function in R. Data formatting and visualization were performed using the *tidyverse* in RStudio 2 (Wickham et al., 2019).

Results

Monthly Nutrient Sampling

NH_4^+ concentrations in the nearshore regions of the SBC were lowest June through October (*Figure 1*). NH_4^+ concentrations from 2017 to 2019 ranged from 0.05 to 4.59 µM with a mean value of 0.37 ± 0.50 µM.

Physical Conditions

Winds ranged from 0 to 6.3 m s^{-1} and were typically strongest in the afternoon. Wind directions varied over the course of the three sampling campaigns but were most often offshore from the northwest or northeast (*Figure 2*). Sampling was scheduled to coincide with neap, midway, and spring tide conditions on August 3, 7, and 10, respectively. Using the NOAA dataset, the lowest tidal height reported was -0.31 m while the highest tidal height was 2.23 m, both of which occurred during the last sampling campaign on August 10th to 11th (*Figure 2*).

Water temperature fluctuated on a tidal basis. Recorded temperatures ranged from approximately 16º to 23º C (*Figure 2*). On most days, the water column was stratified during early morning. Over the course of the day and into the early evening, temperatures increased. On all dates sampled, a warmer surface layer appeared around 14:00 that reached a depth of at least 3 m. Only occasionally was the water column isothermal, as at 22:00 on August 10th, when the temperature of the full water column was approximately 21º C. Tidal height and

temperature were significantly positively correlated ($F(88) = 11.77$, $R^2 = 0.11$, $p = 0.0009$), with higher temperatures recorded during higher tides.

Measured salinity ranged from approximately 33.6 to 33.8 Practical Salinity Units (PSU) (*Figure 2*). Early morning waters appeared slightly more stratified, but midday and evening values fluctuated on an approximately 6-hour timescale, more closely matched to tidal height. Salinity and tidal height were significantly positively correlated ($F(88) = 7.89$, $R^2 = 0.07$, $p = 0.006$), with more saline water extending deeper into the water column during higher tides. Salinity was also significantly correlated with temperature ($F(88) = 165.2$, $R^2 = 0.65$, $p < 0.0001$), with higher seawater salinity measured during periods of higher temperatures.

Patterns in temperature and salinity co-varied. Typically, warmer, more saline water flowed into the sampling region as tidal height increased. As the tidal height decreased, cooler, less saline water flowed into the sampling region, typically below 1 or 2 m and to within 1 m of the bottom. Coldest and least saline water occurred at low tide and was more typically found between 3 and 7 m. The coldest, least saline water mass was detected during the neap tide conditions of the first sampling period (August 3-4) and the warmest, most saline water mass was present during the midway tide conditions of the second sampling period (August 7-8).

Dissolved Nutrients and Chlorophyll a

During August 2018, NH_4^+ concentrations varied over diel cycles (*Figure 3, Appendix 2*). Mean NH_4^+ concentration of all depths and times measured over the course of all sampling campaigns was 0.65 μM, and concentrations ranged from 0.05 to 2.01 μM. These values are consistent with dissolved nutrient data collected during the stratified

summer period of 2016 (*Appendix 3*) and during a study by Brzezinski et al. (2013). Concentrations were typically highest in the early morning (2:00-6:00), decreased throughout the day (10:00-18:00), sometimes to below the limit of detection (0.05 µM), and increased during the night (22:00-2:00). Values were not consistently highest at the surface or near the bottom. Surface waters typically contained the highest NH_4^+ concentrations between 06:00 and 10:00 while bottom waters contained the highest NH_4^+ concentrations between 2:00 and 6:00.

NO_3^- concentrations did not vary on a diel pattern. At most sampling times, concentrations were below the limit of detection (0.2 µM) (*Figure 3*). The mean NO_3^- concentration of all depths and times measured during the sampling campaigns was 0.22 µM, and concentrations ranged from below detection to 0.38 µM. NO_3^- concentrations were often an order of magnitude less than NH_4^+ concentrations.

Mean dissolved organic carbon (DOC) concentration was 95 µM, and values ranged from 82 to 174 µM (*Figure 3*). There appeared to be two outliers, the first at 10:00 on August 8th (174 µM) and the second at 14:00 on August 11th (158 µM). Higher DOC concentrations were usually recorded at shallower depths (1 and 3 m). DOC concentrations fluctuated little during the first sampling campaign from August 3rd to 4th. On all dates sampled, DOC concentrations varied less than 25 µM in samples collected at 5 m.

Chlorophyll a (*chl a*) concentrations fluctuated, but not in a diel pattern. The mean *chl a* concentration of all samples was 1.52 µg/L, and concentrations ranged from 0.58 to 4.12 µg/L (*Figure 3*). *Chl a* concentrations decreased between 18:00 and 22:00 each evening and increased between 2:00 and 6:00 each morning. For the latter two sampling periods, tidal height increased during this time and warmer, more saline water flowed to the study site.

However, patterns varied over the course of the day and throughout the water column. There were particularly large increases during both mornings of the last sampling period (August 10^{th} – 11^{th}) at high tides. Extrema of *chl a* measured during a given sampling campaign were inversely related to the extrema in measured NH_4^+ concentrations (see *Figure 7*).

Ammonium Concentrations in Relation to Physical and Biological Measurements

NH_4^+ concentrations were inversely related to tidal height for all dates sampled ($F(88) = 39.8$, $R^2 = 0.30$, $p < 0.0001$) (*Figure 4*). Each consecutive sampling campaign progressed towards the spring tide, hence the final sampling dates had the broadest distribution in tidal height. At tidal heights above 0.5 m, NH_4^+ concentrations noticeably decreased, with more samples falling below 0.5 µM than in lower tidal heights (<0.5 m).

NH_4^+ concentrations were inversely related to seawater temperature for all dates sampled ($F(88) = 20.36$, $R^2 = 0.18$, $p < 0.0001$) (*Figure 5*). NH_4^+ concentrations began to drop below the limit of detection (0.05 µM) around 19º C, and at approximately 21.5º C, nearly all samples dropped below the limit of detection.

NH_4^+ concentrations were inversely related to seawater salinity for all dates sampled ($F(88) = 13.01$, $R^2 = 0.12$, $p = 0.0005$) (*Figure 6*). Unlike tidal height and temperature, however, NH_4^+ concentrations had greater variability about the predicted relationship, and the range in salinity spanned 33.64 to 33.76 PSU.

In addition to physical parameters, NH_4^+ concentrations were inversely related to chlorophyll a (*chl a*) for all dates sampled ($F(86) = 5.785$, $R^2 = 0.05$, $p = 0.02$) (*Figure 7*). Above *chl a* values of 2.5 µg/L, NH_4^+ concentrations all dropped below 0.5µM.

As illustrated in temperature-salinity diagrams overlaid with *chl a* and NH_4^+ concentrations (Figure 8), higher *chl a* concentrations were associated with cooler

temperatures and less saline water. The same trend was true for NH_4^+ concentrations, with higher concentrations measured in cooler, less saline water. This is consistent with the inverse correlations found for NH_4^+ concentrations and temperature (*Figure 5*) and salinity (*Figure 6*).

Based on the predictor variables that were most strongly correlated with NH_4^+ concentrations using the linear regressions presented above (*Figure 4-7*), we performed a multiple linear regression including temperature, tidal height, and their interaction term as predictors of NH_4^+ concentrations (*Table 1*). Initially, salinity was also included as an independent predictor variable and as part of the interaction term, but it was removed after assessing model fit using Akaike Information Criterion values as well as the significance of each predictor variable. Salinity covaried with temperature, hence its inclusion in the final model structure was not appropriate. Both temperature ($p = 0.0002$) and tidal height ($p = 0.002$) were significant predictors of NH_4^+ concentrations, as was their interaction term ($p = 0.005$).

Discussion

Physical Drivers of Periodicity in Ammonium Concentrations

Based on physical measurements, tidal height appeared to be the best predictor of NH_4^+ concentrations ($p < 0.0001$, *Figure 4*) followed by temperature ($p < 0.0001$, *Figure 5*). However, within each sampling period, temperature co-varied with tidal height. In a multiple linear regression model including both predictors, the interaction between tidal height and temperature was a significant predictor of NH_4^+ concentrations ($p = 0.005$, *Table 1*). At lower tidal heights, NH_4^+ concentrations were significantly greater. We propose that this

increase in nutrient concentrations may be due to the export of nutrients remineralized in nearshore beach and subtidal sediments. Local beaches have high concentrations of nutrients (>100 μM) in their pore waters due to deposition of macroalgal wrack (Dugan et al., 2011) and remineralization by beach invertebrates (Lowman et al., 2019). Furthermore, beach pore waters flush regularly, approximately every 4.4 – 6.4 days, and pore water residence time has been significantly positively correlated with tidal height (Goodridge and Melack, 2014). If NH_4^+ concentrations in nearshore waters also correspond with tidal cycles, this suggests that tidal flushing of high-nutrient, beach pore waters may be exported to shallow, coastal areas during low tide. Located behind the beach, immediately onshore of the sampling site, is the Goleta Slough, an estuary where four creeks converge before emptying into the ocean. The outlet to the slough was open during August 2018, which suggests there could also have been export from the creeks and the slough to nearshore waters. Subtidal marine sediments in this region also have high NH_4^+ concentrations (approximately 40 μM) in their pore waters (Smith et al., 2018) that could be supplied to the overlying water column by tidal and current flushing. In addition, our results indicate that NH_4^+ concentrations significantly decreased as tidal height and temperature increased. We propose that this relationship may be due to the advection of warm, low-nutrient water from offshore areas. Tidal height and temperature were significantly positively correlated ($p = 0.0009$), suggesting warmer water was advected onshore during high tides. Nutrient concentrations in the SBC are low (<0.5 μM) during the summer months (Brzezinski et al., 2013, *Figure 2*), so the advection of offshore water to nearshore regions would likely not bring high concentrations of NH_4^+ with it. High tides would therefore deliver warm, low-nutrient water and decrease measured NH_4^+ concentrations.

Salinity was also identified as a significant predictor of NH_4^+ concentrations ($p = 0.0005$, *Figure 6*), although it was not included as an independent variable in the final multiple linear regression structure. During high tides, salinity increased ($p = 0.006$). More saline water is typically indicative of water from further offshore and supports the above suggestion that offshore water was delivered to coastal regions during high tides. In addition, salinity was significantly inversely correlated with NH_4^+ concentrations ($p = 0.0005$, *Figure 6*) which means higher NH_4^+ concentrations were measured in less saline water. Beach pore water typically consists of a mix of fresh groundwater sources and recycled seawater from the nearby surf zone, and when this water is released back into the ocean, it is labeled submarine groundwater discharge (SGD) (Burnett et al., 2003). However the freshwater influence at most SBC beaches is low, especially during dry summer conditions (Swarzenski and Izbicki, 2009; Goodridge and Melack, 2014). The correlations between tidal height, salinity, and NH_4^+ concentrations further support our suggestion that low tides delivered water from nearby beaches to shallow, coastal areas.

Other physical transport processes may have been active during the sampling period, such as internal waves and seasonal or wind-driven upwelling. Internal waves are a demonstrated source of diel oscillations in DIN in some nearby locations in the SBC (McPhee-Shaw et al., 2007), although they can be unpredictable (Nash et al., 2012). Longer period internal waves are not related to tidal cycles (Noble et al., 2009), but internal tides are a form of internal waves driven by diel changes in wind velocity (Fram et al., 2008). Seasonal upwelling has also been demonstrated to cause changes in DIN concentrations on daily timescales, but periods of seasonal upwelling are uncommon during the stratified season (McPhee-Shaw et al., 2007). A threshold of 13º C has been found to be indicative of

seasonal upwelling in the region (Fram et al., 2008), and we did not measure temperatures below 16º C. Therefore, we suggest that NH_4^+ was not replenished by seasonal upwelling events during our sampling period. Shorter periods of upwelling cause by winds have been demonstrated at nearby locations such as Mission beach (Armstrong and LaFond, 1966) and San Luis Obispo Bay (Walter et al., 2017). In these instances, offshore winds displace nearshore surface waters and cause fluctuations in thermocline depth. In the SBC, winds are generally weak at sunrise and strongest in the early afternoon, and local measurements have a diel variability in wind strength during the summer (Dorman and Winant, 2000). We also found that wind speeds had a weakly diel pattern, with stronger, generally northerly winds occurring in the afternoon (*Figure 1*). If such winds were strong enough to induce shorter periods of upwelling, this could moderate the amplitude of the NH_4^+ concentration signal we detected in relation to the tidal height. For example, if strong winds were blowing offshore during a low tide, it could dampen the detected nutrient signal we propose is coming from high nutrient beach pore waters by diluting it with upwelled, low-nutrient seawater from further offshore. Such a dampening may be visible between the afternoons of August 8th and 11th. On both days, low tide occurs at approximately 2:00, and there is a noticeable spike in NH_4^+ concentration around that time on both dates. However, on August 8th, the NH_4^+ signal is lower (0.5 – 1.0 μM), and the offshore wind speed is much greater, suggesting the potential of a small upwelling event. On August 11th, there is almost no wind during the same period, and measured NH_4^+ concentrations are greater (1.5 – 2.0 μM), suggesting greater influence from beach pore waters. Fram et al. (2008) found the transport of colder water onshore at depth (~9 m) and warmer water offshore at the surface both inside and outside of an SBC kelp forest following a late afternoon high tide. This further supports the potential for

strong, offshore afternoon winds to encourage offshore movement of surface waters and onshore movement of upwelled bottom waters, therefore moderating the tidal signal in NH_4^+ concentrations. Additional data regarding seawater current speeds relative to wind speeds would be required to determine with confidence if winds caused significant fluctuations in NH_4^+ concentrations. Nevertheless, it may be an important physical factor moderating the periodicity of measured NH_4^+ concentrations, particularly if winds in the SBC vary most on a diel timescale.

Biological Drivers of Periodicity in Ammonium Concentrations

NH_4^+ concentrations fluctuated with a diel pattern in nearshore waters of the SBC during the stratified summer period of August 2018 (*Figure 3, Appendix 2*) and in June through August 2016 (*Appendix 3*). Concentrations frequently decreased or remained low during the day and increased at night. Previous studies performed within giant kelp forests of the SBC have either inferred NO_3^- concentrations from temperature measurements (Zimmerman and Kremer, 1984) or reported only daytime NH_4^+ concentrations (Brzezinski et al., 2013). The NO_3^- concentrations detected during this study were similar to low NO_3^- concentrations (<1.0 μM) measured by others in the SBC (Brzezinski et al., 2013; Washburn et al., 2019). Our sampling is the first to demonstrate a diel periodicity in NH_4^+ concentrations in nearshore waters of the SBC based on *in situ* sampling on a full 24-hour timescale. This pattern of low NH_4^+ concentrations during the day and high NH_4^+ concentrations at night has been reported by others, including in nearby surficial waters of the Southern California Bight (Ward and Bronk, 2001; Bronk and Ward, 2005). However, analysis of physical drivers demonstrate a clear influence of tidal height on measured NH_4^+ concentrations in the coastal waters we sampled (*Figure 4, Table 1*). We suggest that the

periodicity of fluctuations in NH_4^+ concentrations was determined foremost by a tidal influence, but that biological processes may have further moderated these fluctuations on a diel basis.

Phytoplankton chlorophyll a (*chl a*) and NH_4^+ concentrations were inversely correlated ($p = 0.02$, *Figure 7*). Phytoplankton prefer to uptake NH_4^+ over NO_3^- (Glibert et al., 1982b; Dortch, 1990), and this has been demonstrated in the Southern California Bight, which includes the Santa Barba Channel (Bronk and Ward, 2005). NH_4^+ may also be transformed into NO_3^- by nitrifying microbes, although nitrification rates in the Southern California Bight are relatively low (Bronk and Ward, 2005). NH_4^+ uptake rates are significantly correlated with both temperature and light (Glibert et al., 1982a), and therefore NH_4^+ uptake by phytoplankton is likely to be higher during the day than at night (Wheeler et al., 1989; Cochlan et al., 1991). Bronk and Ward (2005) found total NH_4^+ uptake rates in nearshore waters of the Southern California Bight in October to be approximately 71 nM hr^{-1} at *chl a* concentrations of 0.24 µg/L. The mean *chl a* concentrations measured during this study (1.52 µg/L) would therefore suggest rates of NH_4^+ uptake of approximately 0.45 µM hr^{-1}. In addition to uptake by phytoplankton, NH_4^+ regeneration by grazing and zooplankton excretion may have contributed to a diel pattern. During experiments carried out in the South California Bight, NH_4^+ regeneration rates were higher at night than during the day (Ward and Bronk, 2001; Bronk and Ward, 2005). Zooplankton also perform diel migration, and since their main excretion product is NH_4^+, they too might contribute to nightly NH_4^+ concentration increases (Jawed, 1973; Hammer, 1981; Harris and Malej, 1986). Greater uptake by phytoplankton in warm water may also contribute to the inverse correlation found between seawater temperature and NH_4^+ concentrations ($p < 0.0001$, *Figure 5)*, in addition to

the possibility that warmer waters were low-nutrient water delivered from offshore areas during high tides. Although phytoplankton *chl a* has been shown to increase with increasing stratification (Goodman et al., 2012), we found no significant relationship between *chl a* and tidal height or temperature ($p > 0.05$ for both). Therefore, we suggest phytoplankton were not being advected to our study site from offshore waters during high tides. A combination of greater uptake by phytoplankton during the day and greater regeneration and excretion by microbes and zooplankton at night may contribute to the diel signal in NH_4^+ concentrations visible across most dates sampled (*Figure 3, Appendix 2 and 3*).

Proposed Local Mechanism Responsible for Periodicity of Ammonium Concentrations Pattern

Due to the inverse correlation between NH_4^+ concentrations and tidal height, we propose that fluctuations in NH_4^+ are due primarily to the export of remineralized nutrients from nearby beaches and subtidal sediments during low tides and the advection of warm, low-nutrient waters from offshore during high tides (*Figure 9*). We also suggest biological processes overlap physical processes to cause a weakly diel signal in NH_4^+ concentrations.

The amplitude of fluctuations in NH_4^+ concentrations was likely affected by the interaction between tidal height and diel biological processes. For example, higher tides were significantly correlated with lower NH_4^+ concentrations. If a high tide took place during the day, uptake by phytoplankton could further dampen the NH_4^+ signal. Alternatively, high NH_4^+ concentrations occurred during low tides which could be further enhanced at night, when remineralization and excretion dominate.

Water samples and physical measurements collected in Goleta Bay in August 2018 confirm the existence of a periodicity in NH_4^+ concentrations driven by tidal cycles as well as

diel fluctuations likely driven by biological uptake and remineralization of NH_4^+. Our data also indicates a consistent presence of recycled nitrogen available to giant kelp forests in nearshore areas during stratified, low-nutrient conditions in the SBC. The mean concentration of NH_4^+ reported for seawater surrounding kelp forests during the summer season is 0.5 µM (Brzezinski et al., 2013), a value that was exceeded on 60% of our sampling times (n = 18). These data imply a greater presence of recycled nitrogen (NH_4^+) than previously recognized in coastal waters of the SBC during stratified conditions. Although low tides appeared to significantly increase nutrient concentrations in shallow waters (8 m), it is unclear if this effect would be as strong at depths where kelp forests are located (10-20 m). For example, some reefs are found immediately offshore and may be supplied by this process. When kelp is further offshore, other species of macroalgae and plants occur between it and the nearshore and may take advantage of the nutrients supplied from the beach. In deeper kelp forest waters, beach pore waters are unlikely to influence nutrient concentrations, but biological processes such as remineralization and excretion could add nutrients. Excretion may be even greater due to the diversity of invertebrates, fish, and mammals in kelp forests (Miller et al., 2018). We anticipate patterns of lower nutrients detected during high tides would remain similar in kelp forest habitats. To be certain, though, additional research should be conducted to determine if the advection of warm, low-nutrient water into kelp forests during high tides overwhelms or simply dilutes contributions from internal recycling processes. Local production, for instance by attached bryozoans (Arkema, 2009), would be retained in the recirculating eddies that form as water flows past kelp stipes and fronds. More information regarding nutrients, specifically NH_4^+, availability in giant kelp

forests as well as fluctuations in nutrient supply may be used to better understand rates of primary productivity during stratified conditions typical of summer months.

Tables and Figures

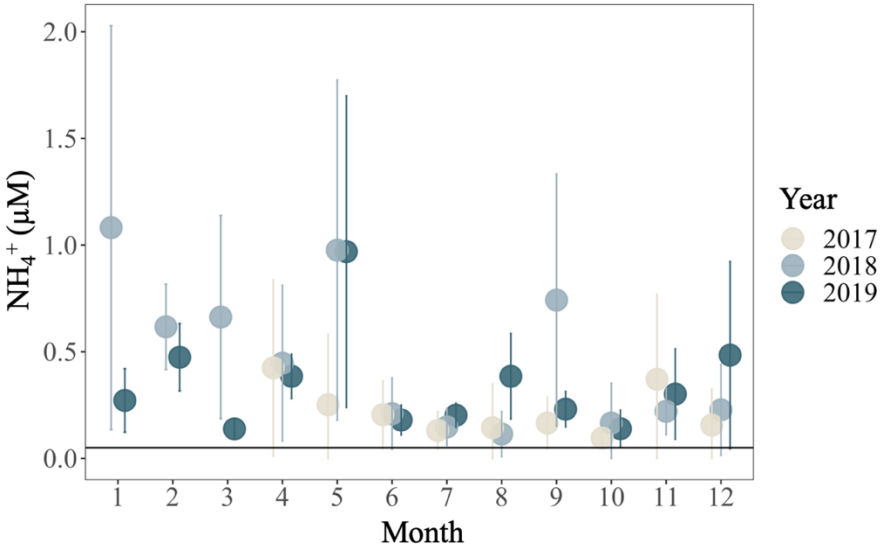

Figure 1: Mean monthly ammonium (NH_4^+) concentrations collected at midday from five kelp forest locations in the Santa Barbara Channel by the Santa Barbara Long Term Ecological Research project. Error bars represent standard deviation of values measured at all five sites. Horizontal black line indicates the limit of detection of the OPA fluorometric method (0.05 µM).

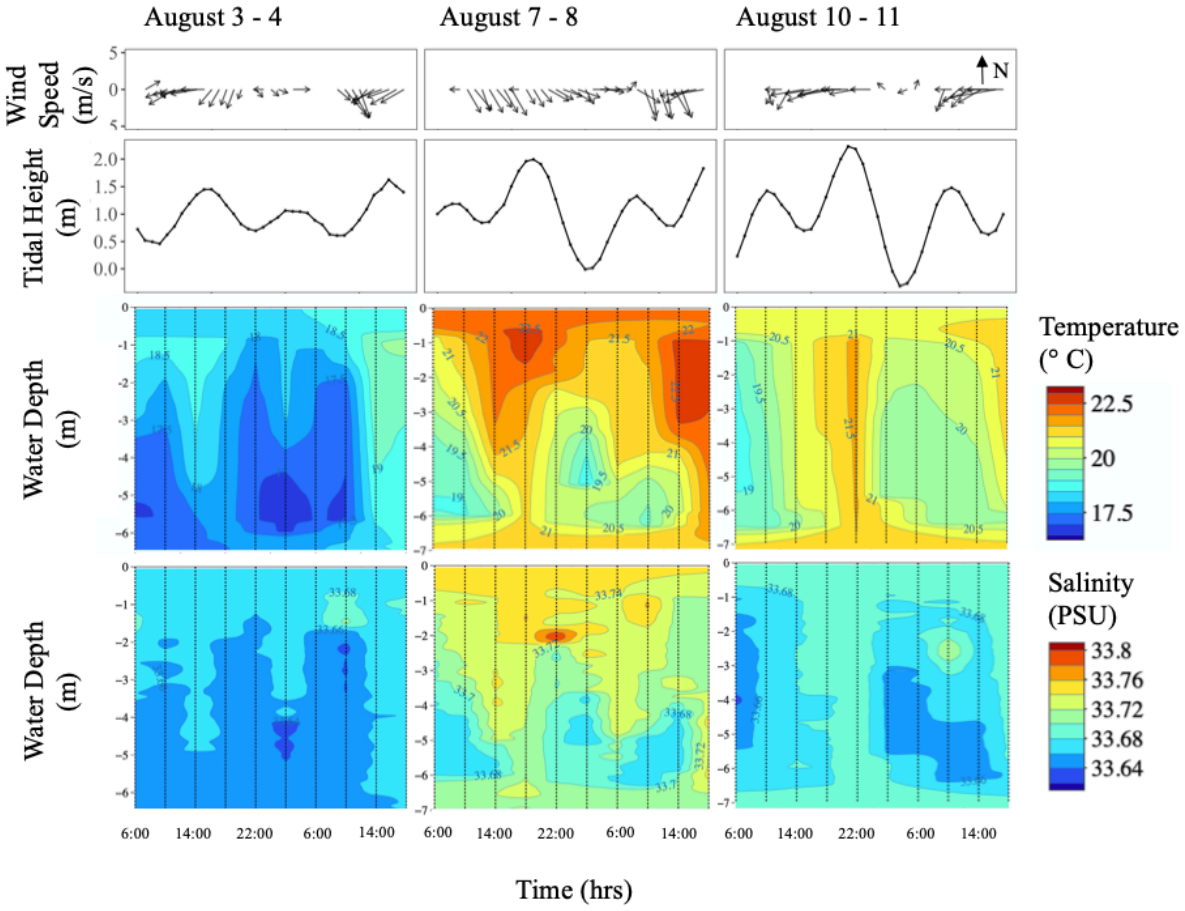

Figure 2: Directional wind speed, tidal height, temperature, and salinity of seawater for sampling dates in August 2018. Neap, midway, and spring tide conditions occurred during the August 3-4, 7-8, and 10-11 sampling dates, respectively. Vertical dashed lines on the temperature and salinity panels indicate sampling times.

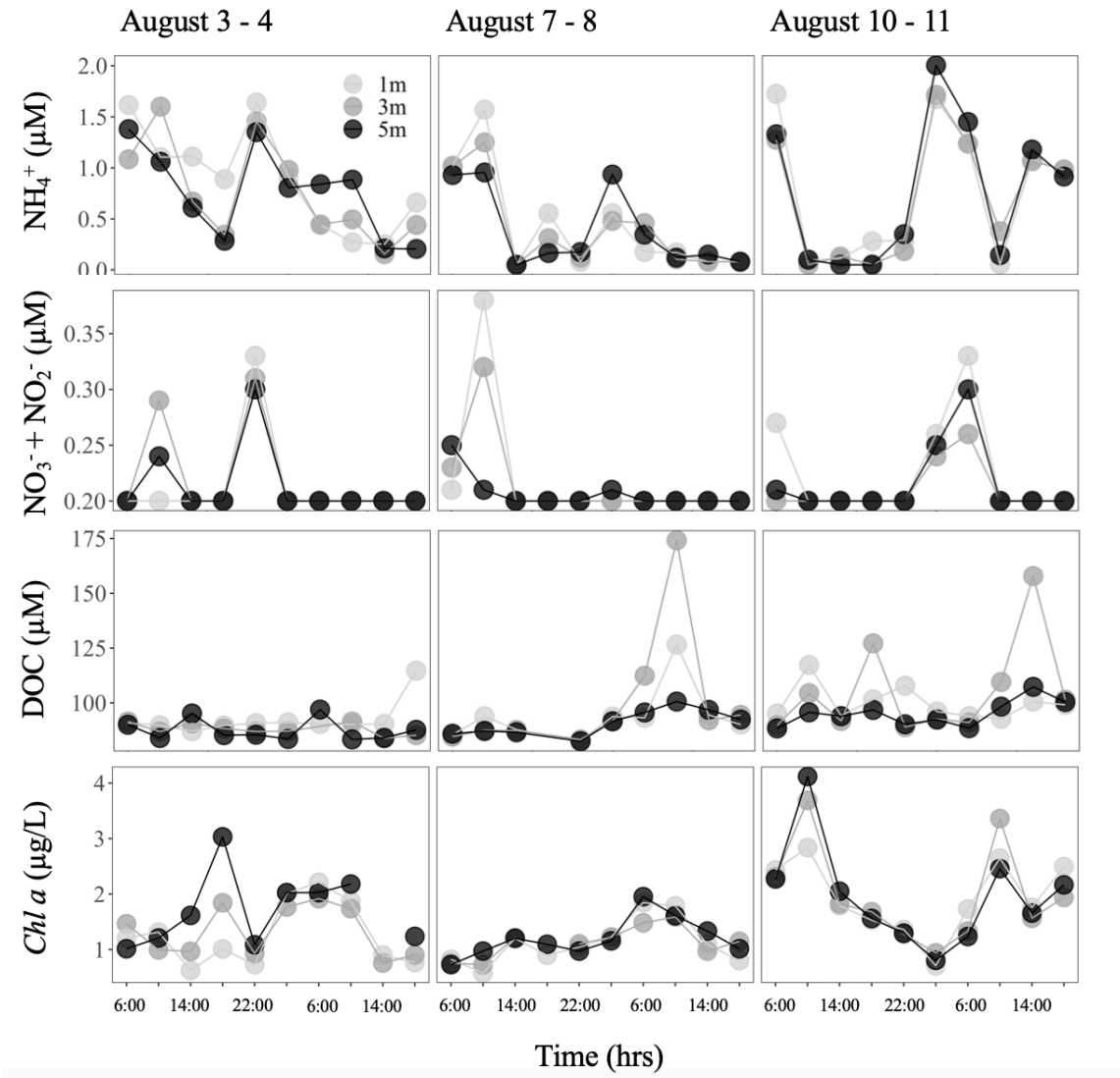

Figure 3: Ammonium (NH_4^+), nitrate ($NO_3^- + NO_2^-$), dissolved organic carbon (DOC), and chlorophyll a (chl a) concentrations of seawater collected in August 2018.

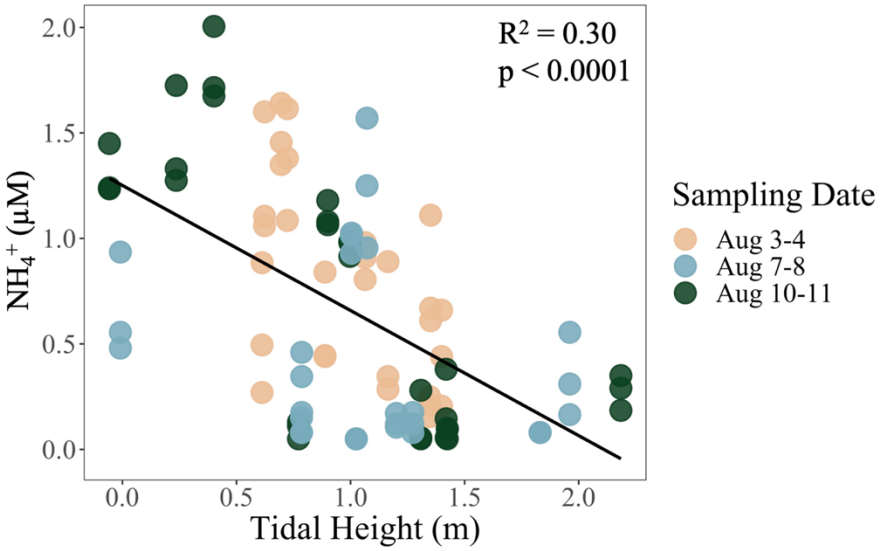

Figure 4: Ammonium (NH_4^+) concentrations versus tidal height during the August 2018 sampling period.

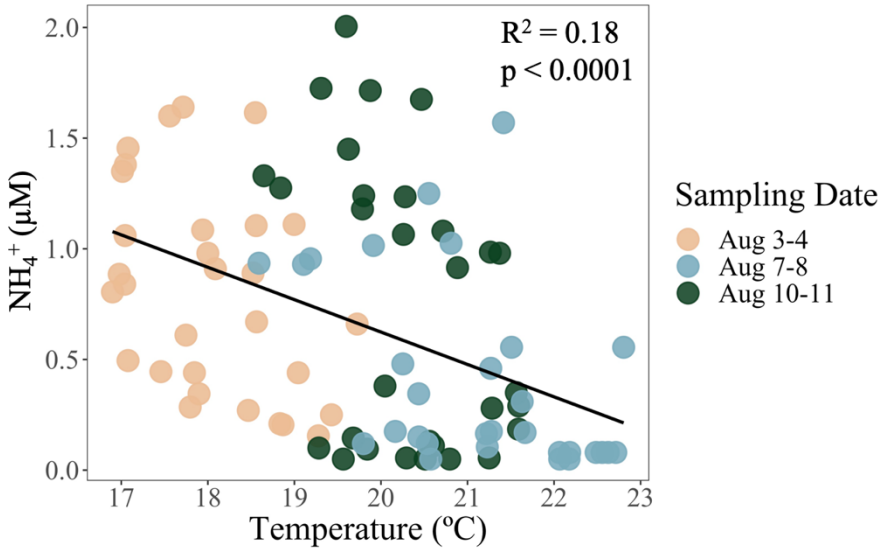

Figure 5: Ammonium (NH_4^+) concentrations versus seawater temperature during the August 2018 sampling period.

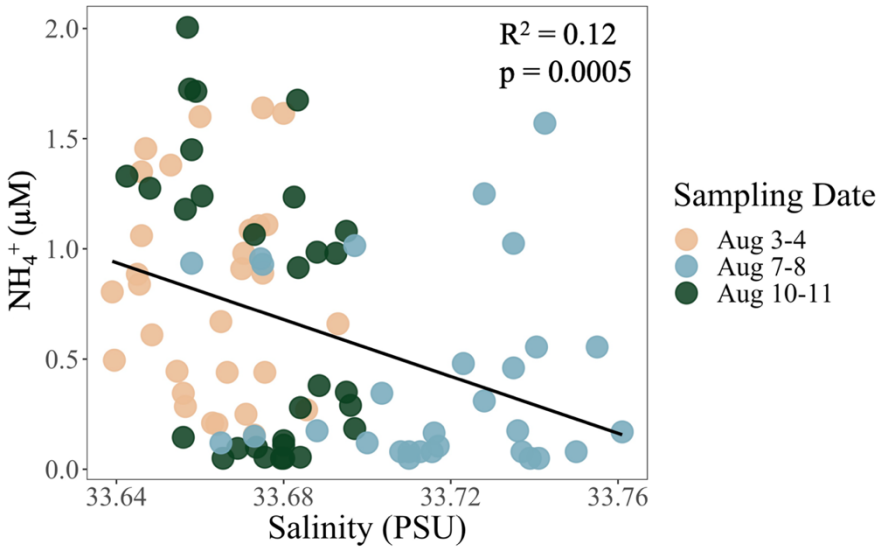

Figure 6: Ammonium (NH_4^+) concentrations versus seawater salinity during the August 2018 sampling period.

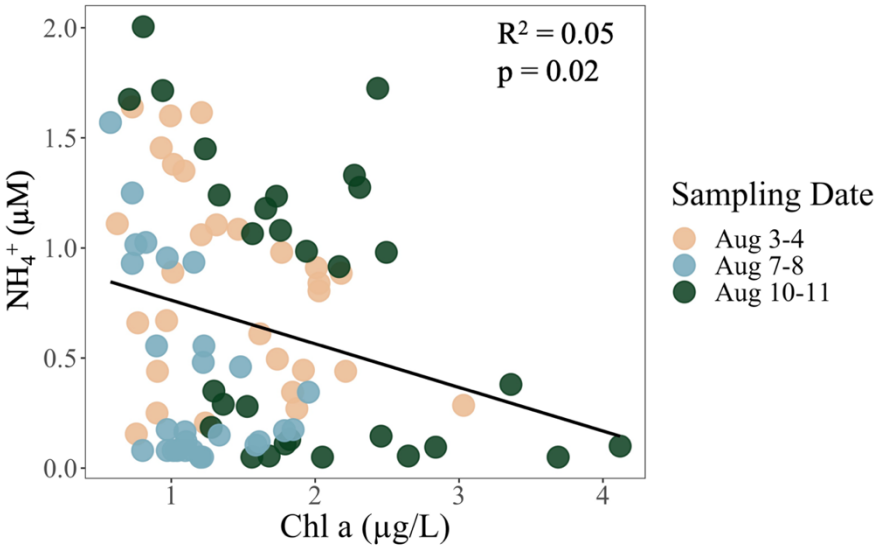

Figure 7: Ammonium (NH_4^+) concentrations versus phytoplankton chlorophyll a (chl a) during the August 2018 sampling period.

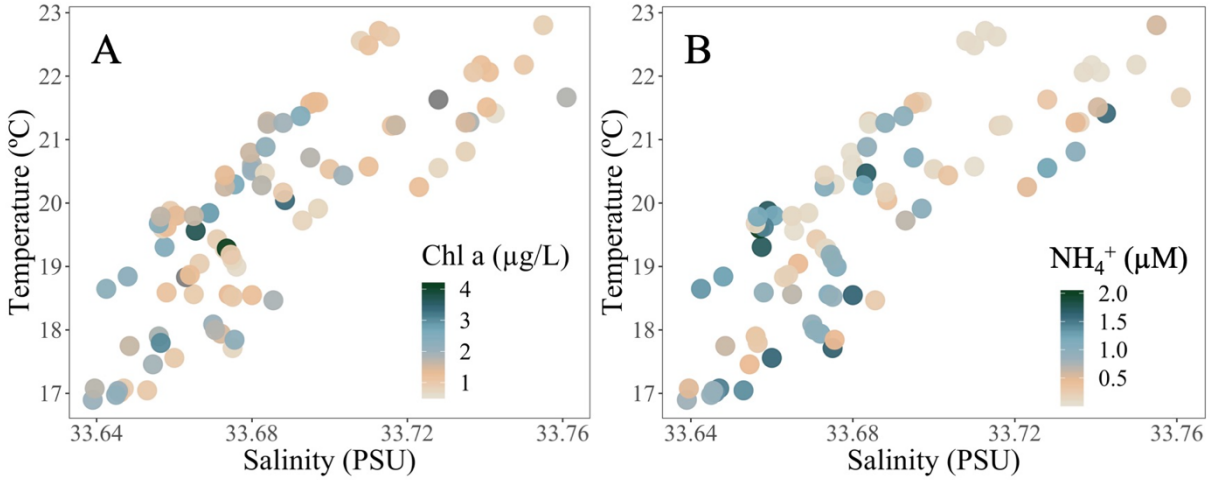

Figure 8: Temperature-salinity plots of seawater collected in August 2018 colored by chlorophyll (Panel A) and ammonium concentrations (Panel B).

Table 1: Multiple linear regression results for ammonium concentrations (μM) using two predictor variables, temperature (ºC) and tidal height (m), as well as their interaction term. The model significantly predicts ammonium concentration ($F(3,86) = 21.9$, $p < 0.0001$, $R^2 = 0.41$).

	Coefficient	**Standard Error**	***t***	***p***	**Overall adjusted R^2**
Intercept	6.759	1.417	4.771	< 0.0001	0.41
Temperature (ºC)	- 0.280	0.071	- 3.945	0.0002	
Tidal Height (m)	- 4.314	1.323	- 3.262	0.002	
*Temperature * Tidal Height*	0.187	0.065	2.896	0.005	

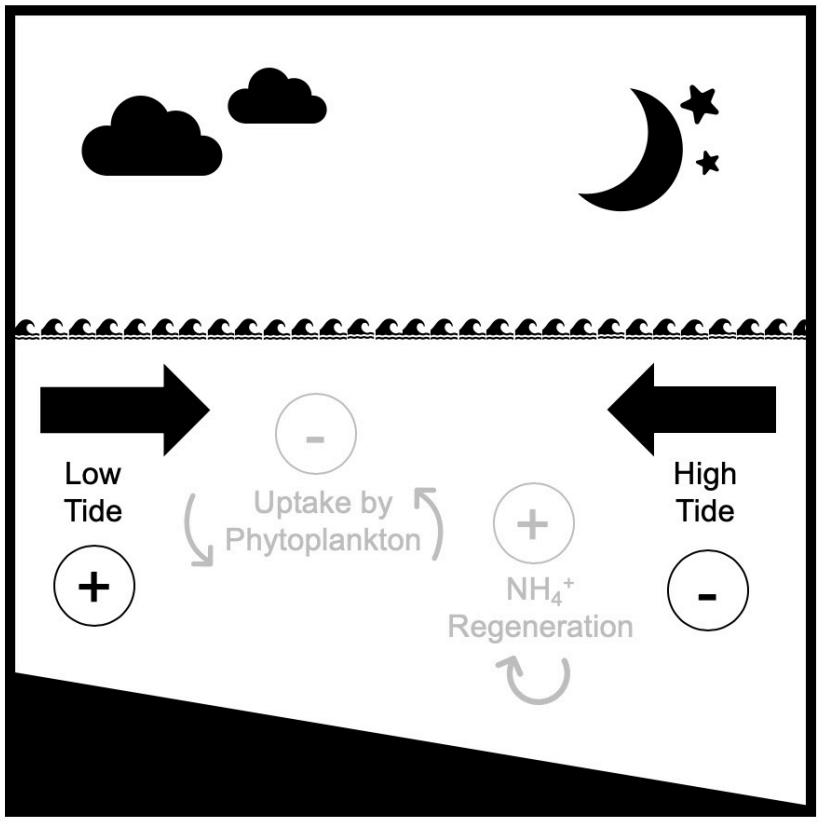

Figure 9: Conceptual diagram of biophysical coupling in nearshore waters of Goleta Bay during the stratified season. Physical processes are depicted with black arrows while biological processes are depicted with grey arrows. Symbols of "+" and "-" indicate whether a given process increases or decreases ammonium concentrations.

Appendix

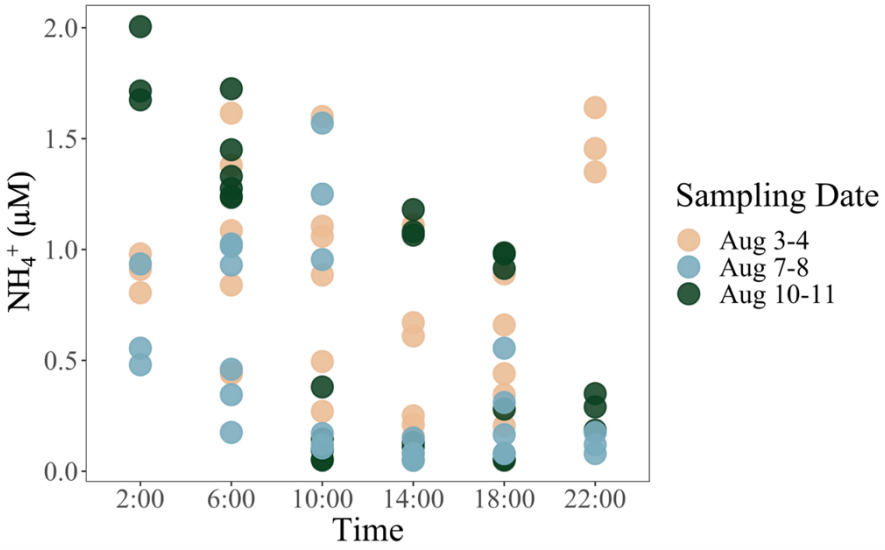

Appendix Figure 1: Ammonium (NH_4^+) concentrations of seawater collected in August 2018 presented temporally.

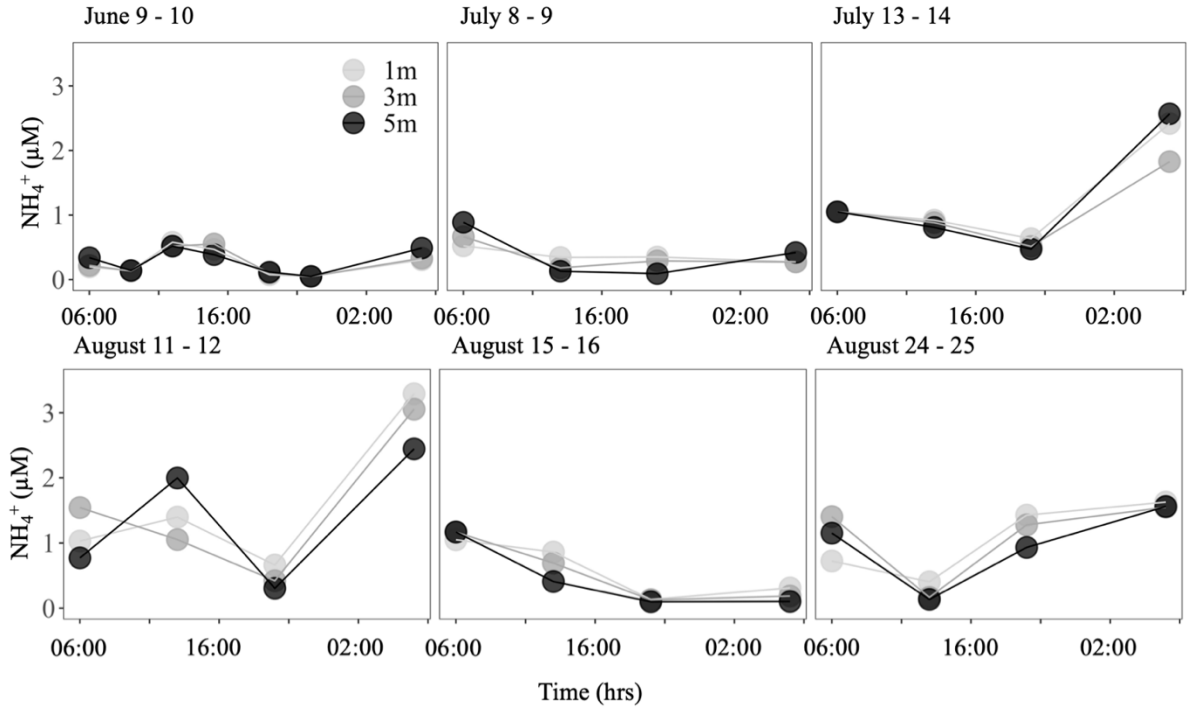

Appendix Figure 2: Ammonium (NH_4^+) concentrations of seawater collected in June through August 2016. Note, samples were collected at one of two sites – Stearns Wharf, Santa Barbara, CA or Goleta Pier, Goleta, CA – during this sampling campaign.

References

Aguilera, R., Melack, J. M., 2018. Concentration-discharge responses to storm events in coastal California watersheds. *Water Resources Research* 54, 407–424. https://doi.org/10.1002/2017WR021578

Arkema, K., 2009. Flow-mediated feeding in the field: Consequences for the performance and abundance of a sessile marine invertebrate. *Marine Ecology Progress Series* 388, 207–220. https://doi.org/10.3354/meps08140

Armstrong, F. A. J., LaFond, E. C., 1966. Chemical nutrient concentrations and their relationship to internal waves and turbidity off southern California: Nutrient concentrations related to internal waves and turbidity. *Limnology and Oceanography* 11, 538–547. https://doi.org/10.4319/lo.1966.11.4.0538

Bronk, D. A., Ward, B. B., 2005. Inorganic and organic nitrogen cycling in the Southern California Bight. *Deep Sea Research Part I: Oceanographic Research Papers* 52, 2285–2300. https://doi.org/10.1016/j.dsr.2005.08.002

Brzezinski, M., 1988. Vertical distribution of ammonium in stratified oligotrophic waters. *Limnology and Oceanography* 33, 1176–1182.

Brzezinski, M., Reed, D., Harrer, S., Rassweiler, A., Melack, J., Goodridge, B., Dugan, J., 2013. Multiple sources and forms of nitrogen sustain year-round kelp growth on the inner continental shelf of the Santa Barbara Channel. *Oceanography* 26, 114–123. https://doi.org/10.5670/oceanog.2013.53

Burnett, W. C., Bokuniewicz, H., Huettel, M., Moore, W. S., Taniguchi, M., 2003. Groundwater and pore water inputs to the coastal zone. *Biogeochemistry* 66, 3–33. https://doi.org/10.1023/B:BIOG.0000006066.21240.53

Capone, D. G., Bronk, D. A., Mulholland, M. R., Carpenter, E. J., 2008. *Nitrogen in the Marine Environment*, 2nd ed. Academic Press, New York.

Cochlan, W. P., Harrison, P. J., Denman, K. L., 1991. Diel periodicity of nitrogen uptake by marine phytoplankton in nitrate-rich environments. *Limnology and Oceanography* 36, 1689–1700.

Dorman, C. E., Winant, C. D., 2000. The structure and variability of the marine atmosphere around the Santa Barbara Channel. *Monthly Weather Review* 128, 261-282. https://doi.org/10.1175/1520-0493%282000%29128<0261%3ATSAVOT>2.0.CO%3B2

Dortch, Q., 1990. The interaction between ammonium and nitrate uptake in phytoplankton. *Marine Ecology Progress Series* 61, 183–201. https://doi.org/10.3354/meps061183

Dugan, J. E., Hubbard, D. M., Page, H. M., Schimel, J. P., 2011. Marine macrophyte wrack inputs and dissolved nutrients in beach sands. *Estuaries and Coasts* 34, 839–850. https://doi.org/10.1007/s12237-011-9375-9

Fewings, M. R., Washburn, L., Ohlmann, J. C., 2015. Coastal water circulation patterns around the Northern Channel Islands and Point Conception, California. P*rogress in Oceanography* 138, 283–304. https://doi.org/10.1016/j.pocean.2015.10.001

Fram, J. P., Stewart, H. L., Brzezinski, M. A., Gaylord, B., Reed, D. C., Williams, S. L., MacIntyre, S., 2008. Physical pathways and utilization of nitrate supply to the giant kelp, Macrocystis pyrifera. *Limnology and Oceanography* 53, 1589. https://doi.org/10.4319/lo.2008.53.4.1589

Glibert, P. M., Goldman, J. C., Carpenter, E. J., 1982a. Seasonal variations in the utilization of ammonium and nitrate by photoplankton in Vineyard Sound, Massachusetts, USA. *Marine Biology* 70, 237–249.

Glibert, P. M., Lipschultz, F., McCarthy, J. J., Altabet, M. A., 1982b. Isotope dilution models of uptake and remineralization of ammonium by marine plankton. *Limnology and Oceanography* 27, 639–650.

Glibert, P. M., Wilkerson, F. P., Dugdale, R. C., Raven, J. A., Dupont, C. L., Leavitt, P. R., Parker, A. E., Burkholder, J. M., Kana, T. M., 2016. Pluses and minuses of ammonium and nitrate uptake and assimilation by phytoplankton and implications for productivity and community composition, with emphasis on nitrogen-enriched conditions. *Limnology and Oceanography* 61, 165–197. https://doi.org/10.1002/lno.10203

Goodman, J., Brzezinski, M. A., Halewood, E. R., Carlson, C. A., 2012. Sources of phytoplankton to the inner continental shelf in the Santa Barbara Channel inferred from cross-shelf gradients in biological, physical and chemical parameters. *Continental Shelf Research* 48, 27–39. https://doi.org/10.1016/j.csr.2012.08.011

Goodridge, B. M., Melack, J. M., 2014. Temporal evolution and variability of dissolved inorganic nitrogen in beach pore water revealed using radon residence times. *Environmental Science & Technology* 48, 14211–14218. https://doi.org/10.1021/es504017j

Hammer, R. M., 1981. Day-night differences in the emergence of demersal zooplankton from a sand substrate in a kelp forest. *Marine Biology* 62, 275–280.

Harms, S., Winant, C. D., 1998. Characteristic patterns of the circulation in the Santa Barbara Channel. *Journal of Geophysical Research: Oceans* 103, 3041–3065. https://doi.org/10.1029/97JC02393

Harris, R. P., Malej, A., 1986. Diel patterns of ammonium excretion and grazing rhythms in Calanus helgolandicus in surface stratified waters. *Marine Ecology Progress Series* 31, 75–85.

Holmes, R. M., Aminot, A., Kérouel, R., Hooker, B. A., Peterson, B. J., 1999. A simple and precise method for measuring ammonium in marine and freshwater ecosystems. *Canadian Journal of Fisheries and Aquatic Sciences* 56, 1801–1808.

Jawed, M., 1973. Ammonia excretion by zooplankton and its significance to primary productivity during summer. *Marine Biology* 23, 115–120.

Lowman, H. E., Emery, K. A., Kubler-Dudgeon, L., Dugan, J. E., Melack, J. M., 2019. Contribution of macroalgal wrack consumers to dissolved inorganic nitrogen concentrations in intertidal pore waters of sandy beaches. *Estuarine, Coastal and Shelf Science* 219, 363-371. https://doi.org/10.1016/j.ecss.2019.02.004

McPhee-Shaw, E. E., Siegel, D. A., Washburn, L., Brzezinski, M. A., Jones, J. L., Leydecker, A., Melack, J., 2007. Mechanisms for nutrient delivery to the inner shelf: Observations from the Santa Barbara Channel. *Limnology and Oceanography* 52, 1748–1766. https://doi.org/10.4319/lo.2007.52.5.1748

Miller, R. J., Lafferty, K. D., Lamy, T., Kui, L., Rassweiler, A., Reed, D. C., 2018. Giant kelp, Macrocystis pyrifera, increases faunal diversity through physical engineering. *Proceedings of the Royal Society B* 285, 20172571. https://doi.org/10.1098/rspb.2017.2571

Mopper, K., Lindroth, P., 1982. Diel and depth variations in dissolved free amino acids and ammonium in the Baltic Sea determined by shipboard HPLC analysis. *Limnology and Oceanography* 27, 336–347.

Nash, J., Shroyer, E., Kelly, S., Inall, M., Duda, T., Levine, M., Jones, N., Musgrave, R., 2012. Are any coastal internal tides predictable? *Oceanography* 25, 80–95. https://doi.org/10.5670/oceanog.2012.44

National Oceanographic and Atmospheric Administration, 2020. Tides & Currents: Station ID 9411340.

NOAA National Centers for Environmental Information, 2020. NOAA National Centers for Environmental Information (2001): Global Surface Hourly DS3505.

Noble, M., Jones, B., Hamilton, P., Xu, J., Robertson, G., Rosenfeld, L., Largier, J., 2009. Cross-shelf transport into nearshore waters due to shoaling internal tides in San Pedro Bay, CA. *Continental Shelf Research* 29, 1768–1785. https://doi.org/10.1016/j.csr.2009.04.008

Raven, J. A., 1980. Nutrient transport in microalgae. *Advances in Microbiological Physiology* 21, 47–226.

Reed, D. C., Carlson, C. A., Halewood, E. R., Nelson, J. C., Harrer, S. L., Rassweiler, A., Miller, R. J., 2015. Patterns and controls of reef-scale production of dissolved organic carbon by giant kelp Macrocystis pyrifera. *Limnology and Oceanography* 60, 1996–2008. https://doi.org/10.1002/lno.10154

Smith, J. M., Reed, D. C., Melack, J. M., 2018. SBC LTER: OCEAN: Sediment porewater ammonium and urea concentrations. *Environmental Data Initiative*. https://doi.org/10.6073/pasta/deb7e37cb76c0da76de533dc64c5e383

Smith, R. C., Baker, K. S., Dustan, P., 1981. *Fluorometric techniques for the measurement of oceanic chlorophyll in the support of remote sensing*. Scripps Institution of Oceanography, University of California, San Diego.

Strickland, J. D. H., Parsons, T. R., 1968. *A Practical Handbook of Seawater Analysis*. Fisheries Research Board of Canada, Ottawa.

Swarzenski, P. W., Izbicki, J. A., 2009. Coastal groundwater dynamics off Santa Barbara, California: Combining geochemical tracers, electromagnetic seepmeters, and electrical resistivity. *Estuarine, Coastal and Shelf Science* 83, 77–89. https://doi.org/10.1016/j.ecss.2009.03.027

Syrett, P. J., 1981. Nitrogen metabolism of microalgae. *Canadian Bulletin of Fisheries and Aquatic Sciences* 210, 182–210.

Taylor, B. W., Keep, C. F., Hall Jr, R. O., Koch, B. J., Tronstad, L. M., Flecker, A. S., Ulseth, A. J., 2007. Improving the fluorometric ammonium method: matrix effects, background fluorescence, and standard additions. *Journal of the North American Benthological Society* 26, 167–177. https://doi.org/ 10.1899/0887-3593(2007)26[167:ITFAMM]2.0.CO;2

Walter, R. K., Reid, E. C., Davis, K. A., Armenta, K. J., Merhoff, K., Nidzieko, N. J., 2017. Local diurnal wind-driven variability and upwelling in a small coastal embayment. *Journal of Geophysical Research Oceans* 122, 955–972. https://doi.org/10.1002/2016JC012466

Ward, B., Bronk, D., 2001. Net nitrogen uptake and DON release in surface waters: importance of trophic interactions implied from size fractionation experiments. *Marine Ecology Progress Series* 219, 11–24. https://doi.org/10.3354/meps219011

Washburn, L., Brzezinski, M. A., Carlson, C. A., Siegel, D. A., 2019. SBC LTER: Ocean: Ocean currents and biogeochemistry: Nearshore water profiles (monthly CTD and chemistry). Santa Barbara Coastal Long Term Ecological Research Project, *Environmental Data Initiative*. https://doi.org/10.6073/pasta/b73d76d8d1465207be6d7fed19291fda

Wheeler, P. A., Kirchman, D. L., Landry, M. R., Kokkinakis, S. A., 1989. Diel periodicity in ammonium uptake and regeneration in the oceanic subarctic Pacific: Implications for interactions in microbial food webs. *Limnology and Oceanography* 34, 1025–1033.

Wickham, H., Averick, M., Bryan, J., Chang, W., D'Agostino McGowan, L., François, R., Grolemund, G., Hayes, A., Henry, L., Hester, J., Kuhn, M., Lin Pedersen, T., Miller, E., Milton Bache, S., Müller, K., Ooms, J., Robinson, D., Paige Seidel, D., Spinu, V., Takahashi, K., Vaughan, D., Wilke, C., Woo, K., Yutani, H., 2019. Welcome to the Tidyverse. *Journal of Open Source Software* 4, 1686. https://doi.org/10.21105/joss.01686

Zhu, Y., Liu, J., Huang, T., Wang, L., Trull, T. W., Dai, M., 2018. On the fluorometric measurement of ammonium in oligotrophic seawater: Assessment of reagent blanks and interferences. *Limnology and Oceanography Methods* 16, 516–524. https://doi.org/10.1002/lom3.10263

Zimmerman, R. C., Kremer, J. N., 1984. Episodic nutrient supply to a kelp forest ecosystem in Southern California. *Journal of Marine Research* 42, 591–604.

CHAPTER 3:

PERMEABLE MARINE SEDIMENTS SURROUNDING GIANT KELP FORESTS PROVIDE RECYCLED NUTRIENTS TO THE OVERLYING WATER COLUMN

Abstract:

Permeable marine sediments are biogeochemically active environments. This study examined the potential of permeable marine sediment to remineralize organic material and to serve as a source of dissolved inorganic nitrogen to the overlying water column during warm, low-nutrient oceanographic conditions. The results of flow-through bioreactor incubations conducted using sediment from three sites off coastal California over the course of three consecutive summers indicate that the top 2 cm of sediment are capable of supplying the surrounding seawater with 0.47 ± 0.73 mmol NH_4^+ m^{-2} day^{-1}. In contrast, sediment collected from a nearby slough indicates that estuarine sediment is a sink of both NH_4^+ and NO_3^-. Timeseries analyses of sediment porewater temperatures indicate that at 5 cm depth sediment porewater flushes every 10 minutes and at 15 cm depth porewater flushes every 2 hours. These measured rates suggest marine sediment provides a significant source of nitrogen to the water column during summer months in nearshore regions of the Santa Barbara Channel.

Introduction

Permeable marine sediments have been dismissed as sites of significant biogeochemical activity due to their low organic matter content (Boudreau et al., 2001). However, recent work suggests that sandy marine sediment is more biogeochemically active than silts, muds, and other cohesive sediment (Rocha, 2008). Nearshore marine sediment

along the continental shelf is typically coarser than offshore sediment (Huettel et al., 2014), and this slight increase in permeability has an outsized effect on biogeochemical processes (Marchant et al., 2016). Permeable marine sediment is subject to advective flow of porewater (Janssen et al., 2005), which creates heterogeneity of oxygenation and organic material distribution and has a significant, although as yet poorly resolved, connection with sediment meiofauna and microbial communities (Rocha, 2008). Thus, nearshore permeable marine sediments have the potential to remineralize significant quantities of organic matter and contribute nutrients and inorganic carbon to coastal waters (Huettel et al., 2014).

Physical exchange of sediment porewater with overlying waters occurs due to pressure gradients created by currents, tides, or waves in the overlying water column (Janssen et al., 2005). Porewater flushing may lead to changes in temperature, which can enhance or suppress biogeochemical processes (Moriarty et al., 2016; Boynton et al., 2018). Advective flow of porewater also delivers oxygen to greater depths than diffusive processes (Janssen et al., 2005; Woulds et al., 2016). Despite delivery of oxygen within permeable marine sediment, anoxic patches may be present and lead to the occurrence of oxic and anoxic biogeochemical processes within the same region (Cook et al., 2017).

In addition, physical exchange leads to the increased delivery of organic material into sediments (Janssen et al., 2005; Rocha, 2008). Sediment redox structure is a function of both porewater transport and organic matter loading (Falter and Sansone, 2000), and the quantity and quality of organic material influences benthic biogeochemistry and metabolism (Herbert, 1999; Boynton et al., 2018). The cycling of organic material is closely coupled to oxygen availability. With greater organic matter loading and remineralization rates, oxygen concentrations decrease, and the surrounding environment is likely to progress towards

anoxia (Marchant et al., 2016). However, because advective flows can recharge oxygen as well as organic matter, remineralization rates can be up to 25 times greater in oxygenated near-surface sediments than in deeper, anoxic sediment (Laverman et al., 2012).

Nutrient and organic matter fluxes from permeable sediments have been investigated in seagrass beds (Gustafsson and Norkko, 2016), coral reefs (Falter and Sansone, 2000), intertidal sand flats (de Beer et al., 2005), subtidal bays (Berg et al., 2003), and, most commonly, in estuarine (Sumi and Koike, 1990) and nearshore marine (Bonaglia et al., 2017) regions. Others have focused on the impacts of organisms such as plankton (Fernex et al., 1996), worms (Saaltink et al., 2019), and farmed oysters and clams (Smyth et al., 2018) on sediment fluxes. In addition to spatial heterogeneity, seasonal changes in the fluxes of various chemical species from sediment have been recorded (Nielsen et al., 2017; Smyth et al., 2018), which could be due to additional physical forces such as sediment resuspension during storms (Ståhlberg et al., 2006).

Sites in nearshore estuarine and marine environments of the Santa Barbara Channel (SBC) were investigated in this study. In the SBC, higher nitrate concentrations are typically measured in winter and spring due to runoff from storms and upwelling while nitrate concentrations remain below the limit of detection (0.2μM) for much of the summer and into the fall (July – November) (McPhee-Shaw et al., 2007; Brzezinski et al., 2013). Despite the apparent low nitrogen availability during summer, nearshore forests of *Macrocystis pyrifera* (giant kelp) continue to have high rates of net primary production (Brzezinski et al., 2013; Reed et al., 2016). Giant kelp does not have the physiological capacity to store nitrogen reserves for longer than approximately three weeks (Gerard, 1982), so alternative sources of nitrogen are expected to support its growth (Fram et al., 2008). We hypothesize that

permeable marine sediments surrounding giant kelp forests may serve as a source of nitrogen, specifically ammonium, supplementing the lack of nitrate measured in the water column during summer months. Permeable marine sediments have been shown to be a net source of inorganic nitrogen to the overlying water column (Rowe et al., 1975; Kitidis et al., 2017) , and in certain systems, sediments have been demonstrated to supply over 30% of pelagic nitrogen demand (Boynton et al., 2018). Further investigation of ammonium cycling in marine waters is warranted since ammonium is in high demand by both phototrophs, for use in primary production, and by nitrifiers, as the substrate for nitrification (Gustafsson and Norkko, 2016).

To obtain flux measurements and to address the spatial variability inherent in marine sediments, we developed a novel closed-system, flow-through bioreactor to mimic *in situ* conditions (advective flow of porewater and seawater temperature). The bioreactor's recirculating design decreased the chances of establishing microbial or redox gradients within the core (Roychoudhury et al., 1998) and created fewer experimental artifacts than sediment slurries (Pallud et al., 2007) by keeping sediments intact. This study measured dissolved nutrient fluxes from permeable marine sediments surrounding three giant kelp forest sites and one estuarine surf zone site during three consecutive summers in the SBC.

Methods

Site Description

Three kelp forest sites located in the Santa Barbara Channel were included in this study: Arroyo Burro (34° 23.623 N, 119° 44.608 W), Goleta Bay (34° 24.175 N, 119° 49.450 W), and Mission Creek (34° 23.821 N, 119° 40.185 W). These sites are routinely sampled as

part of the Santa Barbara Coastal Long Term Ecological Research (SBC LTER) program for dissolved and particulate constituents and giant kelp net primary production (Reed, 2018; Washburn et al., 2019). Average sediment depth at these sites ranges from 1 – 10 m, with several patches of exposed bedrock along the coast (Sommerfield et al., 2009). One additional estuarine site was sampled (Goleta Slough - 34° 25.047 N, 119° 49.628 W) to serve as a contrasting environment. This site is located approximately 1.5 km due north of the Goleta Bay site (Page et al., 2018).

Oceanographic conditions in the SBC have three seasons: seasonal upwelling of cold, nutrient rich water in spring (April – June), warm, stratified water in summer and fall (July – November), and episodic runoff from streams during winter storms (December – March) (Brzezinski et al., 2013). Sampling for this study was done during the warm, stratified summer period at both kelp forest and estuarine sites. Nearshore cross-shelf currents along the benthos average approximately 0.01 to 0.02 m s^{-1} with flow offshore (southward) (Fewings et al., 2015). The summer wave base in the SBC, i.e., the depth to which marine sediment may be disturbed or resuspended due to waves, is up to 20 m (Sommerfield et al., 2009).

Porewater Nutrient Concentrations and Temperature

Prior to core incubations, information regarding *in situ* conditions was collected to aid design and operation of bioreactors. In June 2016, three replicate sediment cores (5 cm diameter x 20 cm long) were collected by SCUBA divers using hand corers at three kelp forest sites (Arroyo Burro - 34° 23.791 N, 119° 44.609 W, Mission Creek - 34° 24.454 N, 119° 40.794 W, Refugio - 34° 27.432 N, 120° 04.200 W) at 15 m depth. In August 2016, additional sediment cores, three replicates per location, were collected at a single kelp forest

site (Mohawk Reef - 34° 23.251 N, 119° 43.685 W) at 5, 7, 10, 15, and 20 m depths. At each of these sampling locations, water samples from the overlying water column were also collected by SCUBA divers using syringes; three samples were collected at each location: one at ~1 m, one in the middle of the water column, and one ~50 cm above the sediment surface. Water samples were filtered through GF/F filters (0.7 µm, Whatman) aboard the boat and were transported in ice-filled coolers. Upon return to shore, sediment cores were immediately sectioned into approximately 2 cm intervals. Each core section was then homogenized, and 15 to 30 g of sediment from each section was placed in a finely perforated scintillation vial fitted into a larger plastic centrifuge tube. All samples were centrifuged at 5000 rpm for 5 minutes, and the resulting porewater collected in the tubes was filtered through GF/C filters (1.2 µm, Whatman) and stored frozen (-20°C). Water and porewater samples were analyzed for ammonium (NH_4^+) using the *ortho*-phthaldialdehyde method (Holmes et al., 1999) and a Turner Trilogy Laboratory Fluorometer (limit of detection, 0.05 µM). Standard curves were created using artificial seawater.

During the summer of 2016, an array of temperature loggers (Tidbit, Onset Computer Corporation, Bourne, MA; precision = 0.2°C) was also deployed at the Mohawk site. Six loggers were attached to a fiberglass pole using stainless steel screws and covered with anti-fouling tape. The array was deployed on August 8 by a team of SCUBA divers. It was buried in the sediment with loggers positioned at 5, 15, and 30 cm sediment depth as well as 50 cm above the seafloor. The full array recovered on September 1.

Sample Collection

Sediment cores and seawater were collected from each of the four sites in August of 2017, 2018, and 2019. At the Goleta Slough estuarine site, four replicate sediment cores (5

cm diameter x 20 cm long) were collected using hand corers by wading into the water where the surf zone met the mouth of the slough; water was collected from the surf zone along the beach just offshore of the mouth of Goleta Slough. At all three kelp forest sites, four replicate sediment cores (5 cm diameter x 20 cm long) at 20 m were collected by SCUBA divers using hand corers; water was also collected by divers from approximately 1 m above the benthos. All samples were transported in ice-filled coolers to the laboratory. Sediment cores were stored overnight (20 h maximum) with the top section exposed in a flow-through seawater tank to maintain oxygenation and *in situ* temperatures. Seawater remained unfiltered and was stored overnight in a 4°C cold room.

Bioreactor Design and Use

For the experiments in August 2017, a series of five hand-cut acrylic bioreactors were used to conduct the sediment efflux measurements. Each bioreactor housed one sediment core sample and was designed to connect to a seawater reservoir via peristaltic pump to allow water to be pumped through the core in a recirculating, closed-loop fashion. One replicate was used as a control containing only seawater, and the remaining four were used to house the replicate sediment cores. A section of PVC pipe was used as a container for the sediment, fit between the hand-cut acrylic end-pieces. End pieces were sealed against the pipe containing the core by pulling the two end caps together using zip ties fit through all four corners of the bioreactor apparatus. In 2018, eight acrylic bioreactors were manufactured using a Trotec Speedy 300 Laser Engraver (80W), which allowed for greater precision and replication of the flow-through design. The new bioreactors allowed for silicone bands to connect the PVC pipe containing the sediment core to each acrylic end-piece, creating an

even seal (*Figure 1*). For the trials in August 2018 and 2019, four replicates were run for both control and experimental bioreactors.

Bioreactors were assembled with a combusted GF/B filter on the bottom end piece (with the perforated patterning) of each setup to prevent sediment from eroding into the reservoirs and clogging the tubing. Sediment cores were removed from the seawater tank, overlying water was siphoned off, and the top 2 cm of each replicate core was extruded, sectioned, and placed in a bioreactor. Seawater accompanying the sediment samples was removed from the cold room, mixed thoroughly, and measured with a thermometer. Samples were warmed to the appropriate temperature prior to use. All bioreactors were assembled by placing the top acrylic section (with the snowflake-patterned channels) over the core and sealed, taking care not to compress or shear the surface of the core. Control bioreactors were assembled in the same fashion, but without sediment. All replicates were attached to a series of peristaltic pumps using PTFE tubing, and unfiltered seawater was flushed through the bioreactors for 1 hour at a rate of approximately 5.5 mL minute^{-1}. Each setup was allowed to drip freely during this period to allow existing porewater to be flushed out. Flushing time was determined by breakthrough curve analyses examining how much time was required for estuarine and kelp forest sediment porewater nutrient concentrations to match inflow conditions.

Bioreactor Incubations

After flushing for 1 hour, each bioreactor was attached to a new reservoir of unfiltered seawater, which was held in a 15°C water bath, and the entire setup was run in a recirculating fashion via a closed system for 3 hours at the same rate as the initial flushing. At the conclusion of each trial, the seawater reservoirs were sealed and assembled for

dissolved nutrient analyses, and each sediment core was kept for additional meiofaunal and organic matter analyses.

A set of control incubations containing no sediment was paired with each run to account for microbial activity in the water column (Boynton et al., 2018). Sediment cores placed in each of the experimental incubations were sectioned at 2 cm to reduce the formation of unnatural flow paths or channels that others have found using bromide breakthrough curves in longer cores (Roychoudhury et al., 1998). No terminal electron acceptors were added so as not to influence biogeochemical processes. Cores were processed within 20 hours of collection. Cores were run for a maximum of 3 h to maintain oxygenation; a series of experiments confirmed that oxygen concentrations were not significantly depleted during this time.

Water samples were filtered through GF/F filters (0.7 μm, Whatman) prior to analyses of dissolved nutrients. Standard curves were made with low nutrient seawater that had previously been collected from the Santa Barbara Channel and incubated for over 6 months. Samples were analyzed for NH_4^+ using the *ortho*-phthaldialdehyde method and a Turner Trilogy Laboratory Fluorometer (limit of detection, 0.05 μM). A subset of filtered seawater reservoir samples were stored frozen (-20°C) and analyzed for combined nitrate (NO_3^-) and nitrite (NO_2^-) via flow injection analysis on a Lachat QuickChem 8500 Series 2 Analyzer (Hach Company, limit of detection, 0.50 μM for 2017 samples and 0.20 μM for 2018-2019 samples). Another subset of the filtered water samples was acidified using 4N HCl, refrigerated (4°C), and analyzed for dissolved organic carbon (DOC, limit of detection, 25 μM, precision, 1-2 μM) and total dissolved nitrogen (TDN, limit of detection, 2 μM, precision, 1-2 μM) performed via high temperature combustion on a Shimadzu TOC-V

Analyzer. TDN is interpreted as a combination of dissolved inorganic nitrogen (NH_4^+, NO_3^-, NO_2^-) and the numerous compounds considered dissolved organic nitrogen (DON).

In August 2017, two cores from each site sampled were analyzed for water and organic matter content after the conclusion of each experiment. Approximately 20 grams of thawed sediment was dried at 60°C for 48 hours and re-weighed to determine water content. These same samples were then combusted at 450°C for 4 hours and re-weighed to determine organic matter content. In August 2018 and 2019, two sediment cores from each site sampled were sifted through a 1 mm sieve, and live organisms were counted the same day and, when possible, identified to family.

Data Analyses

Data organization and analyses were performed using Excel (v 16.24) and R Statistical Software (v 3.4.3). Cross-covariance analyses were performed using the ccf() function. Data formatting and visualization were performed using the *tidyverse* in RStudio 2 (Wickham, 2019). Values reported following a "±" symbol denote standard deviation, unless otherwise stated.

Net fluxes reported below refer to the fluxes generated by the sediment alone. To calculate net fluxes from the sediments examined in this study, we first calculated the change in nutrient concentrations (μM) between starting and concluding concentrations measured in the seawater reservoirs (*Equation 1*).

$$[NH_4^+]_{AFTER} - [NH_4^+]_{BEFORE} = \Delta [NH_4^+] \quad (1)$$

These values were then converted to rates (μM hr^{-1}) by dividing by the length of the experiment (3 hr). For each bioreactor experiment conducted, we calculated the mean rates of change by control (seawater) and experimental (sediment core) treatments (*Equation 2*), with the number of successful replicates of each treatment denoted by "n".

$$\frac{\Sigma\, \Delta\, [NH_4^+]_{CONTROL}}{n} = \bar{x}_{CONTROL} \pm \sigma \qquad (2)$$

The net change in concentration from sediment alone was then determined by subtracting mean rates of change of control incubations from mean rates of change of experimental treatments (*Equations 3 and 4*). Standard deviations of net changes in concentration were also determined by summing standard deviations of both treatments and then taking the square root.

$$\bar{X}_{EXPERIMENTAL} - \bar{x}_{CONTROL} = \bar{x}_{NET} \qquad (3)$$

$$\sqrt{(\sigma^2_{EXPERIMENTAL} + \sigma^2_{CONTROL})} = \sigma_{NET} \qquad (4)$$

Net changes in nutrient concentrations were scaled up to a larger surface area of benthos (m^2) and converted to net nutrient fluxes (μmol m^{-2} hr^{-1}) (*Equation 5*) by multiplying by the volume of the seawater reservoirs used (250 mL) and the surface area of the sediment core (19.6 cm^2). The same conversions were applied to standard deviation values.

$$\bar{x}_{NET} \times 0.25\ L \times 19.6\ cm^{-2} \times \frac{10{,}000\ cm^2}{1\ m^2} = \bar{x}_{NET} \qquad (5)$$

We use ammonium (NH_4^+) in the equations above, but all nutrient effluxes were calculated the same way.

Results

Sediment Porewater Ammonium Concentrations

Porewater ammonium (NH_4^+) concentrations measured in sediments near kelp forests during summer 2016 ranged from 1.59 to 96.99 µM, and the mean porewater NH_4^+ concentration across all sites and water and sediment depths sampled was 43.13 ± 19.79 µM (*Table 1*). NH_4^+ concentrations in sediment porewaters did not increase with sediment depth, except at Arroyo Burro Reef at 15 m water depth and Mohawk Reef at 20 m water depth. Seawater NH_4^+ concentrations ranged from 0.05 to 0.98 µM, and the mean water column NH_4^+ concentration at all sites and water depths sampled was 0.30 ± 0.29 µM (*Table 2*). At several sites, NH_4^+ concentrations were at the limit of detection (0.05 µM) in surface waters. The mean NH_4^+ concentrations for surface, midway, and bottom water depths were 0.11 ± 0.09 µM, 0.21 ± 0.19 µM, and 0.59 ± 0.28 µM, respectively. At all sites sampled, NH_4^+ concentrations in water near the bottom were greater than both surface and midway concentrations in all but one location (Mohawk, 5 m).

Sediment Porewater Temperatures

Between August 10 and September 1, 2016, temperatures measured in the sediment ranged from 13.6 to 19.7°C, and water temperatures measured 50 cm about the sediment ranged from 13.3 to 20.0°C (Figure 2). Temperatures in the water column and in the upper 5 cm of the sediments varied over approximately tidal cycles with maxima and minima in water temperatures only slightly more than changes in the upper 5 cm of sediments. In

contrast, those at 15 cm fluctuated but over a smaller range and the changes at 30 cm were minor. These differences indicate rapid flushing of the upper 5 cm of sediments and a lagged response below. We determined the lag by computing the cross-covariance between each sediment temperature logger (n = 3) and the overlying water column for the 22-day dataset. The values at which the cross-covariance values are greatest indicate the timestep, or lag, at which there is the strongest correlation between the two time-series. Temperatures at 5 cm depth in the sediment had the strongest correlation with overlying water temperature changes (i.e., the highest cross-covariance value) and the shortest lag (10 minutes). At 15 cm sediment depth, the lag was 100 minutes or approximately 2 hours. At 30 cm sediment depth, the lag was 1,845 minutes or approximately 31 hours. Thus, the top 5 cm of sediment flushes approximately 144 times daily, the porewater to 15 cm sediment depth flushes approximately 12 times daily, and the porewater to 30 cm sediment depth flushes approximately once a day.

Sediment Porosity and Organic Matter Content

Mean porosity of kelp forest sediment cores was 29% ± 3.4%, and porosity of estuarine cores was approximately 23% ± 2.5%. Mean organic matter content of kelp forest sediment cores was 1.4% ± 0.4%, and mean organic matter content of estuarine cores was 0.6% ± 0.1%.

Seawater Nutrient Fluxes

Each trial included a series of replicates containing only unfiltered seawater; these control treatments were intended to measure microbial activity within the water column so that net nutrient fluxes from the sediment core incubations could be calculated. Previous studies have found this correction to be minimal, so net fluxes rather than separate control and sediment results are typically presented (Boynton et al., 2018). For all dissolved nitrogen

species, our results suggested little change in concentrations in the control incubations. In particular, there was no measurable difference in dissolved inorganic nitrogen (DIN) concentrations. However, we were able to detect variability in dissolved organic carbon (DOC) concentrations, which we suggest was due to higher DOC concentrations than DIN concentrations.

Dissolved Organic Carbon Fluxes

Dissolved organic carbon (DOC) concentrations in the seawater near the kelp forests used for the bioreactor experiments ranged from 67 – 99 μM. Brackish water DOC concentrations ranged from 92 – 239 μM. Including all years and sites sampled, the mean net DOC flux from marine sediment was 617 ± 617 μmol m^{-2} $hour^{-1}$ (15 ± 15 mmol m^{-2} day^{-1}). The mean net flux from estuarine surf zone sediment was -896 ± 556 μmol m^{-2} $hour^{-1}$ (-21 ± 13 mmol m^{-2} day^{-1}) (Figure 3). All samples analyzed for DOC were above the limit of detection (25 μM). The acrylic sheets used to manufacture the bioreactors may have contributed a small amount of DOC to our samples, but to decrease the potential for leaching, each end piece was soaked in deionized water prior to its first use and rinsed in deionized water before and after each subsequent use.

Dissolved Nitrogen Fluxes

Samples were not assayed for total dissolved nitrogen (TDN) in 2017. In 2018 and 2019, TDN concentrations in the seawater used for the bioreactor experiments ranged from 5 to 7 μM. Brackish water TDN concentrations ranged from 6 to 12 μM. Including both years and all sites sampled, the mean net TDN flux from kelp forest sediment was 78 ± 52 μmol m^{-2} $hour^{-1}$ (1.9 ± 1.3 mmol m^{-2} day^{-1}), and the mean net flux from estuarine surf zone sediment

was -65 ± 85 μmol m^{-2} $hour^{-1}$ (-1.6 ± 2.1 mmol m^{-2} day^{-1}) (Figure 3). All samples measured for TDN were above the limit of detection (2 μM).

Ammonium (NH_4^+) effluxes measured in bioreactors containing sediment collected near giant kelp forests were an order of magnitude greater than from bioreactors containing only unfiltered seawater collected at the same sites. NH_4^+ concentrations in the seawater used for the bioreactor experiments ranged from 0.06 to 0.91 μM. Brackish water NH_4^+ concentrations ranged from 0.06 to 2.48 μM. Across all years and sites sampled, the mean net flux of NH_4^+ from kelp forest sediment was 20 ± 30 μmol m^{-2} $hour^{-1}$ (0.47 ± 0.73 mmol m^{-2} day^{-1}), and the mean net flux from estuarine surf zone sediment was -28 ± 62 μmol m^{-2} $hour^{-1}$ (-0.68 ± 1.5 mmol m^{-2} day^{-1}) (Figure 3). All samples measured for NH_4^+ were above the limit of detection (0.05 μM).

Measurements of nitrate concentrations included both nitrate and nitrite and will be referred to jointly as "nitrate". Nitrate concentrations in the kelp forest seawater used for the bioreactor experiments ranged from 0.2 to 1.3 μM and brackish water concentrations ranged from 0.2 to 0.6 μM. Kelp forest sediments across all sites and years sampled had a mean net NO_3^- flux of 3.7 ± 22 μmol m^{-2} $hour^{-1}$, and estuarine surf zone sediments had a mean net NO_3^- flux of 5.5 ± 7.0 μmol m^{-2} $hour^{-1}$ (Figure 3). On a daily basis, the mean net NO_3^- flux from kelp forest and estuarine surf zone sediment cores is approximately 0.09 ± 0.52 mmol m^{-2} day^{-1} and 0.13 ± 0.17 mmol m^{-2} day^{-1}, respectively. Approximately 30% of the samples (n = 31) analyzed for NO_3^- concentrations were below the limit of detection (0.20 μM).

Since over a third of the samples analyzed for nitrate (NO_3^-) fell below the limit of detection, precise rates of NO_3^- production and consumption should be interpreted with caution. Due to the variability in NO_3^- effluxes and analytical constraints, the remainder of

the discussion concerning dissolved inorganic nitrogen fluxes will focus instead on NH_4^+ effluxes from the kelp forest sediment cores, which were well above the method's limit of detection (0.05 μM) and are often used as a proxy for organic matter remineralization (Laverman et al., 2012).

Subtracting NH_4^+ and NO_3^- from TDN measurements provides an estimate of dissolved organic nitrogen (DON) fluxes. We calculated DON fluxes from kelp forest sediment cores to be approximately 1.3 ± 0.5 mmol m^{-2} day^{-1} from the top 2 cm sediment horizon.

Sediment Meiofauna

Sediment cores were not analyzed for meiofauna in 2017. Sediment cores collected in 2018 and 2019 from Goleta Slough contained no meiofauna larger than 1mm. Each of the two cores analyzed from Arroyo Burro, Goleta Beach, and Mission Creek in 2018 and 2019 contained approximately 9 ± 3 organisms (>1 mm) per core. Tube-building polychaetes, in Spionidae, Pectinariidae, and Sabellidae families, and other polychaetes in the Terebellidae and Nereididae families were most common. Burrowing mollusks in the Fustiariidae family were also common. Upon inspection under a microscope (10x magnification), all of the organisms appeared intact, which suggests they resided in the top 2 cm horizon of the sediment sampled. Changes to sediment redox state due to bioturbation, such as alternating darker and lighter regions indicative of sulfate reduction and oxygenation, respectively, were not visible, but multiple faunal tubes and burrows were visible in each core. Some burrows were visible during core sectioning, but did not contain meiofauna upon inspection following the incubations; this suggests certain organisms may have burrowed during sample processing and decreased counts.

Discussion

Our efflux measurements suggest that permeable sediments surrounding giant kelp forests contribute a significant quantity of nutrients to the overlying water column and may help to offset the nitrogen deficit giant kelp and other primary producers face during summer. The uncertainty associated with these measurements is to be expected due to the heterogeneity of organic material and microbial assemblages in marine sediment. The results indicate that permeable marine sediments near kelp forests receive sufficient organic matter that is remineralized by faunal communities and released into the overlying water as appreciable fluxes of DOC, DON, and NH_4^+.

Studies of marine sediments have usually used benthic chambers deployed *in situ* or sediment core incubations, with samples collected from the overlying water in both designs. A few studies have used eddy-correlation techniques (Huettel et al., 2014). Considering the inherent heterogeneity, both spatial and temporal, of permeable sediments, these approaches possess drawbacks. Benthic chamber deployments and full core incubations may not reproduce advective flow of porewater (Rao et al., 2007) and underestimate the effects of bioturbation (Berg et al., 2003), two conditions that control diagenetic processes (Huettel et al., 2014). Eddy correlation approaches require significant instrumentation, have a small footprint, and may be limited in scope due to cost and replication constraints (Berg et al., 2003). Information regarding temporal trends is also lacking; to date, only 17% of studies examining fluxes along the sediment-water interface have collected samples for three years or more (Boynton et al., 2018).

Nutrient concentrations and calculated fluxes from our bioreactor experiments were comparable to published values (*Table 3*). These results imply that this bioreactor design can be used to approximate *in situ* conditions and measure nutrient effluxes from marine sediments. Mean DOC efflux measured from permeable sediments surrounding kelp forests was two orders of magnitude greater than the mean DOC flux for coastal (17 m) bay sediments from Buzzards Bay, Massachusetts (Burdige et al., 1992) and an order of magnitude greater than DOC fluxes measured in continental margin sediment (99 m) in Monterey Bay, California (Burdige et al., 1999). In addition, seawater collected from near kelp forests had high DOC concentrations (67 - 239 μM), and these concentrations are consistent with past work in the SBC that found organic matter is partitioned mainly in the dissolved phase during the stratified, summer months (Halewood et al., 2012). Furthermore, our measured rates of NH_4^+ efflux from sediments collected near giant kelp forests are a similar order of magnitude to fluxes reported in studies using *in situ* chambers, batch incubations, and flow-through cores. The mean NH_4^+ flux from SBC sediments was on the lower end of most published estuarine and marine sediment NH_4^+ fluxes (*Table 3,* Boynton et al., 2018). NO_3^- and DON flux rates from SBC sediment cores were similar to published results from coastal marine sediment core incubations (*Table 3*).

The DOC and DON fluxes from estuarine surf zone and sediments near kelp forests differed considerably. During all but one trial (Goleta Bay 2017), sediments collected near kelp forests were net sources of both DOC and DON. However, estuarine surf zone sediments were a net sink of both DOC and DON. This difference is likely due to organic matter supply, meiofaunal density, and microbial nutrient uptake. Sediment collected near kelp forests contained approximately double the amount of organic material of estuarine surf

zone sediment. The low quantities of organic matter in the estuarine surf zone may be due to reworking and resuspension of sediments by waves and tides, which may also cause the remaining organic material to be more refractory (Wainright and Hopkinson Jr., 1997) and less readily remineralized.

Sediments from near kelp forests were a net source of DOC and NH_4^+ during most times at most sites (*Figure 3*). Burdige et al. (1999) found a positive correlation between benthic DOC fluxes and sediment carbon oxidation rates. This suggests high DOC fluxes from marine sediments in the SBC may be indicative of high organic matter remineralization rates, which are reported to be greatest at water depths of 50 m or less (Huettel et al., 2014). However, the bioreactor data reflect fluxes from only the top 2 cm of sediment, and the data suggest that sediment porewaters flush to depths of 15 cm (*Figure 2*). This is consistent with the findings of Huettel et al. (2014), which suggest the greatest transport of porewater and, therefore, organic material typically occurs in the top 20 cm of permeable marine sediment. Due to this organic matter and oxygen resupply, sediments in this horizon should consistently release both organic and inorganic constituents.

Remineralization rates may vary laterally as well as with depth due to a variety of physical and biological factors (Kitidis et al., 2017). If remineralization rates are assumed to be roughly equivalent throughout the top 15 cm of our sediments, faster flushing rates in surficial sediments would yield lower porewater nutrient concentrations, and slower flushing rates at depth would maintain higher porewater nutrient concentrations. This distribution of nutrients with depth was found in sediment porewater NH_4^+ concentrations at 20 m depth at Mohawk Reef (*Table 1*). However, fast flushing of low nutrient concentrations and slow flushing of high concentrations would yield similar overall fluxes to one another. Provided

the marine sediments examined in this study flushed quickly at the surface, more slowly at depth, and displayed similar rates of remineralization across all depths, results from 2 cm of sediment were extended to 15 cm of sediment by multiplying calculated fluxes by 7.5. Hence, permeable sediments surrounding giant kelp forests are capable of producing 113 ± 113 mmol DOC, 9.8 ± 3.8 mmol DON, and 3.5 ± 5.5 mmol NH_4^+ m^{-2} day^{-1}. These values are greater than published DOC effluxes and comparable to published DON and NH_4^+ effluxes for coastal marine sediments (*Table 3*).

Fluxes from the bioreactors indicated that marine sediments were a net source of NH_4^+, but calculated NH_4^+ production rates were not high enough to explain *in situ* NH_4^+ concentrations. Sediment cores collected during the summer of 2016 had mean NH_4^+ concentrations of 43.1 ± 19.8 μM, but mean NH_4^+ concentrations in the 0-2 cm sediment horizon at 20 m water depth, the same horizon that was used for the bioreactor incubations, were 14.0 ± 7.5 μM. These concentrations are orders of magnitude greater than seawater NH_4^+ concentrations in this study (0.30 ± 0.29 μM) and average NH_4^+ concentrations in the overlying water column (0.5 μM) during the summer season (Brzezinski et al., 2013). Using the measured porosity of the sediment (29%) and the mean net NH_4^+ flux (20 μmol m^{-2} $hour^{-1}$), *in situ* NH_4^+ concentrations measured in the 0-2 cm sediment horizon at 20 m water depth could be renewed in 4 ± 2 hours. This regeneration rate is slower than the calculated flushing rate for this horizon (~6 minutes). Two conditions within the bioreactors may have dampened NH_4^+ production below rates necessary to resupply existing concentrations. First, the seawater reservoir was a closed system and did not supply fresh organic matter. Instead, it resupplied the same substrate for multiple hours, which could lead the organic material within the sediment to become more refractory (Wainright and Hopkinson Jr., 1997) and

cause remineralization rates to decrease. Second, though oxygen concentrations were not depleted over the course of the measurements, they may have dropped below optimal concentrations for the microbial communities that aerobically remineralize organic material within the sediments, again preventing remineralization processes from reaching maximal rates.

Remineralization of organic matter in coastal marine sediments may be dependent on subsidies from nearby ecosystems, including giant kelp forests and beaches. We hypothesize that much of the organic matter in our sediment cores may be in the form of kelp detritus, which is the fate for up to 66% of giant kelp primary production off the coast of California (Krumhansl and Scheibling, 2012). In addition, beach porewater may contribute DOC to nearshore waters and elevate concentrations by 0.4 to 6.6 μM (Goodridge, 2018). Similar to marine sediments, beaches along the California Bight have demonstrated significant remineralization potential, with positive relationships between DON and DIN concentrations of beach porewater and the quantity of macrophyte wrack deposited on the beach (Dugan et al., 2011). The remineralization of giant kelp and the release of DIN is significantly facilitated by beach invertebrates such as talitrid amphipods (Lowman et al., 2019), indicating that kelp detritus is a suitable remineralization substrate for microbial and macrofaunal consumers alike. Although beach porewater DIN concentrations are an order of magnitude greater than SBC sediment porewater concentrations, the average flushing turnover time of these sediments is 4.4 to 6.4 days (Goodridge and Melack, 2014; Lowman et al., 2019), several orders of magnitude slower than the surficial marine sediments discussed in this study.

The release of NH_4^+ from sediment porewater into the overlying water column is mediated by several microbial processes, including ammonification, nitrification, assimilation, and annamox (Bronk and Steinberg, 2008; L'Helguen et al., 2014). NH_4^+ is a byproduct of organic matter remineralization, for which there must be sufficiently high concentrations of organic material and terminal electron acceptors, such as oxygen (Laverman et al., 2012). Frequent flushing of sediment porewater maintains aerobic conditions (Woulds et al., 2016). Remineralization can be further stimulated if the redox boundary oscillates due to advective porewater flow (Rocha, 2008). The remineralized NH_4^+ is a competitive substrate for both microalgae and nitrifiers, who use this reduced form of nitrogen to fuel primary production and produce NO_3^-, respectively (Huettel et al., 2014; Gustafsson and Norkko, 2016). Under anaerobic conditions, NH_4^+ may also be removed through the anaerobic oxidation of ammonium, known as annamox, and oxidized into N_2 (Engström et al., 2005). Most past work examines anaerobic processes, and therefore sediment cores are typically stored for several days prior to use (Roychoudhury et al., 1998; de Beer et al., 2005; Pallud et al., 2007; Rao et al., 2007; Laverman et al., 2012;). However, sediment temperature profiles in nearshore regions of the SBC suggest the top 15 cm layer flushes with the overlying water column (*Figure 2*), which likely oxygenates the sediments enough to prevent significant rates of annamox but allow nitrification to occur (Herbert, 1999). If high rates of nitrification did occur in our bioreactor incubations, our measured rates of NH_4^+ production may be underestimations. For example, both NO_3^- and NH_4^+ concentrations increased in 7 of the 9 experiments conducted using marine sediment. Some of this increase in NO_3^- concentrations may have been due to nitrification.

Permeable sediments contain microbial communities poised to take advantage of episodic organic matter inputs and rapidly produce inorganic nutrients (Huettel et al., 2014). Woulds et al. (2016) found bacterial populations in estuarine sediment with low organic matter content are particularly adept at processing organic carbon inputs. In the surf zone where our estuarine samples were collected, seawater may supply high concentrations of organic material in the form of DOC (121μM) (Goodridge and Melack, 2014) and DON (22.7 – 75.2 μM) (Dugan et al., 2011). Although concentrations of NH_4^+ and NO_3^- in surf zone seawater are reported to be low (<1 μM), DIN concentrations are high (>100 μM) in intertidal sediment porewater (Goodridge and Melack, 2014; Lowman et al., 2019), which is evidence of microbial remineralization in the sediment. Our data support this finding and indicate estuarine surf zone sediments were a net sink of DOC and DON, which suggests microbial communities in this sediment rapidly remineralize organic matter subsidies.

In addition, biogeochemical processes in permeable marine sediment are influenced by meiofaunal communities. Larger fauna may bioturbate, or displace the sediment, and cause bioirrigation by flushing burrows (Schulz and Zabel, 2000). Bioturbation and bioirrigation lead to the transport of organic matter into deeper layers (Berner and Westrich, 1985), maintain concentrations of electron acceptors (Hines and Jones, 1985), and restructure microbial communities (Laverock et al., 2010; Chen et al., 2017). Although processes such as bioturbation and bioirrigation have been shown to dominate in cohesive sediments (Huettel et al., 2014), it is important to consider the effects of meiofauna in permeable sediments also. Meiofaunal burrows can encourage the growth of certain microbial communities through "microbial gardening" (Huettel et al., 2014; Boynton et al., 2018), and their associated microbial communities have been shown to increase rates of ammonium release

(Widdicombe and Needham, 2007) and denitrification (Sciberras et al., 2017). Since estuarine surf zone sediment contained no macrofauna while marine sediments near kelp forests routinely contained 10+ organisms per core, we propose that the greater NH_4^+ effluxes measured from marine sediment may have been due in part to the presence of more macrofauna and the products of their excretion. However, the biogeochemical response of sediments to the presence of meiofauna remains poorly constrained (Rocha, 2008; Boynton et al., 2018). Bacterial activity has been shown to dominate in permeable marine sediments such as the ones considered in this study (Woulds et al., 2016).

Permeable sediments are a source of dissolved inorganic nitrogen in marine environments (Bronk and Steinberg, 2008; Boynton et al., 2018), and approximately 32% of phytoplankton nitrogen demand between latitudes 30 to 59 degrees North is satisfied by sediment-water fluxes of NH_4^+ (Boynton et al., 2018). We suggest that nutrient efflux measured from permeable sediments surrounding giant kelp forests may also be an important source of nutrients for benthic communities. In addition, we propose sediment flux rates are comparable to excretion rates by sessile and mobile benthic invertebrates. A study conducted in the same kelp forest reefs as in this study concluded that invertebrates may contribute 3.5 – 18.3 μmol NH_4^+ m^{-2} hr^{-1} via excretion (Peters et al., 2019). These values, and our calculated sediment efflux of 20 ± 30 μmol NH_4^+ m^{-2} $hour^{-1}$, indicate that excretion and remineralization taking place in permeable sediments may be significant sources of nutrients during the summer. Since water temperatures are highest in summer in the SBC and nutrient fluxes from marine sediment increase with increasing temperatures (Boynton et al., 2018), we propose the flux rates reported in this study are likely near their annual maximum rates. The period during which nutrient concentrations in the SBC are lowest, namely July through

November (McPhee-Shaw et al., 2007; Brzezinski et al., 2013), likely coincides with the period during which sediments possess the greatest potential to serve as a source of recycled nutrients to giant kelp forests and other primary producers.

Tables and Figures

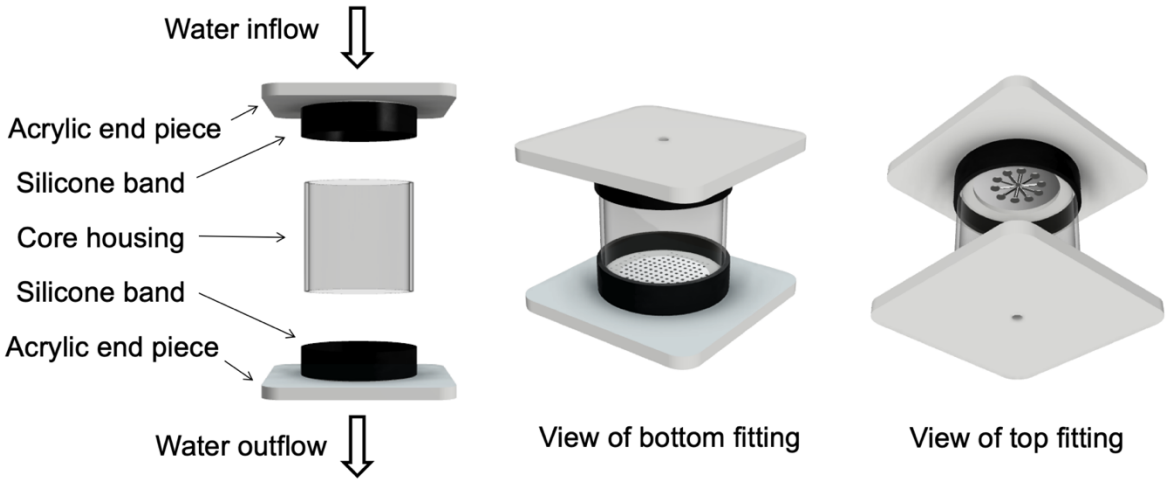

Figure 1: Flow-through sediment bioreactor design manufactured by laser cutting acrylic sheets for experimental runs performed in 2018 and 2019. This entire setup was connected to a seawater reservoir by PTFE tubing and run using a peristaltic pump. Note: Bioreactor housings used in 2017 followed a similar design but were manufactured by hand.

Table 1: Mean porewater ammonium concentrations (μM) with one standard deviation reported in sediment cores collected near kelp forest sites in summer 2016 (Smith et al., 2018a). Sediment depth reported in 2 cm horizons.

Depth	Arroyo Burro	Mission Creek	Refugio	Mohawk				
(cm)	15 m	15 m	15 m	5 m	7 m	10 m	15 m	20 m
0-2	45.16	43.95	61.84	50.89	12.94	33.46	54.65	14.02
	± 18.88	± 22.05	± 26.42	± 11.70	± 2.47	± 5.10	± 20.04	± 7.45
2-4	59.09	66.74	42.60	53.26	20.82	51.42	51.32	19.87
	± 22.59	± 3.23	± 18.34	± 27.76	± 3.27	± 19.47	± 3.97	± 4.21
4-6	65.77	47.13	46.03	49.45	18.32	47.19	53.80	19.57
	± 27.10	± 9.72	± 16.69	± 11.43	± 4.16	± 16.59	± 7.61	± 8.63
6-8	66.17	41.32	53.00	65.99	22.99	54.07	53.54	25.67
	± 26.86	± 15.33	± 24.75	± 6.01	± 0.06	± 31.08	± 4.93	± 4.57
8-10	-	36.49	-	49.62	25.19	28.54	56.53	26.53
		± 10.94		± 20.97	± 6.04	± 25.34	± 4.93	± 13.71
10-15	-	-	-	53.44	19.77	31.44	44.58	34.61
				± 14.66	± 4.49	± 8.41	± 10.83	± 5.68

Table 2: Seawater ammonium concentrations (μM) measured near kelp forest sites in summer 2016 (Smith et al., 2018a). Exact water sampling depth reported in parentheses, and deeper water depths are located further offshore.

	Arroyo Burro	Mission Creek	Refugio	Mohawk				
	15 m	15 m	15 m	5 m	7 m	10 m	15 m	20 m
Surface	0.05 (1)	0.05 (1)	0.09 (1)	0.31 (1)	0.16 (1)	0.06 (1)	0.05 (1)	0.07 (1)
Midway	0.05 (7.5)	0.05 (7.5)	0.05 (7.5)	0.36 (2.5)	0.32 (3.5)	0.57 (5.5)	0.08 (6.5)	0.20 (7.5)
Bottom	0.33 (14.5)	0.98 (14.5)	0.20 (14.5)	0.36 (4.5)	0.57 (6.5)	0.71 (10.5)	0.93 (12.5)	0.65 (14.5)

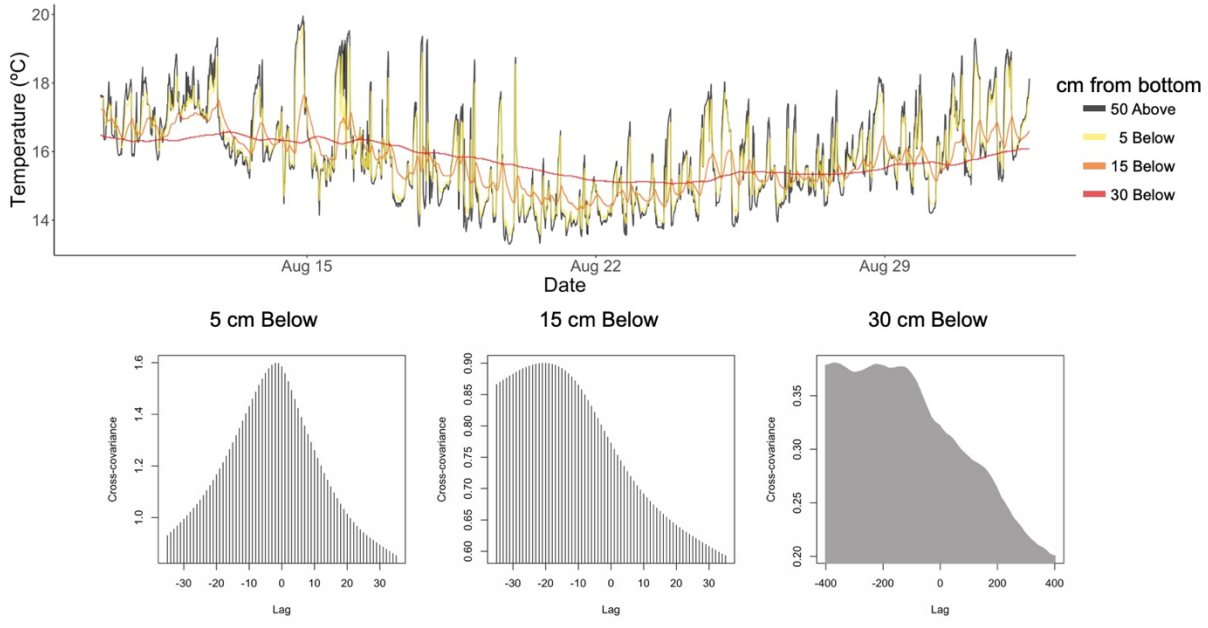

Figure 2: Sediment porewater temperature measured at Mohawk Reef (34° 23.251 N, 119° 43.685 W) using Tidbit temperature loggers in August 2016 (Smith et al., 2018b). The top panel displays the full dataset, while the bottom panels display the cross-covariance between temperature at a given depth in the sediment versus the overlying water columns. Lags are denoted by the time step at which the data was collected (every 5 minutes). Therefore, a lag value of -10 refers to a 50 minute delay. Note, the results of the "30 cm Below" panel appear as a solid fill due to the 800 time steps included, rather than the 70 time steps included in the two previous panels.

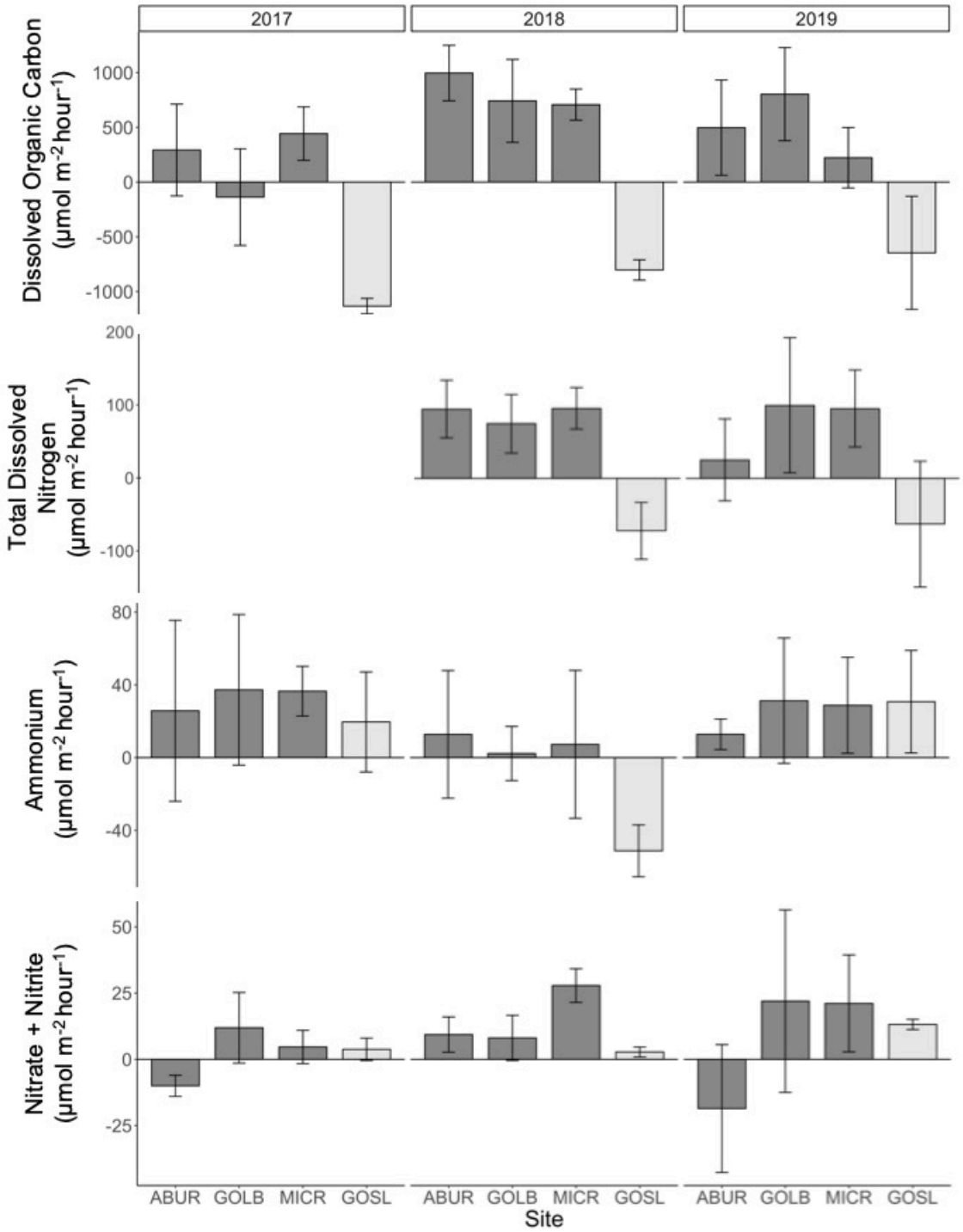

Figure 3: Dissolved nutrient fluxes (µmol m^{-2} hr^{-1}) measured during bioreactor experiments conducted in August 2017-2019. Error bars denote one standard deviation. Sites listed along the x-axis include Arroyo Burro (ABUR), Goleta Bay (GOLB), and Mission Creek (MICR) kelp forest reefs as well as the Goleta Slough (GOSL) estuarine surf zone site.

Table 3: Dissolved nutrient fluxes (mmol N m^{-2} hr^{-1}) measured from coastal marine sediments.

Location	Source	NH_4^+	NO_3^-	DON	DOC
Santa Barbara Channel, CA, USA	*This study* [a]	0.47 ± 0.73	0.09 ± 0.52	1.3 ± 0.5	15 ± 15
Svalbard, Norway	(Blackburn et al., 1996)[a]	0.054 ± 0.493		0.899 ± 3.166	
Buzzards Bay, MA, USA	(Burdige et al., 1992)[b]				0.55 ± 0.25
Monterey Bay, CA, USA	(Burdige et al., 1999)[c]				2.12 ± 1.29
Concepciòn Bay, Chile	(Graco et al., 2001)[a]	12.92 ± 10.10	-1.33 ± 2.10		
Georgia Bight, GA, USA	(Hopkinson, 1987)[a]	1.38	2.62	0.197	
Upwelling region, Chile	(Molina et al., 2004)[a]	1.2 - 5.6	-0.6 - -4.3	4.9 - 75	

[a] Determined by measuring concentration changes in sediment cores.
[b] Determined using porewater concentrations.
[c] Determined using benthic chamber incubations.

References

Berg, P., Røy, H., Janssen, F., Meyer, V., Jørgensen, B. B., Huettel, M., de Beer, D., 2003. Oxygen uptake by aquatic sediments measured with a novel non-invasive eddy-correlation technique. *Marine Ecology Progress Series* 261, 75–83. https://doi.org/10.3354/meps261075

Berner, R. A., Westrich, J. T., 1985. Bioturbation and the early diagenesis of carbon and sulfur. *American Journal of Science* 285, 193–206. https://doi.org/10.2475/ajs.285.3.193

Blackburn, T. H., Hall, P. O. J., Hulth, S., Landen, A., 1996. Organic-N loss by efflux and burial associated with a low efflux of inorganic N and with nitrate assimilation in Arctic sediments (Svalbard, Norway). *Marine Ecology Progress Series* 141, 283–293.

Bonaglia, S., Hylén, A., Rattray, J. E., Kononets, M. Y., Ekeroth, N., Roos, P., Thamdrup, B., Brüchert, V., Hall, P. O. J., 2017. The fate of fixed nitrogen in marine sediments with low organic loading: an in situ study. *Biogeosciences* 14, 285–300. https://doi.org/10.5194/bg-14-285-2017

Boudreau, B. P., Huettel, M., Forster, S., Jahnke, R. A., McLachlan, A., Middelburg, J. J., Nielsen, P., Sansone, F., Taghon, G., Van Raaphorst, W., Webster, I., Weslawski, J. M., Wiberg, P., Sundby, B., 2001. Permeable marine sediments: Overturning an old paradigm. *EOS Transactions American Geophysical Union* 82, 133-136. https://doi.org/10.1029/EO082i011p00133-01

Boynton, W. R., Ceballos, M. A. C., Bailey, E. M., Hodgkins, C. L. S., Humphrey, J. L., Testa, J. M., 2018. Oxygen and nutrient exchanges at the sediment-water interface: A

global synthesis and critique of estuarine and coastal data. *Estuaries and Coasts* 41, 301–333. https://doi.org/10.1007/s12237-017-0275-5

Bronk, D. A., Steinberg, D. K., 2008. Nitrogen regeneration, in: Capone, D.G., Bronk, D.A., Mulholland, M., Carpenter, E.J. (Eds.), *Nitrogen in the Marine Environment*. Academic Press, New York, pp. 385–467.

Brzezinski, M., Reed, D., Harrer, S., Rassweiler, A., Melack, J., Goodridge, B., Dugan, J., 2013. Multiple sources and forms of nitrogen sustain year-round kelp growth on the inner continental shelf of the Santa Barbara Channel. *Oceanography* 26, 114–123. https://doi.org/10.5670/oceanog.2013.53

Burdige, D. J., Alperin, M. J., Homstead, J., Martens, C. S., 1992. The role of benthic fluxes of dissolved organic carbon in oceanic and sedimentary carbon cycling. *Geophysical Research Letters* 19, 1851–1854. https://doi.org/10.1029/92GL02159

Burdige, D. J., Berelson, W. M., Coale, K. H., McManus, J., Johnson, K. S., 1999. Fluxes of dissolved organic carbon from California continental margin sediments. *Geochimica et Cosmochimica Acta* 63, 1507–1515. https://doi.org/10.1016/S0016-7037(99)00066-6

Chen, X., Andersen, T. J., Morono, Y., Inagaki, F., Jørgensen, B. B., Lever, M. A., 2017. Bioturbation as a key driver behind the dominance of Bacteria over Archaea in near-surface sediment. *Scientific Reports* 7, 2400. https://doi.org/10.1038/s41598-017-02295-x

Cook, P. L. M., Kessler, A. J., Eyre, B. D., 2017. Does denitirification occur within porous carbonate sand grains? *Biogeosciences* 14, 4061–4069. https://doi.org/10.5194/bg-14-4061-2017

de Beer, D., Wenzhöfer, F., Ferdelman, T. G., Boehme, S. E., Huettel, M., van Beusekom, J. E., Böttcher, M. E., Musat, N., Dubilier, N., 2005. Transport and mineralization rates in North Sea sandy intertidal sediments, Sylt-Rømø Basin, Wadden Sea. *Limnology and Oceanography* 50, 113–127. https://doi.org/10.4319/lo.2005.50.1.0113

Dugan, J. E., Hubbard, D. M., Page, H. M., Schimel, J. P., 2011. Marine macrophyte wrack inputs and dissolved nutrients in beach sands. *Estuaries and Coasts* 34, 839–850. https://doi.org/10.1007/s12237-011-9375-9

Engström, P., Dalsgaard, T., Hulth, S., Aller, R. C., 2005. Anaerobic ammonium oxidation by nitrite (anammox): Implications for N2 production in coastal marine sediments. *Geochimica et Cosmochimica Acta* 69, 2057–2065. https://doi.org/10.1016/j.gca.2004.09.032

Falter, J. L., Sansone, F. J., 2000. Hydraulic control of pore water geochemistry within the oxic-suboxic zone of a permeable sediment. *Limnology and Oceanography* 45, 550–557. https://doi.org/10.4319/lo.2000.45.3.0550

Fernex, F. E., Braconnot, J.-C., Dallot, S., Boisson, M., 1996. Is ammonification rate in marine sediment related to plankton composition and abundance? A time-series study in Villefranche Bay (NW Mediterranean). *Estuarine, Coastal and Shelf Science* 43, 359–371.

Fewings, M. R., Washburn, L., Ohlmann, J. C., 2015. Coastal water circulation patterns around the Northern Channel Islands and Point Conception, California. *Progress in Oceanography* 138, 283–304. https://doi.org/10.1016/j.pocean.2015.10.001

Fram, J. P., Stewart, H. L., Brzezinski, M. A., Gaylord, B., Reed, D. C., Williams, S. L., MacIntyre, S., 2008. Physical pathways and utilization of nitrate supply to the giant

kelp, Macrocystis pyrifera. *Limnology and Oceanography* 53, 1589-1603. https://doi.org/10.4319/lo.2008.53.4.1589

Gerard, V. A., 1982. Growth and utilization of internal nitrogen reserves by the giant kelp Macrocystis pyrifera in a low-nitrogen environment. *Marine Biology* 66, 27–35.

Goodridge, B., 2018. The influence of submarine groundwater discharge on nearshore marine dissolved organic carbon reactivity, concentration dynamics, and offshore export. *Geochimica et Cosmochimica Acta* 241, 108–119. https://doi.org/10.1016/j.gca.2018.08.040

Goodridge, B. M., Melack, J. M., 2014. Temporal evolution and variability of dissolved inorganic nitrogen in beach pore water revealed using radon residence times. *Environmental Science & Technology* 48, 14211–14218. https://doi.org/10.1021/es504017j

Graco, M., Farias, L., Molina, V., Gutiérres, D., Nielsen, L. P., 2001. Massive developments of microbial mats following phytoplankton blooms in a naturaly eutrophic bay: Implications for nitrogen cycling. *Limnology and Oceanography* 40, 821–832. https://doi.org/10.4319/lo.2001.46.4.0821

Gustafsson, C., Norkko, A., 2016. Not all plants are the same: Exploring metabolism and nitrogen fluxes in a benthic community composed of different aquatic plant species. *Limnology and Oceanography* 61, 1787-1799. https://doi.org/10.1002/lno.10334

Halewood, E., Carlson, C., Brzezinski, M., Reed, D., Goodman, J., 2012. Annual cycle of organic matter partitioning and its availability to bacteria across the Santa Barbara Channel continental shelf. *Aquatic Microbial Ecology* 67, 189–209. https://doi.org/10.3354/ame01586

Herbert, R. A., 1999. Nitrogen cycling in coastal marine ecosystems. *FEMS Microbiology Reviews* 23, 563–590.

Hines, M. E., Jones, G. E., 1985. Microbial biogeochemistry and bioturbation in the sediments of Great Bay, New Hampshire. *Estuarine, Coastal and Shelf Science* 20, 729–742.

Holmes, R. M., Aminot, A., Kérouel, R., Hooker, B. A., Peterson, B. J., 1999. A simple and precise method for measuring ammonium in marine and freshwater ecosystems. *Canadian Journal of Fisheries and Aquatic Sciences* 56, 1801–1808.

Hopkinson, J., 1987. Nutrient regeneration in shallow-water sediments of the estuarine plume region of the nearshore Georgia Bight. *Marine Biology* 94, 127–142.

Huettel, M., Berg, P., Kostka, J. E., 2014. Benthic exchange and biogeochemical cycling in permeable sediments. *Annual Review of Marine Science* 6, 23–51. https://doi.org/10.1146/annurev-marine-051413-012706

Janssen, F., Huettel, M., Witte, U., 2005. Pore-water advection and solute fluxes in permeable marine sediments (II): Benthic respiration at three sandy sites with different permeabilities (German Bight, North Sea). *Limnology and Oceanography* 50, 779–792. https://doi.org/10.4319/lo.2005.50.3.0779

Kitidis, V., Tait, K., Nunes, J., Brown, I., Woodward, E. M. S., Harris, C., Sabadel, A. J. M., Sivyer, D. B., Silburn, B., Kröger, S., 2017. Seasonal benthic nitrogen cycling in a temperate shelf sea: the Celtic Sea. *Biogeochemistry* 135, 103–119. https://doi.org/10.1007/s10533-017-0311-3

Krumhansl, K., Scheibling, R., 2012. Production and fate of kelp detritus. *Marine Ecology Progress Series* 467, 281–302. https://doi.org/10.3354/meps09940

Laverman, A. M., Pallud, C., Abell, J., Cappellen, P. V., 2012. Comparative survey of potential nitrate and sulfate reduction rates in aquatic sediments. *Geochimica et Cosmochimica Acta* 77, 474–488. https://doi.org/10.1016/j.gca.2011.10.033

Laverock, B., Smith, C. J., Tait, K., Osborn, A. M., Widdicombe, S., Gilbert, J. A., 2010. Bioturbating shrimp alter the structure and diversity of bacterial communities in coastal marine sediments. *ISME J* 4, 1531–1544. https://doi.org/10.1038/ismej.2010.86

L'Helguen, S., Chauvaud, L., Cuet, P., Frouin, P., Maguer, J.-F., Clavier, J., 2014. A novel approach using the 15N tracer technique and benthic chambers to determine ammonium fluxes at the sediment–water interface and its application in a back-reef zone on Reunion Island (Indian Ocean). *Journal of Experimental Marine Biology and Ecology* 452, 143–151. https://doi.org/10.1016/j.jembe.2013.12.001

Lowman, H. E., Emery, K. A., Kubler-Dudgeon, L., Dugan, J. E., Melack, J. M., 2019. Contribution of macroalgal wrack consumers to dissolved inorganic nitrogen concentrations in intertidal pore waters of sandy beaches. *Estuarine, Coastal and Shelf Science* 219, 363-371. https://doi.org/10.1016/j.ecss.2019.02.004

Marchant, H. K., Holtappels, M., Lavik, G., Ahmerkamp, S., Winter, C., Kuypers, M. M. M., 2016. Coupled nitrification-denitrification leads to extensive N loss in subtidal permeable sediments. *Limnology and Oceanography* 61, 1033–1048. https://doi.org/10.1002/lno.10271

McPhee-Shaw, E. E., Siegel, D. A., Washburn, L., Brzezinski, M. A., Jones, J. L., Leydecker, A., Melack, J., 2007. Mechanisms for nutrient delivery to the inner shelf:

Observations from the Santa Barbara Channel. *Limnology and Oceanography* 52, 1748–1766. https://doi.org/10.4319/lo.2007.52.5.1748

Molina, V., Farias, L., Graco, M., Rivera, C., Pinto, L., Gallardo, V. A., 2004. Benthic nitrogen renegeration under oxygen and organic matter spatial variability off Concepción (~36°S), central Chile. *Deep Sea Research Part II: Topical Studies in Oceanography* 51, 2507–2522. https://doi.org/10.1016/j.dsr2.2004.08.014

Moriarty, J. M., Harris, C. K., Rabouille, C., Fennel, K., Friedrichs, M. A. M., Xu, K., 2016. The roles of resuspension, diffusion and biogeochemical processes on oxygen dynamics offshore of the Rhone River, France: A numerical modeling study. *Biogeosciences Discussions* 1–39. https://doi.org/10.5194/bg-2016-482

Nielsen, S. L., Risgaard-Petersen, N., Banta, G. T., 2017. Nitrogen retention in coastal marine sediments—a field study of the relative importance of biological and physical removal in a Danish estuary. *Estuaries and Coasts* 40, 1276–1287. https://doi.org/10.1007/s12237-017-0216-3

Page, H. M., Lowman, H. E., Melack, J. M., Smith, J. M., Reed, D. C., 2018. SBC LTER: OCEAN: Particulate organic matter content and composition of stream, estuarine, and marine sediments. *Environmental Data Initiative*. https://doi.org/10.6073/pasta/05ca288d7203107bddab618e95524c0a

Pallud, C., Meile, C., Laverman, A. M., Abell, J., Van Cappellen, P., 2007. The use of flow-through sediment reactors in biogeochemical kinetics: Methodology and examples of applications. *Marine Chemistry* 106, 256–271. https://doi.org/10.1016/j.marchem.2006.12.011

Peters, J. R., Reed, D. C., Burkepile, D. E., 2019. Climate and fishing drive regime shifts in consumer-mediated nutrient cycling in kelp forests. *Global Change Biology* 25, 3179–3192. https://doi.org/10.1111/gcb.14706

Rao, A. M. F., McCarthy, M. J., Gardner, W. S., Jahnke, R. A., 2007. Respiration and denitrification in permeable continental shelf deposits on the South Atlantic Bight: Rates of carbon and nitrogen cycling from sediment column experiments. *Continental Shelf Research* 27, 1801–1819. https://doi.org/10.1016/j.csr.2007.03.001

Reed, D., Washburn, L., Rassweiler, A., Miller, R., Bell, T., Harrer, S., 2016. Extreme warming challenges sentinel status of kelp forests as indicators of climate change. *Nature Communications* 7, 13757. https://doi.org/10.1038/ncomms13757

Reed, D. C., 2018. SBC LTER: Reef: Kelp forest community dynamics: Abundance and size of giant kelp (Macrocystis pyrifera), ongoing since 2000. *Environmental Data Initiative*. https://doi.org/10.6073/pasta/8c079d19baee47eea41ba7b2a27adb35

Rocha, C., 2008. Sandy sediments as active biogeochemical reactors: compound cycling in the fast lane. *Aquatic Microbial Ecology* 53, 119–127. https://doi.org/10.3354/ame01221

Rowe, G. T., Clifford, C. H., Smith, K. L., 1975. Benthic nutrient regeneration and its coupling to primary productivity in coastal waters. *Nature* 255, 215–217. https://doi.org/10.1038/255215a0

Roychoudhury, A. N., Viollier, E., Van Cappellen, P., 1998. A plug flow-through reactor for studying biogeochemical reactions in undisturbed sediments. *Applied Geochemistry* 13, 269–280.

Saaltink, R. M., Honingh, E., Dekker, S. C., Griffioen, J., van Riel, M. C., Verdonschot, P. F. M., Vink, J. P. M., Winterwerp, J. C., Wassen, M. J., 2019. Respiration and aeration by bioturbating Tubificidae alter biogeochemical processes in aquatic sediment. *Aquatic Sciences* 81, 13. https://doi.org/10.1007/s00027-018-0610-3

Schulz, H. D., Zabel, M., 2000. *Marine Geochemistry*. Springer Berlin Heidelberg, Berlin, Heidelberg.

Sciberras, M., Tait, K., Brochain, G., Hiddink, J. G., Hale, R., Godbold, J.A., Solan, M., 2017. Mediation of nitrogen by post-disturbance shelf communities experiencing organic matter enrichment. *Biogeochemistry* 135, 135–153. https://doi.org/10.1007/s10533-017-0370-5

Smith, J. M., Reed, D. C., Melack, J. M., 2018a. SBC LTER: OCEAN: Sediment porewater ammonium and urea concentrations. *Environmental Data Initiative*. https://doi.org/10.6073/pasta/deb7e37cb76c0da76de533dc64c5e383

Smith, J. M., Reed, D. C., Melack, J. M., 2018b. SBC LTER: OCEAN: Time series of sediment temperatures by depth. *Environmental Data Initiative*. https://doi.org/10.6073/pasta/f03abadcd706d64dda456352d311f0c1

Smyth, A. R., Murphy, A. E., Anderson, I. C., Song, B., 2018. Differential effects of bivalves on sediment nitrogen cycling in a shallow coastal bay. *Estuaries and Coasts* 41, 1147–1163. https://doi.org/10.1007/s12237-017-0344-9

Sommerfield, C. K., Lee, H. J., Normark, W. R., 2009. Postglacial sedimentary record of the Southern California continental shelf and slope, Point Conception to Dana Point, in: *Earth Science in the Urban Ocean: The Southern California Continental Borderland*. Geological Society of America. https://doi.org/10.1130/2009.2454(2.5)

Ståhlberg, C., Bastviken, D., Svensson, B. H., Rahm, L., 2006. Mineralisation of organic matter in coastal sediments at different frequency and duration of resuspension. *Estuarine, Coastal and Shelf Science* 70, 317–325. https://doi.org/10.1016/j.ecss.2006.06.022

Sumi, T., Koike, I., 1990. Estimation of ammonification and ammonium assimilation in surficial coastal and estuarine sediments. *Limnology and Oceanography* 35, 270–286.

Wainright, S. C., Hopkinson Jr., C. S., 1997. Effects of sediment resuspension on organic matter processing in coastal environments: a simulation model. *Journal of Marine Systems* 11, 353–368.

Washburn, L., Brzezinski, M. A., Carlson, C. A., Siegel, D. A., 2019. SBC LTER: Ocean: Ocean currents and biogeochemistry: Nearshore water profiles (monthly CTD and chemistry). Santa Barbara Coastal Long Term Ecological Research Project, *Environmental Data Initiative*. https://doi.org/10.6073/pasta/ecf97031bd606f9766f6e665689b483d

Wickham, H., Averick, M., Bryan, J., Chang, W., D'Agostino McGowan, L., François, R., Grolemund, G., Hayes, A., Henry, L., Hester, J., Kuhn, M., Lin Pedersen, T., Miller, E., Milton Bache, S., Müller, K., Ooms, J., Robinson, D., Paige Seidel, D., Spinu, V., Takahashi, K., Vaughan, D., Wilke, C., Woo, K., Yutani, H., 2019. Welcome to the Tidyverse. *Journal of Open Source Software* 4, 1686. https://doi.org/10.21105/joss.01686

Widdicombe, S., Needham, H. R., 2007. Impact of CO_2-induced seawater acidification on the burrowing activity of Nereis virens and sediment nutrient flux. *Marine Ecology Progress Series* 341, 111–122. https://doi.org/10.3354/meps341111

Woulds, C., Bouillon, S., Cowie, G. L., Drake, E., Middelburg, J. J., Witte, U., 2016. Patterns of carbon processing at the seafloor: the role of faunal and microbial communities in moderating carbon flows. *Biogeosciences* 13, 4343–4357. https://doi.org/10.5194/bg-13-4343-2016

CHAPTER 4:

TERRESTRIAL ORGANIC MATTER INPUTS TO NEARSHORE MARINE SEDIMENT UNDER PROLONGED DROUGHT FOLLOWED BY SIGNIFICANT RAINFALL

Abstract:

Terrestrial organic matter (TOM) exported to nearshore marine regions may be altered by drought or large amounts of precipitation. We examined how the 2011-2015 drought in southern California followed by significant precipitation during the winter seasons of 2015-2016 impacted the quantity and quality of TOM transported to nearshore kelp forests of the Santa Barbara Channel. Based on organic matter (OM) content, lignin oxidation by-products, and carbon isotopic signatures, biomarkers of TOM were detected in stream, estuarine, and marine sediment. Quantitative measures of lignin clearly differentiated between the three environments. Qualitative lignin signatures revealed temporal patterns that were mirrored in stream and marine sediment. These patterns were indicative of inputs from less degraded TOM over time, and lignin oxidation compounds can be used as biomarkers of TOM transported during storm events in coastal watersheds and into nearshore marine sediment.

Introduction

The land-ocean boundary is a biogeochemically active region where terrestrial organic matter (TOM) is physically transported from upland areas to nearshore marine environments (Billen et al., 1991). This TOM may be remineralized and then provide a nutrient source to coastal ecosystems (Opsahl and Benner, 1997) or be buried in marine

sediments (Burdige, 2005). TOM transport into nearshore marine areas is a function of landscape and climate (Onstad et al., 2000) and with land use and climatic changes, its transport will likely be affected (McClain et al., 2003). Increased agricultural and urban development may alter both the quantities and sources of TOM while storms and extended droughts may significantly alter sources and export of TOM to nearshore areas (Godin et al., 2017; Masson-Delmotte et al., 2018). Due to the many biological, chemical, and physical processes that TOM may undergo prior to reaching the marine environment, there is need for further study of TOM transport and fate in coastal regions (Xenopoulos et al., 2017).

The purpose of this study was to investigate how storm events impact the quantity and quality of TOM transported into coastal regions. We examined how distance from stream mouths, as a source of storm runoff, and sampling date, following successive winter storms, might impact TOM measured in marine sediments and, as a result, alter OM availability in nearshore environments. Our study area in the Santa Ynez Mountain watersheds and nearshore regions of the Santa Barbara Channel in southern California is of particular interest due to droughts, episodic rainfall, and wildfires that cause significant variability in local runoff and solute and particulate export (Aguilera and Melack, 2018a). Multiple wildfires occurred in the region during the decade preceding this study, and wildfires can lead to an increased export of suspended sediments during the next precipitation event (Coombs and Melack, 2013; Murphy et al., 2015; Aguilera and Melack, 2018b). Fires were spread throughout the sampling region, so our analysis focuses instead on the storms and the preceding drought as controlling factors in organic material condition and transport. In Santa Ynez Mountain watersheds, 50% of annual suspended sediment may be discharged in 0.5-2 days of storm events, suggesting that half of the sediment that reaches the ocean from the

land each year may happen in a single storm (Warrick et al., 2015). The short, intermittent streams and episodic storm events would likely produce pulsed inputs of TOM to the Santa Barbara Channel and moderately sequester it (Blair and Aller, 2012). The episodic nature of runoff events makes this region well suited for a study using lignin as a tracer of the effects of climate variability on loading of particulate organic matter from the landscape.

Lignin can be used as a biomarker to trace the transport and processing of TOM. As a structural compound found in vascular terrestrial plants, lignin is resistant to degradation relative to other organic compounds and can provide a fingerprint of TOM source material (Hedges and Mann, 1979a). Lignin's degradation by chemical and physical processes and microbial remineralization depends on environmental conditions such as oxygen and light availability (Opsahl and Benner, 1995; Thevenot et al., 2010). Lignin oxidation compounds that result from performing cupric oxide (CuO) oxidation (Hedges and Mann, 1979a; Louchouarn et al., 2000; Moingt et al., 2016) are indicative of source materials and biogeochemical and physical processes (Hedges and Ertel, 1982; Hernes et al., 2007; Moingt et al., 2016). Using only stable isotopes as a biomarker of TOM, it may be difficult to distinguish between terrestrial materials and marine organic matter (MOM) (Hedges et al., 1997), and one can overestimate the relative amount of MOM (Burdige, 2005). Lignin provides a parameter that can be combined with isotopic analyses to improve source identification. However, care should be taken in interpreting results since lignin analyses do not provide a measure of absolute TOM content (Louchouarn et al., 2010; Moingt et al., 2016).

Lignin has been used mostly one of two ways: as a measure of TOM present in marine environments or as an integrated record of land use change in a downstream water

body (Prahl et al., 1994; Opsahl and Benner, 1995). TOM has been identified in salt marshes (Chen and Torres, 2018), mangrove forests (Dittmar and Lara, 2001), benthic marine sediments (Hedges and Parker, 1976; Hedges and Mann, 1979b; Prahl et al., 1994; Tesi et al., 2008), and river systems emptying into coastal marine environments (Goñi et al., 1998; Sun et al., 2017). Lignin is also a tracer for land use change, with the downstream water body being a recipient of sediment in runoff and, therefore, a record of human activity such as agriculture (Onstad et al., 2000; Dalzell et al., 2007; Bélanger et al., 2015, 2017), pulp industry (Louchouarn et al., 1999), and logging and mining (Moingt et al., 2014). Lignin is seldom used in studies with varied ecosystems in the context of multiple climate events, our focus in this study. Here, we combine lignin signatures of stream, estuarine, and nearshore marine sediment to evaluate TOM inputs along the land-ocean continuum before and after storm events over the course of two years.

We examined the relative input and degradation state of TOM in stream, estuarine, and marine sediment before and after precipitation events during the 2016 and 2017 winter seasons. Due to the large rainfall predicted during the 2015-2016 El Niño Seasonal Oscillation, we hypothesized that sediment samples collected following the storms would contain greater and fresher lignin content than those collected before the storms. We also hypothesized that following these storms marine sediments located closest to stream mouths would receive higher TOM loading than sites further from streams. With a multi-year design and wide geographic distribution of sites, this project evaluated the quantity and quality of TOM reaching kelp forest ecosystems in the context of a severe drought followed by the first significant precipitation in several years.

Methods

Site Description

Nine stream sites in Santa Ynez Mountain watersheds, two estuarine sites in Santa Barbara County, California, and eight kelp forest sites located offshore in the Santa Barbara Channel (SBC) were sampled (*Figure 1, Appendix 1*). The watershed sizes range from 7 to 50 km^2, and maximum watershed elevation is approximately 1,000 meters above sea level (Aguilera and Melack, 2018a, b). Five marine sites were located immediately downstream of a stream or estuarine site while three others were located near a kelp forest but at least 1 km from the nearest stream mouth. The distance from sampling site to shore ranged from approximately 300 to 2,200 m; Goleta Bay (GOLB) and Mission Creek (MICR) were sampled 1.5-2.2 km from shore due to their bathymetric gradient (see sampling locations along the 20 m isobath in Figure 1). All sites are part of the Santa Barbara Coastal Long Term Ecological Research (SBC LTER) program, which has collected long-term, monthly datasets at these locations for dissolved and particulate constituents (Melack, 2019; Washburn et al., 2019).

The region experiences a Mediterranean climate, with cool winters and warm, dry summers (Aguilera and Melack, 2018b). Oceanographic conditions consist of three periods: seasonal upwelling of cold, nutrient rich water in spring (April – June), warm, stratified water in summer and fall (July – November), and episodic runoff from streams during winter storms (December – March) (Brzezinski et al., 2013). A nearshore current (~15 m water depth) along the mainland typically flows poleward (westward) with speeds up to 0.1 m s^{-1} with stronger currents in summer (Harms and Winant, 1998; Fewings et al., 2015). Average nearshore cross-shelf currents along the benthos typically range from 0.01 to 0.02 m s^{-1} with

flow offshore (southward). In water depths of 15 m or less, seawater residence time is approximately 2 days (Fewings et al., 2015). During fair-weather conditions typical in summer, the wave base, or the depth to which marine sediment is disturbed due to waves, is up to 20 m. In contrast, marine sediment may be disturbed and resuspended in up to 70 m during stormy conditions typical of winter (Sommerfield et al., 2009). Along the mainland, sand is transported each winter from beaches and nearshore areas into offshore regions and is returned the following summer (Revell et al., 2011).

Sampling Design

Sampling was designed to encompass the period immediately before and during El Niño Seasonal Oscillation (ENSO) conditions in southern California, from December 2015 to June 2017. Suspended particulate matter was collected at nine streams during winter storms. Samples were not collected from streams during dry season periods because they lacked appreciable discharge at these times. At estuarine sites, four replicate sediment cores (5 cm diameter x 20 cm long) were collected using hand corers from the shallow subtidal channels near the inlets. At kelp forest sites, four replicate sediment cores (5 cm diameter x 20 cm long) at two water depths (10 m and 20 m) were collected by SCUBA divers using hand corers. Estuarine and marine cores were split into shallow (0-10 cm) and deep (10-20 cm) subsamples. Sediment cores were sectioned by 10 cm increments due to the energetic conditions along the benthos. Samples were transported back to the laboratory and frozen (-20 ºC) prior to additional analyses.

Sample Processing

All samples were analyzed for OM content, grain size, carbon and nitrogen content, carbon and nitrogen stable isotopes, and lignin content. OM content was determined by

weighing 2 g of thawed sediment, drying at 60 ºC for 48 hours, combusting at 450 ºC for 4 hours, and re-weighing the sample. Grain size was determined using 20 g of dried sediment, treating the sample with 5 % sodium hexametaphosphate for 24 hours (Poppe et al., 2000), and analyzing using a Cilas laser diffraction particle size analyzer. For carbon and nitrogen content as well as isotopic signatures, samples were thawed, and shell and other coarse material removed. Sediment was then dried at 60 ºC for 48 hours, ground using mortar and pestle, weighed into silver capsules, acidified with 6 % sulfurous acid to remove carbonates, and re-dried. All samples were analyzed using a Thermo Finnigan Delta-Plus Advantage isotope mass spectrometer coupled with a Costech EAS elemental analyzer housed at the University of California Santa Barbara (UCSB) Marine Science Institute Analytical Laboratory. Instrument precision for both C and N was ± 0.2 ‰, determined by replicate analyses of NBS 1572 standard. Isotope values are presented per mil in standard δ notation relative to the Pee Dee Belemnite standard for carbon and atmospheric N_2 for nitrogen. All samples were analyzed for lignin content using a modified version of the alkaline CuO oxidation method described by Goñi and Montgomery (2000) (Moingt et al., 2016) using a Varian 3800/Saturn 2000^{TM} coupled gas chromatograph – mass spectrometer fitted with a fused capillary column (DB-1 from J&W, 60 m, 320 μm) housed at GEOTOP, Université du Québec à Montréal.

Lignin analyses were performed to evaluate TOM source material in sediments and the degree to which this material had undergone diagenetic processing. Our results for the standard reference material (SAG 05) were consistent with previously published values (Louchouarn et al., 2000; Moingt et al., 2016; Appendix 2). Sigma 8 is a measure of eight total lignin oxidation products indicating total lignin amount per sample, while Lambda is a

measure of the same oxidation products but normalized to organic carbon (OC) content, as an indicator of the proportion of allochthonous to autochthonous OM in aquatic environments (Hedges and Parker, 1976). The ratio of cinnamyl to vanillyl phenols (C/V) is used as a measure of the relative contribution of non-woody source materials (Hedges and Mann, 1979a) and decreases with biodegradation (Opsahl and Benner, 1995; Dittmar and Lara, 2001). The ratio of syringyl to vanillyl phenols (S/V) is used as a measure of the relative contribution of woody angiosperm material (Hedges and Mann, 1979a). S/V decreases or remains unchanged due to degradation processes and increases due to physical sorption and leaching processes in aquatic environments (Opsahl and Benner, 1995; Hernes et al., 2007). The ratio of *p*-hydroxyl phenols to vanillyl and syringyl phenols (P/(V+S)) is used as a measure of the relative contribution of woody versus non-woody materials (Moingt et al., 2016). P/(V+S) and 3,5-dihydroxybenzoic acid to vanillyl phenols (3,5-Bd/V) are also used as measures of degradation (Hedges and Ertel, 1982; Louchouarn et al., 1999; Dittmar and Lara, 2001). Lignin has been detected in seagrasses (Klap et al., 2000) and red algae (Martone et al., 2009), but their lignin content is low. We ensured sampling did not occur in areas with these taxa so as not to confound results using lignin as a terrestrial biomarker.

We examined indicators of overall lignin content (Sigma 8, Lambda) and signatures of source materials and degradation processes (S/V, C/V, P/(V+S), 3,5-Bd/V) to identify spatial and temporal trends in the sediments. While the extraction efficiency of the cupric oxidation method remains fairly constant, the lignin fraction of a given sample may vary based on the characteristics of the TOM of the sample, so calculating precise loadings of TOM is not advised. However, if the lignin content of samples collected from the same location increases through time, one can attribute that to increased TOM input (Louchouarn

et al., 1999; Moingt et al., 2016; Bélanger et al., 2017). Hence, we interpret lignin measures in terms of source material and level of degradation.

Data Analyses

Data organization and analyses were performed using Excel (v 16.24) and R Statistical Software (v 3.4.3). Data formatting and visualization were performed using the *tidyverse* in RStudio 2 (Wickham, 2019). Linear mixed effects models were used to account for the nested sampling design and to address the lack of independence between certain samples (Millar and Anderson, 2004; Chaves, 2010). Prior to model construction, seven outliers in the lignin dataset were removed. All statistical analyses used an alpha (α) value of 0.05 unless otherwise noted. The lme function within the *nlme* package was used to create and validate each model (Pinheiro et al., 2019). Model creation began with fixed effects and random effects using a random intercept structure. Then, model selection followed the protocol outlined by Zuur et al. (2009, Chapter 5), beginning with a linear model, accounting for variance structure, optimizing the fixed structure, and validating best model fit using distribution of residuals and AIC values. If necessary, data were log-transformed. If fixed effects were found to have a significant effect on lignin values, post hoc tests (Tukey's HSD) were run using the glht function of the *multcomp* package (Hothorn et al., 2017). Data are published on the SBC LTER site (Page et al., 2018). Final results aggregated by environment and sampling date are presented in Appendix 3. Results of all linear mixed effects models are reported in Appendix 4.

Results

Precipitation

During a drought from 2011 to 2015, mean annual rainfall in the region measured from Santa Barbara County gauge 234 (34°25’ N, 119°42’ W) was 24.8 cm. From 2015 to 2017, the period of our study, mean annual rainfall approximately doubled to 48.1 cm. The 20-year rainfall average for the two decades preceding our study (1995-2015) was 47.2 cm, with especially large precipitation occurring during the 1997-98 (119 cm) and 2004-05 (94 cm) water years (Santa Barbara County Flood Control District, 2019).

Lignin content

At least one of twelve possible lignin oxidation products (LOPs) were detected in 444 of 457 sediment samples (97 %). Means and standard deviations of LOP values, organic carbon content, and isotopic signatures aggregated by environment and sampling date are reported in Appendix 3.

Lignin quantity measurements

Sigma 8 values of all samples ranged from 0.01 to 15.29 mg/10 g sample, and mean and standard deviation values for the streams, estuaries, and kelp forests were 5.85 ± 3.89 mg/10 g sample, 2.75 ± 2.78 mg/10 g sample, and 0.47 ± 0.44 mg/10 g sample, respectively (Figure 3). Due to the distribution of values from all environments, Sigma 8 values were log-transformed prior to the development of a linear mixed effects model. Our final model structure for the full dataset included environment (stream, estuary, or marine) as a fixed effect and sampling site as a random effect. Sampling date was not considered as a fixed effect since certain environments were sampled only on certain dates (Table 1), and a lack of independence between site type and sampling date would lead to significant correlation issues. The model results revealed a significant effect of environment on Sigma 8 values (linear mixed effects model (LMEM), $p < 0.0001$). Stream Sigma 8 values were significantly

different from the estuary (Tukey's post hoc, $p = 0.0020$) and marine values (Tukey's post hoc, $p < 0.001$), and the estuary values were significantly different from the marine values (Tukey's post hoc, $p = 0.0016$). Due to stream Sigma 8 values being significantly different than all other environments sampled and values being consistently greater, we conclude that stream sediment samples contained the greatest quantities of TOM.

Lambda values of all samples ranged from 0.04 to 6.01 mg/100 mg Organic Carbon (OC), and mean values for the stream, estuary, and kelp forest environments were 2.14 ± 0.99 mg/100 mg OC, 2.17 ± 1.29 mg/100 mg OC, and 1.08 ± 0.76 mg/100 mg OC, respectively (Figure 3). The final model for the full dataset included environment as a fixed effect, sampling site as a random effect, and an additional term to account for multiple variances across environments. Model results suggested a significant effect of environment on Lambda values (LMEM, $p = 0.0001$). The stream and estuary Lambda values were not significantly different, but marine values were significantly different from stream and estuary values (Tukey's post hoc, $p < 0.0001$ for both). Lambda values for stream sediment were significantly different from, and typically greater than, marine sediment, which indicates stream sediment samples contained greater proportions of TOM than marine sediment samples.

Contrary to our initial hypothesis, Sigma 8 and Lambda values in marine sediment did not vary significantly between marine sites located near and far from stream mouths. Marine sediment Sigma 8 values ranged from 0.01 to 3.43 mg/10 g sample. Mean values for sites located near and far from stream mouths were 0.51 ± 0.48 mg/10 g sample and 0.38 ± 0.35 mg/10 g sample, respectively. Marine sediment Lambda values ranged from 0.04 to 4.41 mg/100 mg OC, and mean values for sites located near and far from stream mouths were 1.20

± 0.77 mg/100 mg OC and 0.86 ± 0.70 mg/100 mg OC, respectively. Additional information regarding model structures for marine Sigma 8 and Lambda values can be found in Appendix 4. The lignin quantity measures of Sigma 8 and Lambda were unable to distinguish between marine sites located near and far from stream mouths. Sampling date, water depth, and sediment depth were significant predictors of lignin quantity measures.

Isotopic signatures vs. lignin measurements

Higher Sigma 8 values are indicative of greater lignin content in a given sample, and depleted $\delta^{13}C$ signatures (more negative values) also suggest greater input from terrestrial sources (Hedges and Parker, 1976). Moingt et al. (2016) found a linear relationship between Sigma 8 and $\delta^{13}C$ signatures, but the samples analyzed were forest soils. Since our samples were collected from varied environments as well as different horizons (suspended and benthic), we present the Sigma 8 and $\delta^{13}C$ signature relationship in a more qualitative manner. TOM signatures in the Santa Barbara Channel range from -25 to -23 ‰, kelp forest particulate OM $\delta^{13}C$ signatures range from -23 to -17 ‰, and offshore particulate MOM signatures range from -22 to -19 ‰ (Page et al., 2008). Stream and estuarine sediment had higher Sigma 8 values and more depleted $\delta^{13}C$ signatures, whereas marine sediment had lower Sigma 8 values and more enriched $\delta^{13}C$ signatures (*Figure 4*). Sigma 8 values were most variable at stream and estuarine sites while $\delta^{13}C$ signatures were most variable at marine sites. No distinct grouping emerged in isotopic signatures between marine sites located near or far from streams.

Lignin content and isotopic signatures may be used to indicate material sources and the level of degradation of the OM. Greater values for the 3,5-dihydroxybenzoic acid to vanillyl (3,5-Bd/V) ratio indicate greater levels of TOM degradation (Louchouarn et al.,

1999). Fragments of brown macroalgae in sediment samples can also increase 3,5-Bd/V measures due to the presence of tannin and flavonoid compounds in their tissues (Goñi and Hedges, 1995). We present the relationship between 3,5-Bd/V and $\delta^{13}C$ signatures to examine the relationship between sampling environment and evidence of degradative processes. Stream and estuarine sediments contained low 3,5-Bd/V values with low variability while marine sediments had greater 3,5-Bd/V values with much greater variability (*Figure 5*). There was no significant difference in 3,5-Bd/V values by marine sites located near and far from streams (*Appendix 4*).

Lignin quality measurements

Syringyl to vanillyl (S/V) and cinnamyl to vanillyl (C/V) ratios provide information about material sources and degradation processes. S/V values of all samples ranged from 0.15 to 11.72. Mean values for the streams, estuaries, and kelp forests were 2.45 ± 0.88, 2.73 ± 1.27, and 3.03 ± 1.51, respectively. C/V values of all samples ranged from 0.01 to 0.75. Mean values for the streams, estuaries, and kelp forests were 0.27 ± 0.13, 0.32 ± 0.0.19, and 0.10 ± 0.08, respectively. There was no significant difference in S/V values across environments (LMEM, $p = 0.2479$) and no significant difference in C/V values between stream and estuarine environments (Tukey's post hoc, $p = 0.241$). Consequently, we will focus on linear mixed effect models run for S/V and C/V values within each environments.

Stream S/V and C/V values distinguish patterns in source material quality, prior to significant processing and signature alteration that may occur during transport to the ocean. Stream S/V values ranged from 1.50 to 4.36 while C/V values ranged from 0.09 to 0.54 (*Figure 6*). Linear mixed effects model structure for the stream S/V data only included watershed area and sampling date as fixed effects, sampling site as a random effect, and an

additional term allowing different variances by sampling date. The model structure for the C/V data included sampling date as a fixed effect and sampling site as a random effect. Watershed area (km^2) (LMEM, $p = 0.0099$) and sampling date (LMEM, $p = 0.0004$) had a significant effect on S/V values. Sampling date also had a significant effect on C/V values (LMEM, $p = 0.0019$). For S/V values, post hoc results suggested a significant difference between January and March 2016 (Tukey's post hoc, $p = 0.0014$) and January 2016 and January 2017 (Tukey's post hoc, $p < 0.001$). C/V values were significantly different between January 2016 and January 2017 (Tukey's post hoc, $p = 0.0003$) and March 2016 and January 2017 (Tukey's post hoc, $p = 0.0002$). Based on these findings, we conclude that there was a significant change in either the S/V or C/V signatures of stream sediment between each sampling date, and overall, there was an increase in both S/V and C/V values in stream sediment over the course of the full sampling period coincident with increased stream discharge.

Marine S/V and C/V values were analyzed to determine if patterns in qualitative lignin measures in marine sediment mirrored those found in stream sediment samples. Marine S/V values ranged from 0.15 to 11.72 while C/V values ranged from 0.01 to 0.61 (*Figure 7*). Linear mixed effects model structure for the marine S/V data only included sampling date, water depth, and section of core as fixed effects, sampling site as a random effect, and a variance term by water depth. The model structure for C/V values included date sampled and water depth as fixed effects and sampling site as a random effect. Water depth (LMEM, $p < 0.0001$) had a significant effect on S/V values; post hoc results suggested a significant difference between cores collected at 10 m and 20 m water depth (Tukey's post hoc, $p < 0.0001$). Sampling date (LMEM, $p = 0.0165$) also had a significant effect on S/V

values, with post hoc results suggesting a significant difference between samples collected in December 2015 and March 2017 (Tukey's post hoc, $p = 0.0079$). For C/V values, water depth was found to be a significant fixed effect (LMEM, $p = 0.04$); post hoc results suggested a significant difference between cores collected at 10 m and 20 m water depth (Tukey's post hoc, $p = 0.0384$). Sampling date (LMEM, $p = 0.0001$) had a significant effect on C/V values as well. Post hoc results indicated a significant difference between December 2015 and June 2016 (Tukey's post hoc, $p < 0.001$), December 2015 and March 2017 (Tukey's post hoc, $p = 0.0068$), and June 2016 and June 2017 (Tukey's post hoc, $p = 0.0212$). We conclude that there was a significant change in both S/V and C/V signatures of marine sediment between the initial samples collected prior to significant rainfall (December 2015) and samples collected after two winter storm seasons (March 2017). Similar to stream sediment, there was an increase in S/V values in marine sediment over the course of the full sampling period.

Lignin degradation indices, such as p-hydroxyl to vanillyl and syringyl (P/(V+S)) and 3,5-Bd/V, are typically used to verify patterns observed in source material signatures, such as S/V and C/V, and our results indicate P/(V+S) and 3,5-Bd/V values may also be better interpreted within a single environment. The P/(V+S) and 3,5-Bd/V ratios can be used as measures of diagenetic processing, with higher values for both measures indicating greater degradation (Louchouarn et al., 1999; Dittmar and Lara, 2001). P/(V+S) values of all samples ranged from 0.03 to 2.17, and mean values for streams, estuaries, and kelp forests were 0.20 ± 0.10, 0.15 ± 0.09, and 0.22 ± 0.25, respectively. 3,5-Bd/V values ranged from 0.06 to 4.06, and mean values for streams, estuaries, and kelp forests were 0.18 ± 0.06, 0.20 ± 0.14, and 0.59 ± 0.63, respectively. There was no significant difference in P/V+S values among environments (LMEM, $p = 0.7484$) and no significant difference in 3,5-Bd/V values

between stream and estuarine environments in pairwise comparisons (Tukey's post hoc, $p = 0.996$). Therefore, we present results of linear mixed effects models run for P/(V+S) and 3,5-Bd/V values for each environment separately.

Stream P/(V+S) and 3,5-Bd/V values were analyzed for patterns in degradation parameters prior to transport to marine regions. P/(V+S) values in stream particulate matter ranged from 0.06 to 0.36, and 3,5-Bd/V values in stream particulate matter ranged from 0.08 to 0.37 (*Figure 8*). The final model structure for P/(V+S) data included sampling date as the singular fixed effect and sampling site as the random effect. P/(V+S) varied significantly by sampling date (LMEM, $p < 0.0001$). Post hoc testing revealed that all dates were significantly different from all others (Tukey's post hoc, $p < 0.001$). The final model for 3,5-Bd/V included land use as a fixed effect, site as a random effect, and an additional variance term by sampling date, but values did not vary significantly by land use type (urban, agricultural, or undeveloped). The results of these models indicate that there was a significant change in P/(V+S) signatures of stream sediment between each sampling date, and overall, there was a decrease in P/(V+S) values in stream sediment over the course of the full sampling period.

Marine P/(V+S) and 3,5-Bd/V values were analyzed to determine if trends in upstream samples were mirrored in sediments deposited in nearshore regions. P/(V+S) values in marine sediment ranged from 0.03 to 2.17, and 3,5-Bd/V values ranged from 0.09 to 4.06 (*Figure 9*). The model structure for P/(V+S) data included distance from stream, date sampled, section of core, and water depth as fixed effects, sampling site as a random effect, and a term allowing for different variances by water depth. The model structure for 3,5-Bd/V data included date sampled, section of core, and water depth as fixed effects, sampling site as

a random effect, and a variance term by water depth. P/(V+S) values varied significantly by distance from the nearest stream (LMEM, $p = 0.01$), date sampled (LMEM, $p < 0.0001$), section of core (LMEM, $p = 0.001$), and water depth (LMEM, $p < 0.0001$). Post hoc results suggested a significant difference between sites near and far from stream mouths (Tukey's post hoc, $p = 0.0149$), between 10 m and 20 m water depths ($p < 0.0001$), between top and bottom 10 cm sections of the core (Tukey's post hoc, $p = 0.001$ for all), and nearly all dates sampled (December 2015 and March 2017, December 2015 and June 2017, June 2016 and June 2017, and March 2017 and June 2017 (Tukey's post hoc, $p < 0.001$)). For 3,5-Bd/V values, sampling date (LMEM, $p < 0.0001$), water depth (LMEM, $p < 0.0001$), and core section (LMEM, $p = 0.003$) were all significant fixed effects. Post hoc testing revealed significant differences between 10 and 20 m water depths (Tukey's post hoc, $p < 0.0001$), the top and bottom sections of sediment cores (Tukey's post hoc, $p = 0.0023$) as well as December 2015 and March 2017 and December 2015 and June 2017 (Tukey's post hoc, $p < 0.001$ for both) samples. We conclude that there was a decrease in both P/(V+S) and 3,5-Bd/V signatures of marine sediment between the initial samples collected prior to significant rainfall (December 2015) and samples collected after two winter storm seasons (March/June 2017). Similar to stream sediment, there was a decrease in P/(V+S) values in marine sediment over the course of the full sampling period.

Estuarine sediments did not yield as clear of a trend in lignin quality measures with respect to sampling date as stream and marine sediments. Estuarine S/V values ranged from 0.69 to 8.74 while C/V values ranged from 0.05 to 0.75. Estuarine P/(V+S) values ranged from 0.04 to 0.47 while 3,5-Bd/V values ranged from 0.06 to 0.75.

Discussion

Lignin quantity measures distinguish environments

Quantitative lignin measures (Sigma 8, Lambda) differed among the sampled environments (stream, estuarine, marine), reflecting the greater proportional contribution of TOM to stream as compared to marine particulate organic matter, but these measures did not vary significantly over time. As we hypothesized, sites located close to potential sources of TOM (i.e. streams and estuaries) had the highest mean Sigma 8 and Lambda values (*Figure 3*). Due to runoff caused by episodic storms, the streams located in the Santa Ynez watersheds contain significant quantities of TOM as suspended particulate matter, with TOM content comparable to much larger lotic systems (*Table 2*). Lignin measures at both estuarine sites were comparable to deltaic sediments collected from significantly larger lotic systems, specifically the Mississippi and Atchafalaya rivers (*Table 2*). Estuarine Sigma 8 values were significantly lower than stream values (Tukey's post hoc, $p = 0.0020$), but Lambda values were indistinguishable. Elevated Lambda values at estuarine sites may be due to input of partially degraded TOM, which contains proportionally more lignin than fresh TOM (Benner et al., 1987). If organic material in estuarine sediment consists of more degraded TOM, it would have higher lignin values relative to the total organic matter content. Greater Lambda values may also be due to input from different TOM sources, as suggested by S/V and C/V values (*Figure 6*), or the low OC content of sandy, estuarine sediments (mean OC of estuarine sediment samples = 0.99 ± 0.88 %). Intense deposition of TOM in winter coupled with hypoxic periods in summer (Battalio et al., 2015), may lead to extended periods of low oxygen availability which could slow degradation, increase OM sequestration and, as a

result, further increase Sigma 8 and Lambda values (Opsahl and Benner, 1995; Dittmar and Lara, 2001) at estuarine sites.

Runoff during winter storms transported TOM as far as the deepest water depth of marine sediments sampled (20 m), although the material did not disproportionately travel to or was retained in sediments located closest to stream mouths. Sigma 8 and Lambda measures were unable to distinguish between marine sediment sampled at kelp forest sites located near and far from streams (*Appendix 4*). Instead, water depth was the most significant factor, with Sigma 8 and Lambda values greater in marine sediments collected from deeper locations (20 m) (Tukey's post hoc, $p < 0.0001$ for both). The presence of lignin in most marine sediment samples indicates that TOM reaches these locations and in quantities comparable to global nearshore regions (*Table 2*). However, physical resuspension and transport likely prevent TOM from accumulating in sediments located closer to streams. Indeed, TOM in marine sediments can be transported along shore (Tesi et al., 2008), and storm events that cause strong wave action that may resuspend sediment, exacerbating dilution and dispersion (Airoldi et al., 1996; Cotner et al., 2000). In the energetic system of the Santa Barbara Channel, marine sediment at depths of 10 to 20 m is routinely resuspended due to waves even during fair weather periods (Sommerfield et al., 2009). There is also an annual pattern of scouring, with sand and sediment transported offshore from beaches and nearshore areas in winter and returned the following summer (Revell et al., 2011). These transport mechanisms may homogenize nearshore marine sediments during and after winter storm events. This connectivity may explain why lignin quantity was indistinguishable between marine sediment sampled near and far from streams.

Isotopic signatures and lignin indicators distinguish environments

Lignin and isotopic signatures ($\delta^{13}C$) can be used to differentiate the presence of TOM in freshwater versus marine systems. Our data imply stream and estuarine sediments contained greater TOM content (*Figure 4*), due to greater Sigma 8 values and less enriched (i.e., lighter) $\delta^{13}C$ signatures as compared to isotopic signatures of MOM of the Santa Barbara Channel (Page et al., 2008). In addition to lignin-derived compounds indicative of degradation (3,5-Bd/V), isotopic signatures ($\delta^{13}C$) can also be used as a measure of degradation. Lignin is characterized by $\delta^{13}C$ depleted signatures, and as more degraded TOM contains proportionately more lignin, it displays further depleted $\delta^{13}C$ signatures (up to 4 ‰) (Benner et al., 1987). Tannin and flavonoid compounds found in brown macroalgae can also increase 3,5-Bd content which can inflate 3,5-Bd/V measures (Goñi and Hedges, 1995). Overall, more enriched (i.e., heavier) $\delta^{13}C$ signatures and higher 3,5-Bd/V values in marine sediment suggested TOM in these samples was more degraded (*Figure 5*). Our marine V values were comparable to those measured by Goñi et al. (1998), but our 3,5-Bd/V values were an order of magnitude larger, also indicating potential input from macroalgae. By comparing isotopic signatures with quantitative and qualitative lignin measures, we confirm that stream sediment contained the greatest TOM content and marine sediment contained the most degraded TOM.

Lignin quality measures distinguish temporal trends

Qualitative lignin measures (S/V, C/V, P/(V+S)) detected temporal patterns within stream and marine environments following precipitation events, and changes in lignin signatures measured in stream sediment samples were mirrored in nearshore marine sediment samples. These changes imply input of varied, but increasingly fresh, terrestrial source material. Lignin quality indices (S/V, C/V, P/(V+S)) were more variable within an

environment (i.e., among sampling dates) than across environments (*Appendix 4*). Hence, we focus on the patterns detected within environments, with particular emphasis on temporal changes and measures of degradation.

Over the course of the entire sampling period, changes in marine S/V and C/V signatures broadly mirrored changes in stream S/V and C/V signatures, and S/V values in both stream and marine sediment increased. The relatively high S/V values (>1.00) in stream suspended particulate matter indicate input from woody and non-woody angiosperm tissues (Hedges and Mann, 1979a; Moingt et al., 2016). Higher C/V values (>0.3) suggest input from non-woody material, such as grasses or leaves, while lower values indicate input from woody, structural tissues (Hedges and Mann, 1979a). Moingt et al. (2016) reported significant differences in S/V values according to sample type (i.e. woody and non-woody parts of plants and soils in forests dominated by angiosperms). Therefore, January and March 2016 stream samples likely contained more woody angiosperm tissues, whereas January 2017 stream samples contained more soil or non-woody angiosperm tissues. S/V and C/V signatures may also indicate extent of degradation; S and C phenols are preferentially degraded, decreasing S/V and C/V signatures (Opsahl and Benner, 1995; Bélanger et al., 2017). When interpreted in this context, higher S/V signatures in stream and marine sediments may be due to greater input of TOM that is potentially less degraded.

P/(V+S) values in stream and marine samples decreased over time. Lower P/(V+S) values suggest source materials containing woody tissues while higher values suggest input from soil and non-woody tissues (Moingt et al., 2016). Values in January 2016 stream samples suggest greater input of soil and non-woody material, whereas January 2017 samples suggest more woody material. Similar to other lignin signatures, P/(V+S) may also be

considered a measure of degradation, with higher values suggesting greater levels of TOM degradation (Dittmar and Lara, 2001). In this context, the lower P/(V+S) values measured in stream and marine sediment following storm runoff suggest input of fresh, less degraded TOM. 3,5-Bd/V is another measure of degradation; higher values indicate greater levels of processing (Louchouarn et al., 1999). Marine sediment samples contained significantly different 3,5-Bd/V values through time. Lower 3,5-Bd/V values in December 2015 imply input of less degraded material, whereas higher values in June 2017 imply input of slightly more degraded TOM to marine sediment. We propose decreasing P/(V+S) values measured at stream and marine locations further support the idea that TOM being delivered to these environments during the heavier rains of 2017 was less degraded over time.

Degradation of lignin, as part of the larger pool of bioavailable TOM, depends on the microbial community, physical processes, and light and oxygen availability in a given system (Opsahl and Benner, 1995). In terrestrial environments, white-rot fungi (e.g., *Phlebia tremellosus*) are responsible for significant lignin breakdown (Hedges et al., 1988). Although there is currently no evidence of this fungus in marine environments, breakdown of TOM may occur in marine sediments (Burdige, 2005). Physical processes, such as dissolution and sorption, can alter lignin phenol values (Hernes et al., 2007), and coarse, lignin-rich materials may be subject to more physical processing than finer, lignin-poor organic materials that provide greater physical protection (Louchouarn et al., 1999). Photo-oxidation can lead to a decrease in S/V ratio values (Houel et al., 2006). Anaerobic lignin degradation causes a decrease in C/V ratio values while aerobic degradation causes a decrease in Sigma 8 values (Dittmar and Lara, 2001). There is a lack of consensus on whether these various degradation processes dominate in terrestrial ecosystems (Goñi et al., 1998) or if lignin undergoes

degradation at comparable rates in the ocean (Opsahl and Benner, 1995; Louchouarn et al., 1999). These biologically, chemically, and physically mediated degradation pathways likely occur simultaneously in our system. For this study, stream samples were collected during or immediately after storms while estuarine and marine samples were collected months later. Therefore, degradation taking place while in transport and later *in situ* may have amplified degradation signatures in the latter environments.

Lignin measures as evidence of storm events

With the frequency and intensity of droughts and storm events predicted to increase (Masson-Delmotte et al., 2018; Feng et al., 2019), TOM pulses into the ocean may become increasingly variable. Intense, sporadic storm events lead to large pulses of OC transport (Dalzell et al., 2007). Total suspended particulate matter exported from Santa Ynez Mountain watersheds is correlated with significant storm events (Aguilera and Melack, 2018a), and storm water runoff may contain significantly more lignin (Chen and Torres, 2018). While lignin is nutritionally-poor (Chen and Torres, 2018), it can be used as a marker for the simultaneous transport of labile TOM, which can be a subsidy for nearshore consumers (Savage et al., 2012; Fong and Fong, 2018). Our findings indicate TOM transported by streams into the nearshore ocean changed in terms of source material and level of degradation through time and suggest that antecedent conditions (i.e., drought) as well as precipitation events may have impacted TOM quality and transport.

This study highlights our ability to use lignin oxidation products as terrestrial biomarkers in the context of climate events in coastal regions. Quantitative lignin measures (Sigma 8, Lambda) were able to distinguish between environments sampled but were unable to distinguish between sampling dates. Instead, qualitative lignin measures (S/V, C/V,

P/(V+S), 3,5-Bd/V) yielded the most information regarding changes in sediment TOM content through time. Stream samples had distinct temporal patterns, with both S/V and C/V values increasing and P/(V+S) values decreasing through time. These trends suggest the sequential input of fresh OM and variable vegetation sources. Marine samples mirrored these patterns, also displaying increasing S/V values and decreasing P/(V+S) values. Changes in qualitative lignin signatures over time provide evidence of varied source material from sequential storms and ongoing *in situ* degradation processes which suggests lignin signatures can be used as a tracer of climate variability in fluvial and nearshore marine ecosystems. Due to the parallel trends detected in stream and marine sediment, our findings indicate TOM delivered into the nearshore Santa Barbara Channel from the Santa Ynez Mountain watersheds was less degraded and changed in terms of source material through time.

Tables and Figures

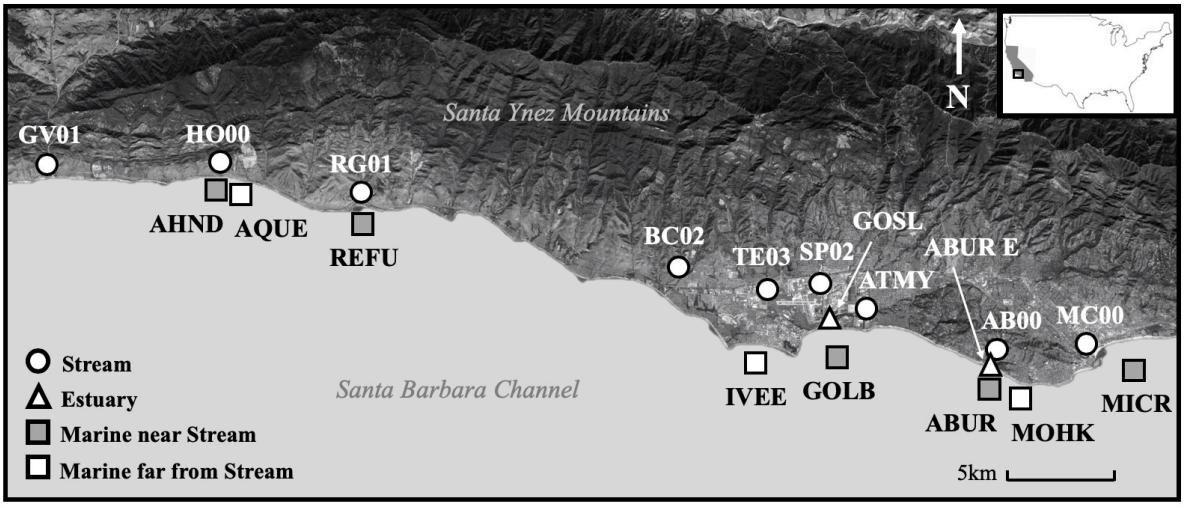

Figure 1: Locations sampled along the Santa Barbara coast from 2015 to 2017 (See Appendix 2 for full site names). All locations are regularly monitored sites of the SBC LTER. Marine locations are marked along the 20 m isobath. Image data provided by Google, SIO, NOAA, U.S. Navy, NGA, GEBCO, and MBARI (*Google Earth Pro*, 2019).

Table 1: Schedule of sampling. Sites were sampled once each time, and sampling all sites within an ecosystem category spanned a few days within each month.

	2015	**2016**		**2017**	
	Dry Season	Rainy Season	Dry Season	Rainy Season	Dry Season
Stream		January, March		January	
Estuary			April, June		March, June
Marine	December		June		March, June

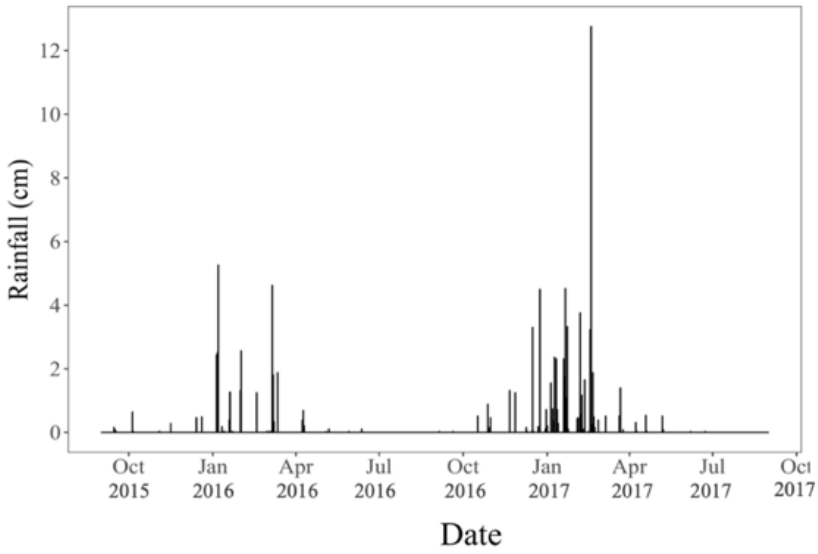

Figure 2: Daily rainfall for 2015-2017 water years (September 1 through August 31) measured at Santa Barbara County Gauge 234 (Santa Barbara County Flood Control District, 2019).

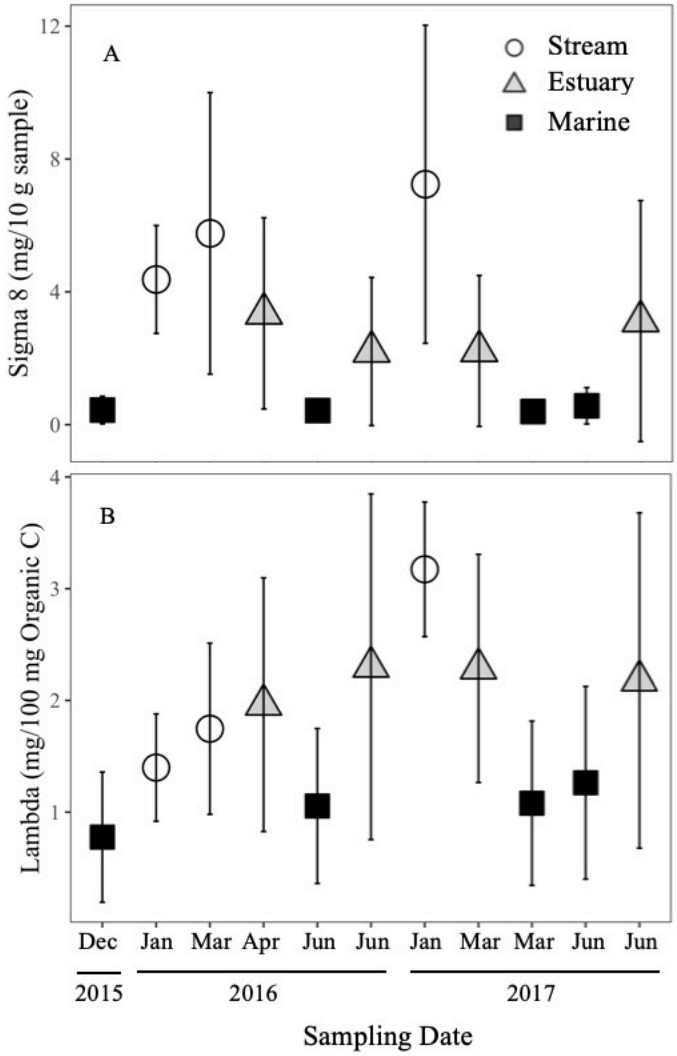

Figure 3: Mean Sigma 8 (A) and Lambda (B) values for all environments sampled. Data are aggregated by chronological sampling date. Error bars denote one standard deviation. Note: December 2015 marine samples were collected prior to significant rainfall.

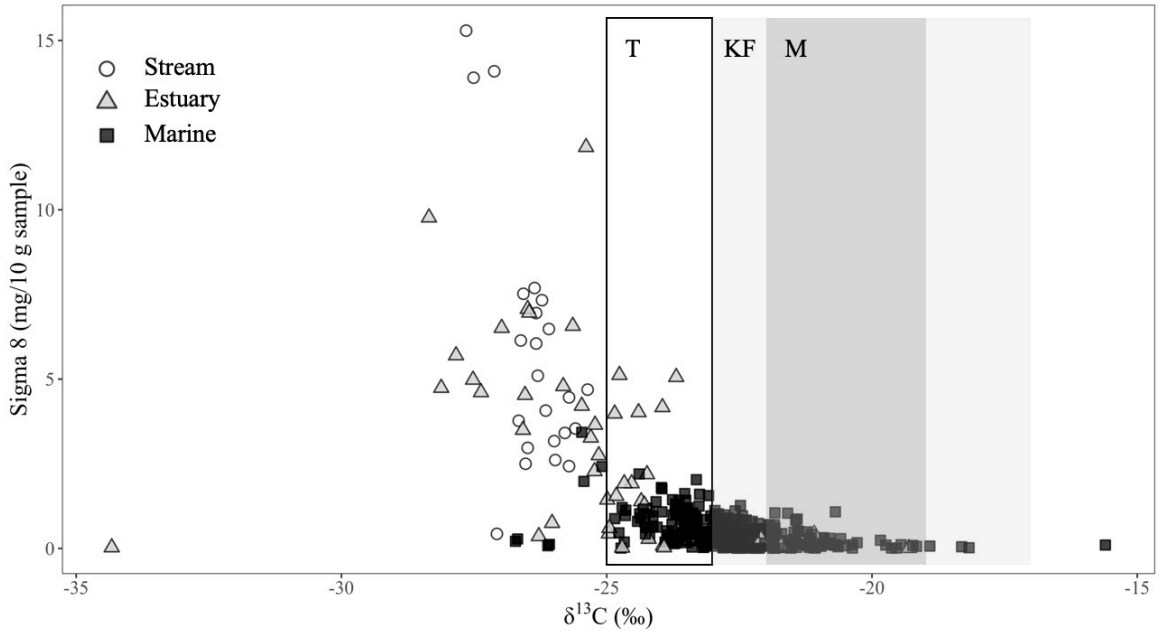

Figure 4: Sigma 8 and $\delta^{13}C$ values for all samples. Boxes are representative of published carbon isotopic signatures of particulate organic matter of various sources sampled from the Santa Barbara Channel nearshore marine environment (Page et al., 2008). “T” refers to terrestrial signatures, “KF” refers to kelp forest signatures, and “M” refers to offshore marine signatures.

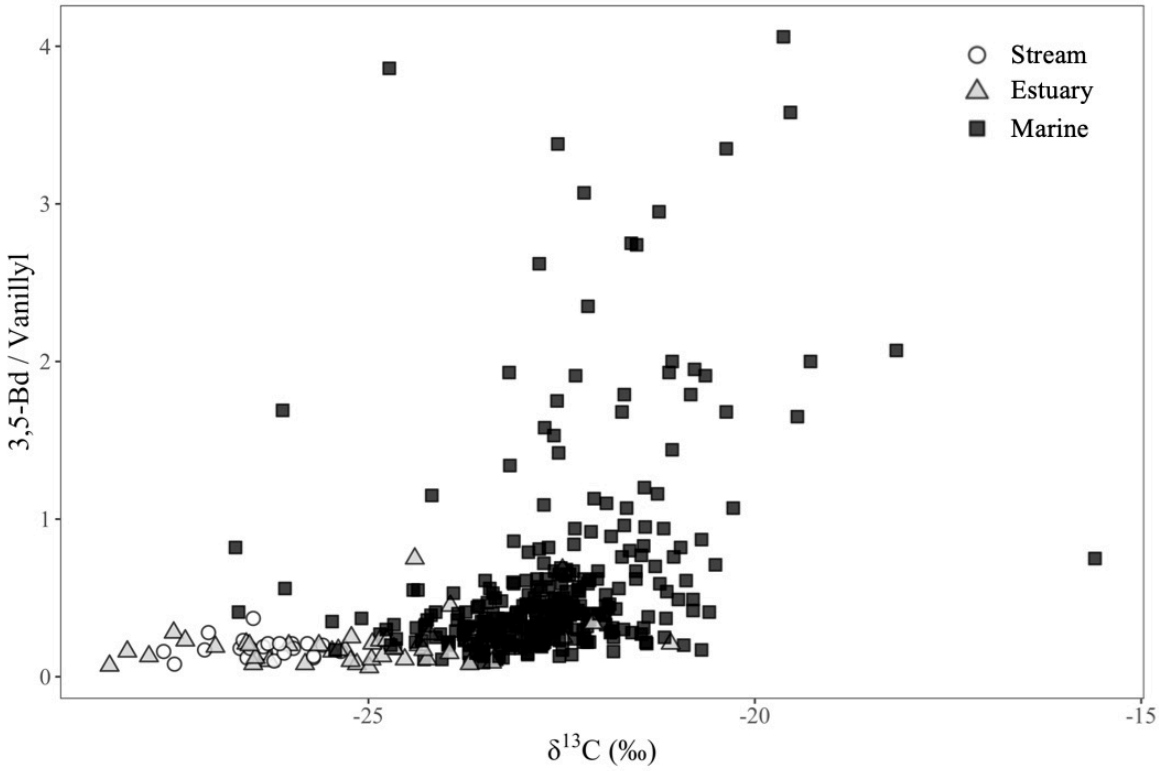

Figure 5: The ratio of 3,5-dihydroxybenzoic acid (3,5-Bd) to vanillyl phenols and $\delta^{13}C$ values for all samples.

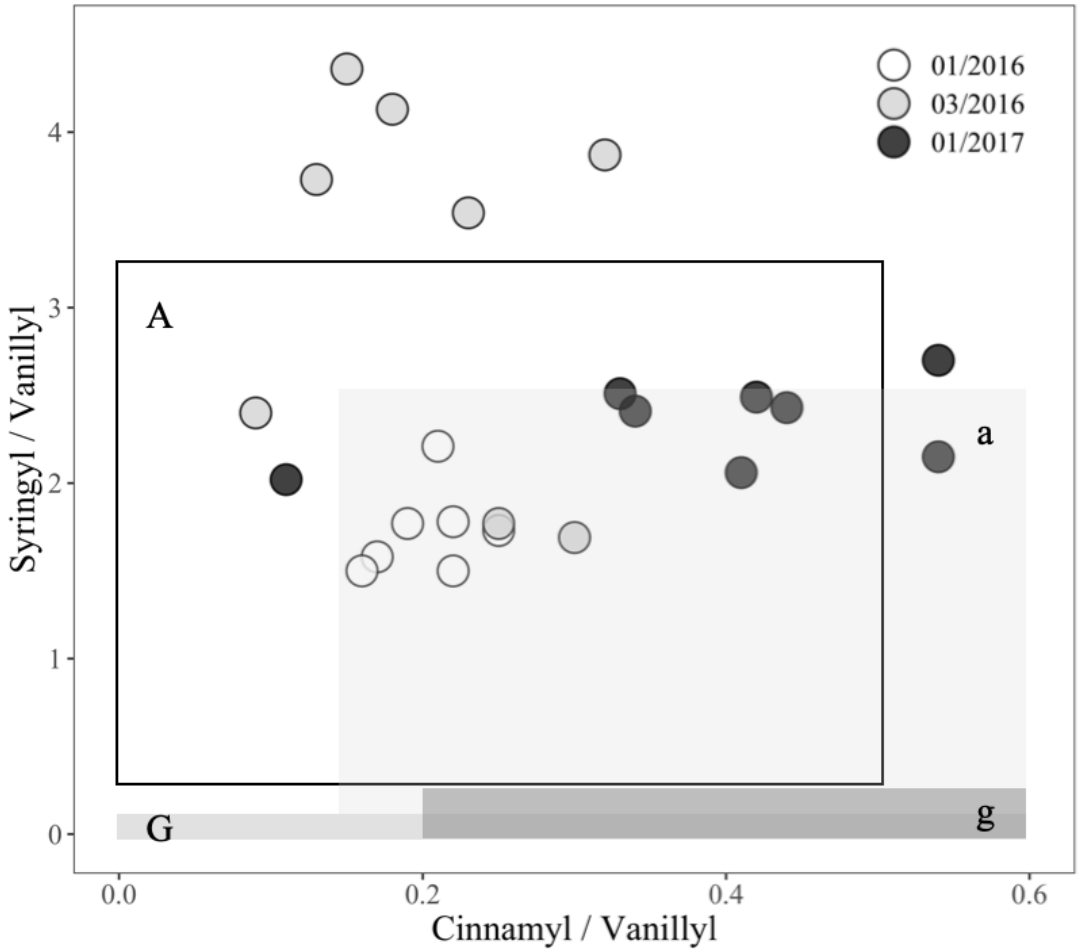

Figure 6: The ratio of S/V and C/V presented for suspended sediments collected from streams only. Boxes are representative of published values of pure terrestrial vegetation tissue sources, both gymnosperm and angiosperm (Hedges and Mann, 1979a; Moingt et al., 2016). “A” refers to woody angiosperm tissue, “a” refers to non-woody angiosperm tissue, “G” refers to woody gymnosperm tissue, and “g” refers to non-woody gymnosperm tissue. Note: All samples were collected during or following storms.

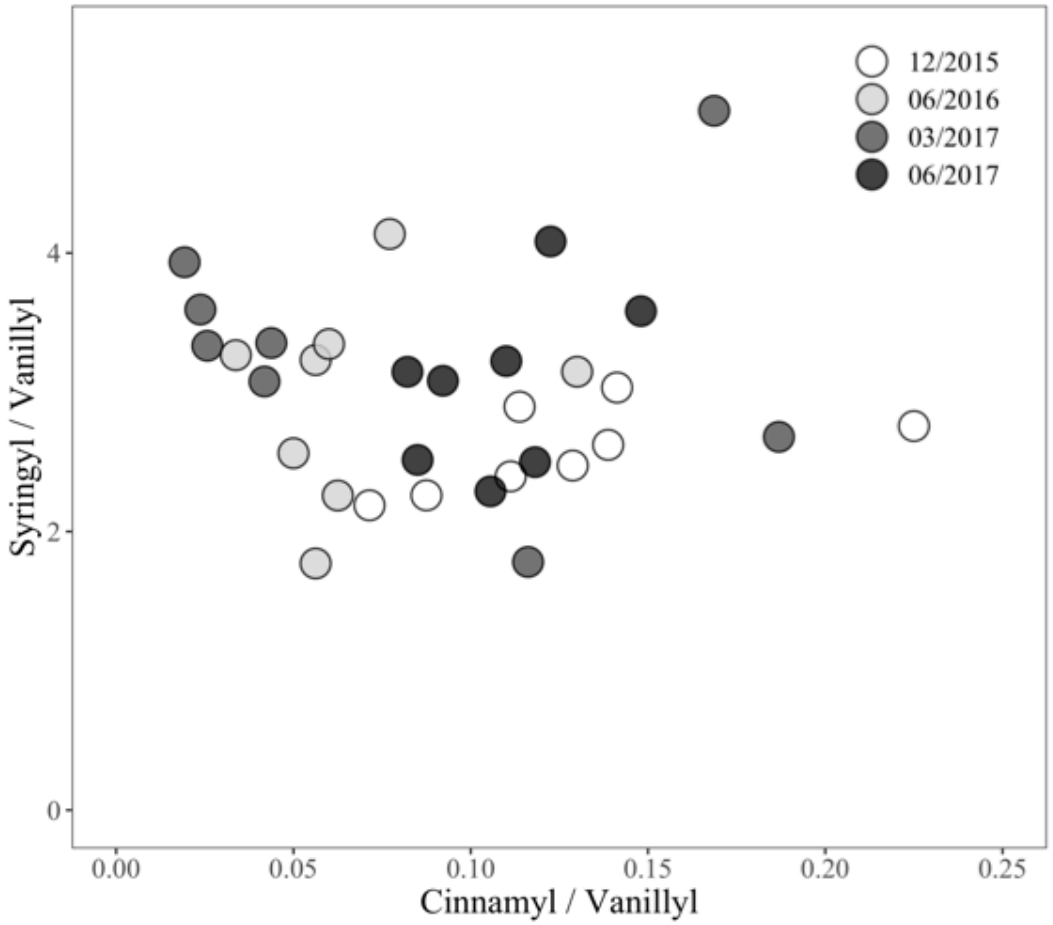

Figure 7: Mean values of the ratio of S/V and C/V presented for sediments collected from marine sites only. Values have been aggregated by site for easier comparison across dates. No distinction between sites near and far from streams has been made since proximity to stream did not have a significant effect on marine sediment S/V or C/V values (*Appendix 4*). Note: December 2015 marine samples were collected prior to significant rainfall.

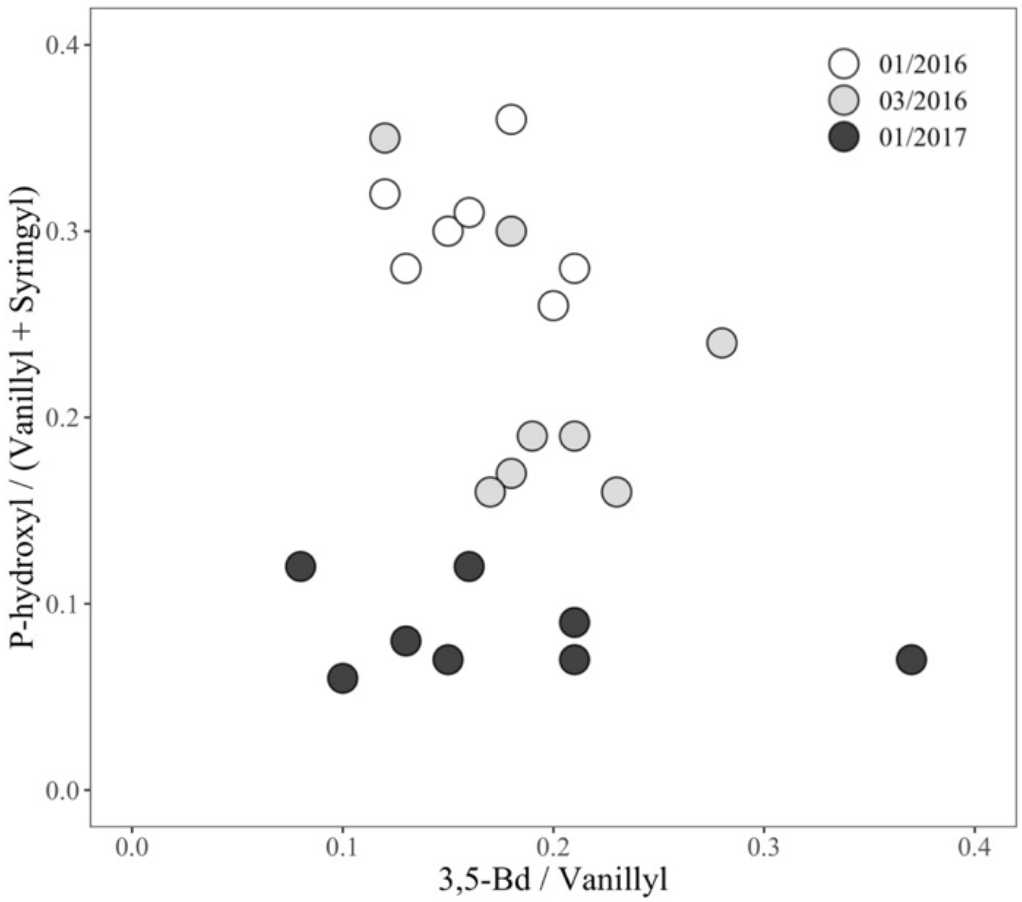

Figure 8: P/(V+S) and 3,5-Bd/V for stream suspended particulate matter only. Note: All samples were collected during or following storms.

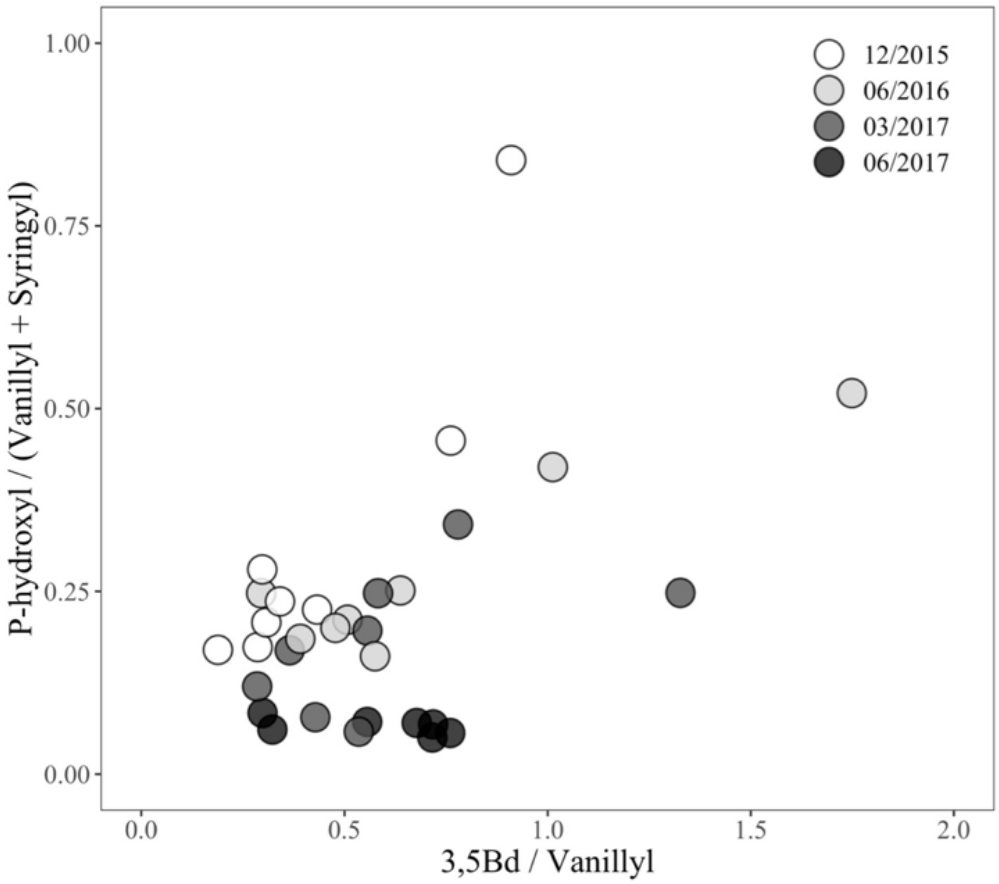

Figure 9: Mean values of the ratios of P/(V+S) and 3,5-Bd/V for marine sediment samples only. Values have been aggregated by site for easier comparison across dates sampled. No distinction between sites near and far from streams has been made since proximity to stream did not have a significant effect on marine sediment 3,5-Bd/V values (*Appendix 4*). Note: December 2015 marine samples were collected prior to significant rainfall.

Table 2: Lignin oxidation product values from studies examining similar environments alongside our data collected from sites located near Santa Barbara (SB), California, USA. Stream/river locations include data measured from suspended sediment only. Marine locations specify the water depth from which samples were collected.

Location	Source	Sigma 8	Lambda	S/V	C/V	3,5-Bd/V
Stream/River						
Santa Ynez Mtns.	This study	5.85	2.14	2.45	0.27	0.18
Central US	Onstad et al., 2000	2.50	1.33	0.82	0.12	-
Indiana, US	Dalzell et al., 2007	1.38	-	1.22	0.61	-
Mississippi R.	Gordon and Goñi, 2003	-	2.82	1.22	0.18	0.30
Amazon R.	Hedges et al., 1986	2.56-7.06	2.15-7.31	0.78-0.85	0.07-0.1	-
Estuary						
SB County	This study	2.75	2.17	2.73	0.32	0.20
Atchafalaya Delta	Gordon and Goñi, 2003	-	3.76	0.99	0.22	0.18
Marine						
SB Channel *10 – 20 m*	This study	0.47	1.08	3.03	0.10	0.59
Gulf of Mexico *10 – 25 m*	Gordon and Goñi, 2003	-	1.06	1.13	0.23	0.43
Gulf of Mexico *74 m*	Goñi et al., 1998	-	0.36	1.01	0.42	0.16
Adriatic Sea *54 m*	Tesi et al., 2008	-	0.94	0.75	0.09	-
Pacific Ocean *55 m*	Prahl et al., 1994	-	3.66	0.27	0.05	-

Appendix

Appendix Table 1: Sampling site codes with corresponding site names and environments.

Site Code	Name	Environment
AB00	Arroyo Burro	Stream
ATMY	Atascadero	Stream
BC02	Bell Canyon	Stream
GV01	Gaviota	Stream
HO00	Arroyo Hondo	Stream
MC00	Mission Creek	Stream
RG01	Refugio	Stream
SP02	San Pedro	Stream
TE03	Tecolotito	Stream
ABUR E	Arroyo Burro	Estuary
GOSL	Goleta Slough	Estuary
ABUR	Arroyo Burro	Marine
AHND	Arroyo Hondo	Marine
AQUE	Arroyo Quemado	Marine
GOLB	Goleta Bay	Marine
IVEE	Isla Vista	Marine
MICR	Mission Creek	Marine
MOHK	Mohawk	Marine
REFU	Refugio	Marine

Appendix Table 2: Lignin CuO indicators from studies using the same reference standard (SAG 05: estuarine sediment) alongside results (Louchouarn et al., 2000; Moingt et al., 2016). ND = not determinable.

	This study (n=58)		Moingt et al., 2016 (n = 13)		Louchouarn et al., 2000 (n=11)	
Lambda	3.50	0.13	3.51	0.19	3.53	0.17
Sigma 8	7.42	0.22	7.35	0.29	ND	ND
S	0.72	0.10	0.64	0.08	0.56	0.05
V	2.46	0.13	2.57	0.17	2.73	0.11
C	0.25	0.05	0.23	0.04	0.23	0.04
P	0.38	0.06	0.35	0.03	0.54	0.10
S/V	0.32	0.05	0.26	0.05	0.21	0.02
C/V	0.10	0.02	0.09	0.01	0.08	0.01
P/(V+S)	0.12	0.01	0.08	0.01	ND	ND
3,5-Bd/V	0.09	0.02	0.10	0.02	0.08	0.02
(Ac/Ad)v	0.34	0.04	0.37	0.03	0.38	0.05
(Ac/Ad)s	0.27	0.09	0.38	0.04	0.38	0.05

Appendix Table 3: Means and standard deviations for carbon, nitrogen, and lignin content.

Environment	Date		% ON	% OC	C/N	$\delta^{13}C$	$\delta^{15}N$	Lambda	Sigma 8
Stream	*01/2016*	Mean	0.33	3.64	11.03	-26.00	4.65	1.40	4.37
		± SD	0.10	1.35	2.01	0.47	1.09	0.48	1.62
	03/2016	Mean	0.35	2.88	7.96	-26.57	1.58	1.75	5.76
		± SD	0.14	1.26	1.48	0.38	1.88	0.77	4.24
	01/2017	Mean	0.18	2.16	11.38	-26.45	3.63	3.17	7.24
		± SD	0.07	1.12	1.83	0.74	0.82	0.60	4.79
Estuary	*04/2016*	Mean	0.10	1.31	12.12	-25.70	2.88	1.96	3.35
		± SD	0.06	0.93	3.63	1.79	2.28	1.14	2.88
	06/2016	Mean	0.08	1.01	12.19	-24.88	4.92	2.30	2.20
		± SD	0.06	0.81	3.68	1.57	1.63	1.55	2.23
	03/2017	Mean	0.06	0.68	9.71	-24.49	3.50	2.29	2.22
		± SD	0.06	0.69	3.95	3.25	1.99	1.02	2.27
	06/2017	Mean	0.06	0.96	11.25	-24.00	0.50	2.18	3.12
		± SD	0.07	1.03	4.21	2.02	3.12	1.50	3.63
Reef near Stream	*12/2015*	Mean	0.05	0.45	9.46	-23.27	2.12	0.97	0.55
		± SD	0.01	0.23	2.71	0.66	1.44	0.60	0.45
	06/2016	Mean	0.04	0.33	8.79	-22.19	3.54	1.22	0.45
		± SD	0.01	0.17	2.42	1.48	1.80	0.71	0.38
	03/2017	Mean	0.04	0.34	7.78	-22.68	3.36	1.15	0.43
		± SD	0.01	0.17	2.03	1.34	1.61	0.74	0.38
	06/2017	Mean	0.04	0.42	11.38	-22.61	3.83	1.35	0.60
		± SD	0.01	0.23	3.08	1.37	1.69	0.89	0.59
Reef far from Stream	*12/2015*	Mean	0.05	0.49	9.73	-22.93	2.72	0.46	0.26
		± SD	0.02	0.28	3.44	0.70	1.27	0.39	0.27
	06/2016	Mean	0.06	0.58	9.44	-22.10	4.62	0.77	0.39
		± SD	0.04	0.51	2.59	1.26	1.84	0.58	0.31
	03/2017	Mean	0.04	0.28	7.39	-22.28	3.80	0.94	0.32
		± SD	0.01	0.10	1.55	1.04	0.73	0.72	0.29
	06/2017	Mean	0.04	0.38	10.37	-22.30	3.44	1.09	0.50
		± SD	0.01	0.19	2.43	0.84	1.59	0.80	0.43

Appendix Table 3: Continued.

Environment	Date		S	V	C	P	S/V	C/V	P/(V+S)	3,5-Bd/V
Stream	*01/2016*	Mean	0.82	0.48	0.10	0.38	1.72	0.20	0.30	0.16
		± SD	0.29	0.17	0.03	0.11	0.25	0.03	0.03	0.03
	03/2016	Mean	1.25	0.40	0.10	0.34	3.19	0.21	0.22	0.20
		± SD	0.61	0.16	0.07	0.15	1.07	0.08	0.07	0.05
	01/2017	Mean	1.99	0.87	0.32	0.25	2.35	0.39	0.09	0.18
		± SD	0.39	0.25	0.11	0.13	0.24	0.14	0.02	0.09
Estuary	*04/2016*	Mean	1.30	0.55	0.11	0.33	2.43	0.19	0.21	0.19
		± SD	0.80	0.31	0.09	0.18	1.06	0.09	0.08	0.11
	06/2016	Mean	1.57	0.59	0.15	0.30	2.74	0.29	0.18	0.18
		± SD	1.09	0.41	0.08	0.15	0.51	0.11	0.10	0.16
	03/2017	Mean	1.44	0.60	0.27	0.17	2.41	0.42	0.08	0.20
		± SD	0.71	0.23	0.12	0.10	0.68	0.19	0.03	0.05
	06/2017	Mean	1.46	0.63	0.31	0.30	3.43	0.45	0.10	0.29
		± SD	0.80	0.46	0.21	0.15	2.19	0.24	0.03	0.19
Reef near Stream	*12/2015*	Mean	0.66	0.28	0.03	0.16	2.52	0.13	0.22	0.31
		± SD	0.41	0.20	0.03	0.06	0.70	0.08	0.13	0.20
	06/2016	Mean	0.86	0.34	0.02	0.19	2.89	0.07	0.20	0.52
		± SD	0.51	0.21	0.02	0.09	1.16	0.06	0.10	0.37
	03/2017	Mean	0.82	0.31	0.03	0.14	3.19	0.11	0.16	0.63
		± SD	0.56	0.23	0.03	0.10	1.70	0.10	0.12	0.68
	06/2017	Mean	0.94	0.39	0.03	0.11	2.73	0.10	0.07	0.53
		± SD	0.61	0.28	0.03	0.04	0.99	0.08	0.03	0.45
Reef far from Stream	*12/2015*	Mean	0.31	0.13	0.02	0.12	2.68	0.13	0.50	0.66
		± SD	0.26	0.12	0.02	0.05	0.92	0.08	0.53	0.62
	06/2016	Mean	0.54	0.23	0.02	0.14	3.08	0.06	0.40	1.02
		± SD	0.40	0.20	0.01	0.06	1.53	0.03	0.35	1.14
	03/2017	Mean	0.70	0.25	0.01	0.16	3.69	0.03	0.25	0.54
		± SD	0.56	0.18	0.00	0.06	2.41	0.01	0.19	0.67
	06/2017	Mean	0.79	0.29	0.03	0.11	3.54	0.11	0.06	0.72
		± SD	0.56	0.23	0.02	0.03	1.80	0.08	0.02	0.71

Appendix Table 4: Linear mixed effects model results, with significant fixed effects denoted in bold. NA indicates no fixed effects significantly predicted dependent variable values.

	Dependent variable	Fixed effect	*df*	*F*	*p*
All samples	log(Sigma 8)	Environment	2, 15	37.2017	**< 0.0001**
	Lambda	Environment	2, 15	17.1210	**0.0001**
	S/V	Environment	2, 15	1.5326	0.2479
	C/V	Environment	2, 15	32.5081	**< 0.0001**
	log(P/(V+S))	Environment	2, 8	0.3005	0.7484
	log(3,5-Bd/V)	Environment	2, 15	20.1071	**< 0.0001**
Stream samples	Sigma 8	Sampling Date	2, 13	2.2677	0.1429
		Land Use	2, 5	1.6135	0.2879
	Lambda	Sampling Date	2, 13	24.6901	**< 0.0001**
		Watershed Area	1, 7	2.2283	0.1861
	S/V	Sampling Date	2, 13	15.2543	**0.0004**
		Watershed Area	1, 6	13.7996	**0.0099**
	C/V	Sampling Date	2, 13	10.5296	**0.0019**
	P/(V+S)	Sampling Date	2, 13	52.0267	**< 0.0001**
	3,5-Bd/V	Land Use	2, 5	3.2429	0.1250
Estuary samples	Sigma 8	NA	-	-	-
	Lambda	Core Section	1, 47	1.9916	0.1648
	S/V	NA	-	-	-
	C/V	Sampling Date	3, 41	7.8450	**0.0003**
	P/(V+S)	Sampling Date	3, 37	11.7140	**< 0.0001**
		Core Section	1, 37	44.8840	**< 0.0001**
	3,5-Bd/V	NA	-	-	-
Marine samples	log(Sigma 8)	Sampling Date	3, 349	2.9342	**0.0335**
		Proximity to Stream	1, 6	1.6298	0.2489
		Water Depth	1, 349	197.8010	**< 0.0001**
		Core Section	1, 349	21.2051	**< 0.0001**
	Lambda	Sampling Date	3, 350	5.6297	**0.0009**
		Proximity to Stream	1, 6	4.7903	0.0712
		Water Depth	1, 350	52.9663	**< 0.0001**
		Core Section	1, 350	14.6094	**0.0002**
	S/V	Sampling Date	3, 341	3.4675	**0.0165**

Appendix Table 4: Continued.

	Dependent variable	Fixed effect	*df*	*F*	*p*
Marine samples	S/V	Water Depth	1, 341	32.0514	< **0.0001**
		Core Section	1, 341	2.3464	0.1265
	C/V	Sampling Date	3, 304	7.2969	**0.0001**
		Water Depth	1, 304	4.2855	**0.0393**
	P/(V+S)	Sampling Date	3, 259	55.5687	< **0.0001**
		Proximity to Stream	1, 6	11.9519	**0.0135**
		Water Depth	1, 259	51.1973	< **0.0001**
		Core Section	1, 259	10.9208	**0.0011**

References

Aguilera, R., Melack, J. M., 2018a. Concentration-discharge responses to storm events in coastal California watersheds. *Water Resources Research* 54, 407–424. https://doi.org/10.1002/2017WR021578

Aguilera, R., Melack, J. M., 2018b. Relationships among nutrient and sediment fluxes, hydrological variability, fire, and land cover in coastal California catchments. *Journal of Geophysical Research: Biogeosciences* 123, 2568–2589. https://doi.org/10.1029/2017JG004119

Airoldi, L., Fabiano, M., Cinelli, F., 1996. Sediment deposition and movement over a turf assemblage in a shallow rocky coastal area of the Ligurian Sea. *Marine Ecology Progress Series* 133, 241–251.

Battalio, B., Behrens, D., Couch, R., Divita, E., Hubbard, D., Lowe, J., Revell, D., Saley, P., 2015. Goleta Slough Area Sea Level Rise and Management Plan. Environmental Science Associates.

Bélanger, E., Lucotte, M., Gregoire, B., Moingt, M., Paquet, S., Davidson, R., Mertens, F., Passos, C.J.S., Romana, C., 2015. Lignin signatures of vegetation and soils in tropical environments. *Advances in Environmental Research* 4, 247–262. https://doi.org/10.12989/aer.2015.4.4.247

Bélanger, É., Lucotte, M., Moingt, M., Paquet, S., Oestreicher, J., Rozon, C., 2017. Altered nature of terrestrial organic matter transferred to aquatic systems following deforestation in the Amazon. *Applied Geochemistry* 87, 136–145. https://doi.org/10.1016/j.apgeochem.2017.10.016

Benner, R., Fogel, M. L., Sprague, E. K., Hodson, R. E., 1987. Depletion of 13C in lignin and its implications for stable carbon isotope studies. *Nature* 329, 708–710. https://doi.org/10.1038/329708a0

Billen, G. C., Lancelot, C., Meybeck, M., 1991. N, P, and Si retention along the aquatic continuum from land to ocean, in: Mantoura, R.F.C., Martin, J.-M., Wollast, R. (Eds.), *Ocean Margin Processes in Global Change*. Wiley, pp. 19–44.

Blair, N. E., Aller, R. C., 2012. The fate of terrestrial organic carbon in the marine environment. *Annual Review of Marine Science* 4, 401–423. https://doi.org/10.1146/annurev-marine-120709-142717

Brzezinski, M., Reed, D., Harrer, S., Rassweiler, A., Melack, J., Goodridge, B., Dugan, J., 2013. Multiple sources and forms of nitrogen sustain year-round kelp growth on the inner continental shelf of the Santa Barbara Channel. *Oceanography* 26, 114–123. https://doi.org/10.5670/oceanog.2013.53

Burdige, D. J., 2005. Burial of terrestrial organic matter in marine sediments: A re-assessment. *Global Biogeochemical Cycles* 19, GB4011. https://doi.org/10.1029/2004GB002368

Chaves, L. F., 2010. An entomologist guide to demystify pseudoreplication: Data analysis of field studies With design constraints. *Journal of Medical Entomology* 47, 291–298. https://doi.org/10.1093/jmedent/47.1.291

Chen, S., Torres, R., 2018. Biogeochemical characteristics and fluxes of suspended particulate organic matter in response to low-tide rainfall: Rainfall-driven POM fluxes and characteristics. *Limnology and Oceanography* 63, S307–S323. https://doi.org/10.1002/lno.10741

Coombs, J. S., Melack, J. M., 2013. Initial impacts of a wildfire on hydrology and suspended sediment and nutrient export in California chaparral watersheds: Wildfire Impacts On Hydrology And Export. *Hydrological Processes* 27, 3842–3851. https://doi.org/10.1002/hyp.9508

Cotner, J. B., Johengen, T. H., Biddanda, B. A., 2000. Intense winter heterotrophic production stimulated by benthic resuspension. *Limnology and Oceanography* 45, 1672–1676. https://doi.org/10.4319/lo.2000.45.7.1672

Dalzell, B. J., Filley, T. R., Harbor, J. M., 2007. The role of hydrology in annual organic carbon loads and terrestrial organic matter export from a midwestern agricultural watershed. *Geochimica et Cosmochimica Acta* 71, 1448–1462. https://doi.org/10.1016/j.gca.2006.12.009

Dittmar, T., Lara, R. J., 2001. Molecular evidence for lignin degradation in sulfate-reducing mangrove sediments (Amazônia, Brazil). *Geochimica et Cosmochimica Acta* 65, 1417–1428. https://doi.org/10.1016/S0016-7037(00)00619-0

Feng, D., Beighley, E., Raoufi, R., Melack, J., Zhao, Y., Iacobellis, S., Cayan, D., 2019. Propagation of future climate conditions into hydrologic response from coastal southern California watersheds. *Climatic Change* 153, 199-218. https://doi.org/10.1007/s10584-019-02371-3

Fewings, M. R., Washburn, L., Ohlmann, J. C., 2015. Coastal water circulation patterns around the Northern Channel Islands and Point Conception, California. *Progress in Oceanography* 138, 283–304. https://doi.org/10.1016/j.pocean.2015.10.001

Fong, C. R., Fong, P., 2018. Nutrient fluctuations in marine systems: Press versus pulse nutrient subsidies affect producer competition and diversity in estuaries and coral reefs. *Estuaries and Coasts* 41, 421–429. https://doi.org/10.1007/s12237-017-0291-5

Godin, P., Macdonald, R. W., Kuzyk, Z. Z. A., Goñi, M. A., Stern, G. A., 2017. Organic matter compositions of rivers draining into Hudson Bay: Present-day trends and potential as recorders of future climate change: Lignins in Hudson Bay Rivers. *Journal of Geophysical Research: Biogeosciences* 122, 1848–1869. https://doi.org/10.1002/2016JG003569

Goñi, M. A., Hedges, J. I., 1995. Sources and reactivities of marine-derived organic matter in coastal sediments as determined by alkaline CuO oxidation. *Geochimica et Cosmochimica Acta* 59, 2965–2981.

Goñi, M. A., Montgomery, S., 2000. Alkaline CuO oxidation with a microwave digestion system: Lignin analyses of geochemical samples. *Analytical Chemistry* 72, 3116–3121. https://doi.org/10.1021/ac991316w

Goñi, M. A., Ruttenberg, K. C., Eglinton, T. I., 1998. A reassessment of the sources and importance of land-derived organic matter in surface sediments from the Gulf of Mexico. *Geochimica et Cosmochimica Acta* 62, 3055–3075. https://doi.org/10.1016/S0016-7037(98)00217-8

Google Earth Pro, 2019.

Gordon, E. S., Goñi, M. A., 2003. Sources and distribution of terrigenous organic matter delivered by the Atchafalaya River to sediments in the northern Gulf of Mexico. *Geochimica et Cosmochimica Acta* 67, 2359–2375. https://doi.org/10.1016/S0016-7037(02)01412-6

Harms, S., Winant, C. D., 1998. Characteristic patterns of the circulation in the Santa Barbara Channel. *Journal of Geophysical Research: Oceans* 103, 3041–3065. https://doi.org/10.1029/97JC02393

Hedges, J. I., Blanchette, R. A., Weliky, K., Devol, A. H., 1988. Effects of fungal degradation on the CuO oxidation products of lignin: A controlled laboratory study. *Geochimica et Cosmochimica Acta* 52, 2717–2726.

Hedges, J. I., Clark, W. A., Quay, P. D., Richey, J. E., Devol, A. H., Santos, U. de M., 1986. Compositions and fluxes of particulate organic material in the Amazon River. *Limnology and Oceanography* 31, 717–738.

Hedges, J. I., Ertel, J. R., 1982. Characterization of lignin by gas capillary chromatography of cupric oxide oxidation products. *Analytical Chemistry* 54, 174–178. https://doi.org/10.1021/ac00239a007

Hedges, J. I., Keil, R. G., Benner, R., 1997. What happens to terrestrial organic matter in the ocean? *Organic Geochemistry* 27, 195–212. https://doi.org/10.1016/S0146-6380(97)00066-1

Hedges, J. I., Mann, D. C., 1979a. The characterization of plant tissues by their lignin oxidation products. *Geochimica et Cosmochimica Acta* 43, 1803–1807. https://doi.org/10.1016/0016-7037(79)90028-0

Hedges, J. I., Mann, D. C., 1979b. The lignin geochemistry of marine sediments from the southern Washington coast. *Geochimica et Cosmochimica Acta* 43, 1809–1818. https://doi.org/10.1016/0016-7037(79)90029-2

Hedges, J. I., Parker, P., 1976. Land-derived organic matter in surface sediments from the Gulf of Mexico. *Geochimica et Cosmochimica Acta* 40, 1019–1029.

Hernes, P. J., Robinson, A. C., Aufdenkampe, A. K., 2007. Fractionation of lignin during leaching and sorption and implications for organic matter "freshness." *Geophysical Research Letters* 34. https://doi.org/10.1029/2007GL031017

Hothorn, T., Bretz, F., Westfall, P., Heiberger, R. M., Schuetzenmeister, A., Scheibe, S., 2017. multcomp: Simultaneous inference in general parametric models.

Houel, S., Louchouarn, P., Lucotte, M., Canuel, R., Ghaleb, B., 2006. Translocation of soil organic matter following reservoir impoundment in boreal systems: Implications for in situ productivity. *Limnology and Oceanography* 51, 1497–1513. https://doi.org/10.4319/lo.2006.51.3.1497

Klap, V. A., Hemminga, M. A., Boon, J. J., 2000. Retention of lignin in seagrasses: angiosperms that returned to the sea. *Marine Ecology Progress Series* 194, 1–11. https://doi.org/10.3354/meps194001

Louchouarn, P., Amon, R. M. W., Duan, S., Pondell, C., Seward, S. M., White, N., 2010. Analysis of lignin-derived phenols in standard reference materials and ocean dissolved organic matter by gas chromatography/tandem mass spectrometry. *Marine Chemistry* 118, 85–97. https://doi.org/10.1016/j.marchem.2009.11.003

Louchouarn, P., Lucotte, M., Farella, N., 1999. Historical and geographical variations of sources and transport of terrigenous organic matter within a large-scale coastal environment. *Organic Geochemistry* 30, 675–699.

Louchouarn, P., Opsahl, S., Benner, R., 2000. Isolation and quantification of dissolved lignin from natural waters using solid-phase extraction and GC/MS. *Analytical Chemistry* 72, 2780–2787. https://doi.org/10.1021/ac9912552

Martone, P. T., Estevez, J. M., Lu, F., Ruel, K., Denny, M. W., Somerville, C., Ralph, J., 2009. Discovery of lignin in seaweed reveals convergent evolution of cell-wall architecture. *Current Biology* 19, 169–175. https://doi.org/10.1016/j.cub.2008.12.031

Masson-Delmotte, V., Zhai, P., Pörtner, H.O., Roberts, D., Skea, J., Shukla, P. R., Pirani, A., Moufouma-Okia, W., Péan, C., Pidcock, R., Connors, S., Matthews, J. B. R., Chen, Y., Zhou, X., Gomis, M. I., Lonnoy, E., Maycock, T., Tignor, M., Waterfield, T. (ed.), 2018. Global Warming of 1.5ºC. An IPCC Special Report on the impacts of global warming of 1.5°C above pre-industrial levels and related global greenhouse gas emission pathways, in the context of strengthening the global response to the threat of climate change, sustainable development, and efforts to eradicate poverty. Intergovernmental Panel on Climate Change. https://www.ipcc.ch/sr15/.

McClain, M. E., Boyer, E. W., Dent, C. L., Gergel, S. E., Grimm, N. B., Groffman, P. M., Hart, S. C., Harvey, J. W., Johnston, C. A., Mayorga, E., McDowell, W. H., Pinay, G., 2003. Biogeochemical hot spots and hot moments at the interface of terrestrial and aquatic ecosystems. *Ecosystems* 6, 301–312. https://doi.org/10.1007/s10021-003-0161-9

Melack, J., 2019. SBC LTER: Land: Stream chemistry in the Santa Barbara Coastal drainage area, ongoing since 2000 ver 16. Santa Barbara Coastal Long Term Ecological Research Project. https://doi.org/10.6073/pasta/67a558a24ceed9a0a5bf5e46ab841174.

Millar, R. B., Anderson, M. J., 2004. Remedies for pseudoreplication. *Fisheries Research* 70, 397–407. https://doi.org/10.1016/j.fishres.2004.08.016

Moingt, M., Lucotte, M., Paquet, S., 2016. Lignin biomarkers signatures of common plants and soils of Eastern Canada. *Biogeochemistry* 129, 133–148. https://doi.org/10.1007/s10533-016-0223-7

Moingt, M., Lucotte, M., Paquet, S., Ghaleb, B., 2014. Deciphering the impact of land-uses on terrestrial organic matter and mercury inputs to large boreal lakes of central Québec using lignin biomarkers. *Applied Geochemistry* 41, 34–48. https://doi.org/10.1016/j.apgeochem.2013.11.008

Murphy, S. F., Writer, J. H., McCleskey, R. B., Martin, D. A., 2015. The role of precipitation type, intensity, and spatial distribution in source water quality after wildfire. *Environmental Research Letters* 10, 084007. https://doi.org/10.1088/1748-9326/10/8/084007

Onstad, G. D., Canfield, D. E., Quay, P. D., Hedges, J. I., 2000. Sources of particulate organic matter in rivers from the continental USA: lignin phenol and stable carbon isotope compositions. *Geochimica et Cosmochimica Acta* 64, 3539–3546. https://doi.org/10.1016/S0016-7037(00)00451-8

Opsahl, S., Benner, R., 1995. Early diagenesis of vascular plant tissues: lignin and cutin decomposition and biogeochemical implications. *Geochimica et Cosmochimica Acta* 59, 4889–4904.

Opsahl, S., Benner, R., 1997. Distribution and cycling of terrigenous dissolved organic matter in the ocean. *Nature* 386, 480–482.

Page, H., Reed, D., Brzezinski, M., Melack, J., Dugan, J., 2008. Assessing the importance of land and marine sources of organic matter to kelp forest food webs. *Marine Ecology Progress Series* 360, 47–62. https://doi.org/10.3354/meps07382

Page, H. M., Lowman, H. E., Melack, J. M., Smith, J. M., Reed, D. C., 2018. SBC LTER: OCEAN: Particulate organic matter content and composition of stream, estuarine, and marine sediments. *Environmental Data Initiative*. https://doi.org/10.6073/pasta/05ca288d720310 7bddab618e95524c0a.

Pinheiro, J., Bates, D., DebRoy, S., Sarkar, D., Heisterkamp, S., Van Willigen, B., 2019. nlme: Linear and nonlinear mixed effects models.

Poppe, L. J., Eliason, A. H., Fredericks, J. J., Rendigs, R. R., Blackwood, D., Polloni, C. F., 2000. USGS East-Coast Sediment Analysis: Procedures, Database, and Georeferenced Displays (Open-File No. 00–358). U.S. Geological Survey.

Prahl, F. G., Ertel, J. R., Goni, M. A., Sparrow, M. A., Eversmeyer, B., 1994. Terrestrial organic carbon contributions to sediments on the Washington margin. *Geochimica et Cosmochimica Acta 58*, 3035–3048.

Revell, D. L., Dugan, J. E., Hubbard, D. M., 2011. Physical and ecological responses of sandy beaches to the 1997-98 El Niño. *Journal of Coastal Research* 27, 718–730. https://doi.org/10.2112/JCOASTRES-D-09-00179.1

Santa Barbara County Flood Control District, 2019. Official Daily Rainfall Record. http://www.countyofsb.org/pwd/hydrology.sbc.

Savage, C., Thrush, S. F., Lohrer, A. M., Hewitt, J. E., 2012. Ecosystem services transcend boundaries: Estuaries provide resource subsidies and influence functional diversity in coastal benthic communities. *PLoS ONE* 7, e42708. https://doi.org/10.1371/journal.pone.0042708

Sommerfield, C. K., Lee, H. J., Normark, W. R., 2009. Postglacial sedimentary record of the Southern California continental shelf and slope, Point Conception to Dana Point, in:

Earth Science in the Urban Ocean: The Southern California Continental Borderland. Geological Society of America. https://doi.org/10.1130/2009.2454(2.5)

Sun, S., Schefuß, E., Mulitza, S., Chiessi, C. M., Sawakuchi, A. O., Zabel, M., Baker, P. A., Hefter, J., Mollenhauer, G., 2017. Origin and processing of terrestrial organic carbon in the Amazon system: lignin phenols in river, shelf, and fan sediments. *Biogeosciences* 14, 2495–2512. https://doi.org/10.5194/bg-14-2495-2017

Tesi, T., Langone, L., Goñi, M. A., Turchetto, M., Miserocchi, S., Boldrin, A., 2008. Source and composition of organic matter in the Bari canyon (Italy): Dense water cascading versus particulate export from the upper ocean. *Deep Sea Research Part I: Oceanographic Research Papers* 55, 813–831. https://doi.org/10.1016/j.dsr.2008.03.007

Thevenot, M., Dignac, M.-F., Rumpel, C., 2010. Fate of lignins in soils: A review. *Soil Biology and Biochemistry* 42, 1200–1211. https://doi.org/10.1016/j.soilbio.2010.03.017

Warrick, J. A., Melack, J. M., Goodridge, B. M., 2015. Sediment yields from small, steep coastal watersheds of California. *Journal of Hydrology: Regional Studies* 4, 516–534. https://doi.org/10.1016/j.ejrh.2015.08.004

Washburn, L., Brzezinski, M. A., Carlson, C. A., Siegel, D.A ., 2019. SBC LTER: Ocean: Ocean currents and biogeochemistry: Nearshore water profiles (monthly CTD and chemistry). Santa Barbara Coastal Long Term Ecological Research Project, *Environmental Data Initiative*. https://doi.org/10.6073/pasta/b73d76d8d1465207be6d7fed19291fda.

Wickham, H., Averick, M., Bryan, J., Chang, W., D'Agostino McGowan, L., François, R., Grolemund, G., Hayes, A., Henry, L., Hester, J., Kuhn, M., Lin Pedersen, T., Miller, E., Milton Bache, S., Müller, K., Ooms, J., Robinson, D., Paige Seidel, D., Spinu, V., Takahashi, K., Vaughan, D., Wilke, C., Woo, K., Yutani, H., 2019. Welcome to the Tidyverse. *Journal of Open Source Software* 4, 1686. https://doi.org/10.21105/joss.01686

Xenopoulos, M. A., Downing, J. A., Kumar, M. D., Menden-Deuer, S., Voss, M., 2017. Headwaters to oceans: Ecological and biogeochemical contrasts across the aquatic continuum. *Limnology and Oceanography* 62, 3-14. https://doi.org/10.1002/lno.10721

Zuur, A. F. (Ed.), 2009. *Mixed effects models and extensions in ecology with R, Statistics for biology and health*. Springer, New York, NY.

CHAPTER 5:

NUTRITIONAL QUALITY OF GIANT KELP DECLINES DUE TO WARMING OCEAN TEMPERATURES

Abstract:

Giant kelp forms extensive forests on temperate reefs, providing habitat and food for a diversity of marine life. Kelp biomass varies in response to changing ocean temperatures, but physiological responses as reflected by the nutritional quality of tissue are not well understood. Over a 17-year period in southern California, we found that nitrogen content of giant kelp tissue declined by ~25%, while carbon content proportionally increased. This decline in nutritional quality was associated with increasing seawater temperatures and the North Pacific Gyre Oscillation. Changes in kelp stoichiometry have important implications for key consumers, such as sea urchins. Our results suggest climate change will affect the physiology of giant kelp, and the consequences of declines in kelp abundance may be compounded by reductions in nutritional quality.

Introduction

Kelp forests are highly productive ecosystems in temperate coastal seas (Steneck et al., 2002) and are a foundation species that structures the surrounding community (Falkenberg et al., 2012; Miller et al., 2018). Kelp forests provide numerous ecological functions including habitat, food resources, nutrient cycling, subsidies to other habitats, and supporting biodiversity (Dayton, 1985; Steneck et al., 2002). Grazers, such as sea urchins, abalone, crustaceans, and gastropods, feed directly on kelp while many other organisms rely

on kelp-derived carbon via indirect pathways (Yorke et al., 2019). More than 80% of kelp forest net primary production is exported as detritus to adjacent marine ecosystems (Cebrian, 1999; Krumhansl and Scheibling, 2012) where it becomes a valuable habitat and food resource (Vetter and Dayton, 1999; Dugan et al., 2003). The availability of kelp as a resource, both within the kelp forest and as a subsidy to adjacent ecosystems, may be threatened as the growing effects of global climate change on primary productivity and ocean circulation are realized (Harley et al., 2006).

Global temperatures have risen significantly in recent decades, and while greater warming has occurred over land, nearly all sea surface temperatures are warmer today relative to a century ago (Hansen et al., 2006). The upper ocean (0-700 m) has warmed significantly since 1970, especially in the Pacific Ocean (Abraham et al., 2013). With continued ocean warming, projections indicate declines in marine biomass at all trophic levels and reduced primary production (Lotze et al., 2019). Temperate coastal ecosystems and their associated flora and fauna are sensitive to warming events, which have produced dramatic change in some regions (Rogers-Bennett and Catton, 2019; Thomsen et al., 2019), including declines in kelp abundance and biomass (Johnson et al., 2011; Raybaud et al., 2013). Such episodic warming events may foreshadow and enhance the projected effects of long-term climate change over easily observed timescales (Di Lorenzo and Mantua, 2016; Smale et al., 2019).

Marine macroalgae form the base of aquatic food webs, thus the effect of climate change on the abundance and nutritional quality of macroalgae is likely to have trophic implications (Harley et al., 2012). Evaluation of changes in macroalgal nutritional quality in the context of abiotic factors like temperature are poorly constrained and often derived from

controlled experiments rather than *in situ* field conditions. Findings from studies of macroalgae grown in warmer seawater have ranged widely, from no effect (Simonson et al., 2015) to mixed effects (Phelps et al., 2017), including increased nitrogen content (Wilson et al., 2015). The nutritional content of macroalgae affect herbivore feeding preference (Van Alstyne et al., 2009), consumption rates (Boyer et al., 2004), and the physiological performance of consumers (Hemmi and Jormalainen, 2002).

Long-term ecological data collection provides a means of exploring questions regarding the *in situ* effects of prolonged and episodic warming events on marine ecosystems. Using data collected as part of the Santa Barbara Coastal Long Term Ecological Research program, we evaluate the nutritional quality (C:N) of giant kelp (*Macrocystis pyrifera*) at reefs off southern California over a 17-year period, and its relationship with local sea surface temperature and Pacific-basin scale ocean climate. Prior analyses showed gradually declining kelp biomass at local reefs over this time period, in addition to pronounced effects on some components of kelp forest and intertidal communities due to an anomalous Pacific warming event (Reed et al., 2016). Kelp canopy cover in the region is temporally and spatially variable, and responses to environmental conditions or perturbations may vary significantly on local and regional scales (Bell et al., 2015). We predict that the nutritional quality of giant kelp tissue declined over the same period that local biomass declined and hypothesize how such change may have compounding effects on kelp forest ecosystems and consumers as well as the ecosystems subsidized by exported kelp production.

Methods

Research conducted by the Santa Barbara Coastal Long Term Ecological Research (SBC LTER) project is based in the Santa Barbara Channel, California, USA (34° 24.300'N 119° 50.650'W). The SBC LTER maintains long-term datasets on giant kelp (*Macrocystis pyrifera*) production along with associated macroalgal and faunal communities. Carbon (C) and nitrogen (N) content of giant kelp blades were measured monthly at three long-term kelp forest monitoring sites (Arroyo Burro, Mohawk and Arroyo Quemado). In this study we used % C, % N, and C:N values for giant kelp measured monthly from May 2002 through July 2019; all %C and %N values refer to content as a percent of dry mass, and C:N values are also mass-based (Reed, 2019). At each site, a surface kelp blade was collected one to two meters back from the growing tip of 15 different individual plants. The blades were scraped to remove epiphytes and a core (2.9cm diameter) was taken from each blade near the pneumatocyst. The cores were dipped in 10% HCl and rinsed with deionized water to remove residual calcium carbonate. The cores were then dried at 60˚ C for a minimum of 48 hours and ground into a homogenous sample. The homogenized samples from each site were analyzed in duplicate for C and N content using an elemental analyzer (CE440 Elemental Analyzer, precision ±0.3%).

We analyzed several oceanographic indices as potential drivers of kelp C:N ratios. Linear regression analyses of mean monthly C:N values through time were conducted for the entire dataset, as well as the period prior to the warming event that began in 2013 (all data up to December 2012). Linear regression analyses were performed for mean monthly C:N values versus the Pacific Decadal Oscillation, the Madden Julian Oscillation, the El Nino Southern Oscillation, the Upwelling Index, the North Pacific Gyre Oscillation (NPGO) (Di Lorenzo et al., 2008), and local (daily, 1km gridded) satellite-derived sea surface temperature

(SST) (National Climatic Data Center, 2007; JPL MUR MEaSUREs Project, 2015). Among the Pacific basin-scale indices explored, the NPGO was the best predictor of C:N values. It is a monthly index and was compared to corresponding C:N values with no temporal lag. SST values were averaged by month and again compared to C:N values with no temporal lag. Local ocean temperature was used in analyses as prior research has shown it is strongly correlated to local nutrient availability (Brzezinski et al., 2013) and kelp growth (Cavanaugh et al., 2011; Cavanaugh et al., 2019). All analyses were conducted in R (R Core Team, 2016) using the 'tidyverse' package (Wickham, 2019).

Results

Mean values of annual carbon to nitrogen (C:N) ratios of giant kelp blades collected from 2002 through 2019 ranged from 6.6 to 48.2 and increased by approximately 0.5 per year ($F(204) = 25.65$, $R^2 = 0.11$, Pearson's $R = 0.33$, $p < 0.0001$, *Figure 1A*). Mean annual values frequently exceeded 20, especially during the warming event (2013-2015) (Di Lorenzo and Mantua, 2016). Prior to the marine heat wave, C:N values of giant kelp were trending upwards ($p < 0.0001$, *Supplemental Figure 3*). Our results suggest that the average C:N content of giant kelp blade tissue has increased from 12.5 to 20 since data collection began in 2002.

The combination of a significant increase in carbon content ($F(204) = 67.94$, $R^2 = 0.25$, Pearson's $R = 0.50$, $p < 0.0001$, *Figure 1B*) and a significant decrease in nitrogen content ($F(204) = 6.56$, $R^2 = 0.03$, Pearson's $R = -0.18$, $p = 0.01$, *Figure 1C*) drove the rise in C:N ratios of giant kelp blade tissue. Mirroring C:N values, carbon content of kelp was greatest from 2013 and 2015, with monthly values routinely exceeding 35% of dry mass.

Nitrogen content was lowest during these same years, and mean monthly values regularly fell below more typical values, 2% to 2.5%, to 1.5% of dry mass. From September 2013 to August 2015, the nitrogen content of multiple samples of kelp fell below 1.1% of dry mass (n = 27) which is considered the threshold at which kelp has exhausted its internal nitrogen reserves (Gerard, 1982). Our results suggest the overall carbon content of giant kelp increased by approximately 25% (29% to 35%) over the past 17 years while overall nitrogen content decreased by approximately 25% (2.5% to 2%).

The availability of dissolved inorganic nitrogen, specifically nitrate, in coastal waters off southern California is driven largely by three dominant oceanographic seasons: December through March, when winter storms cause strong wave action and significant runoff from land to sea; March through May, when wind-driven coastal upwelling delivers nutrient-rich deep waters to the photic zone; and June through November, when warm, stratified conditions can lead to relatively low concentrations of nitrate (NO_3^-) (McPhee-Shaw et al., 2007) and kelp rely on reduced forms of nitrogen (Brzezinski et al., 2013). As a result of this marked seasonality, nitrogen content in kelp tissue displays a strong annual cycle, whereas carbon content does not (Brzezinski et al., 2013). Low tissue nitrogen concentrations in summer influenced the overall trend of increasing C:N values in giant kelp. During the months of July and August, a significant increase in mean C:N of giant kelp was evident between 2002 and 2019 ($p \leq 0.01$, *Figure 2*). In January, kelp also had a significant increase in mean values of C:N over time ($p = 0.02$, *Figure 2*). For the remaining months of the year, relationships between C:N content of giant kelp and year were not significant (*Figure 2*).

Having established that a strong temporal trend in C and N content exists for local populations of giant kelp, we investigated relationships between C:N ratios and abiotic

environmental factors. In southern California, dissolved nutrient concentrations, specifically nitrate, are negatively correlated with seawater temperature through all oceanographic seasons (Zimmerman and Kremer, 1984). C:N values of giant kelp tissue were positively correlated with satellite-derived sea surface temperature ($F(204) = 181.6$, $R^2 = 0.47$, Pearson's $R = 0.69$, $p < 0.0001$, *Figure 3*). This relationship indicates that for every degree (°C) that seawater warms, the C:N content of kelp blade tissue increases by a value of approximately 2 units.

In addition to local seawater temperature, C:N values of giant kelp were negatively correlated with the regional scale North Pacific Gyre Oscillation (NPGO) index ($p < 0.0001$, *Figure 4*). The NPGO index values can be used to explain variations in salinity, nutrients, and chlorophyll-a in the California Current, with larger index values associated with greater circulation and upwelling (Di Lorenzo et al., 2008). Previous analyses found temperature (and nutrient content by proxy) as well as NPGO values to be significant predictors of giant kelp canopy biomass (Bell et al., 2015). Our findings suggest that local seawater temperature, as well as the dynamics of the regional ocean climate, as described by the NPGO, are also significant predictors of C:N content in giant kelp tissue. Analyses involving monthly C:N values versus the Pacific Decadal Oscillation, the Madden Julian Oscillation, the El Nino Southern Oscillation, and the Upwelling Index did not yield significant results and are not presented here.

Discussion

Kelp nutritional state, quantified as C:N content, declined when kelp was exposed to warmer seawater temperatures and has declined by ~50% over a nearly two decade study

period. This study, from 2002 to 2019, is the first to quantify kelp nutritional status with more than a few years of data and indicates the variations in C:N ratios encompass the range over all other kelp species (6 to 60; *Table 1*). This variability may contribute to explaining the fluctuations, observed globally, in kelp biomass correlated over long time periods with ocean climate (Bell et al., 2015; Pfister et al., 2018). These changes, quantified locally, highlight the need to track the nutritional quality of kelps, a key basal resource for many ecosystems and species, elsewhere.

The increase in C:N values means that nutritional quality of the kelp available to consumers has declined over the past 17 years. This finding has implications for kelp forest food webs and for food webs of recipient ecosystems that rely on exported kelp (*Figure 5*) including sandy beaches (Dugan et al., 2003) and deep water benthos (Vetter and Dayton, 1999). In ecosystems where primary producers have high nutritional quality, trophic transfers are more efficient and consumers more productive; therefore, nutritional quality can shape the extent of top-down control by consumers and other processes such as nutrient recycling and carbon accumulation (Cebrian, 1999; Cebrian et al., 2009). Decreased nutritional quality may result in compensatory feeding by consumers (Cruz-Rivera and Hay, 2000); that is they eat a greater quantity of the same food to compensate for reduction in nutritional quality. This behavior can affect the probability of an ecosystem state change, such as shifts from kelp forest to urchin barren, which have been observed following reductions in ecosystem nutrient status elsewhere (Boada et al., 2017).

Our results show that values of C:N in giant kelp blade tissue are significantly correlated with oceanographic conditions, specifically seawater temperature and the NPGO index which is indicative of the extent of upwelling. These findings, combined with the

predicted increase in the frequency of ocean warming events (Hoegh-Guldberg et al., 2018), suggest a future where key marine primary producers, such as kelp, may not only be lower in abundance but also have significantly reduced nutritional value. Warming periods can cause large declines in kelp forest size, at least in some regions (Johnson et al., 2011; Raybaud et al., 2013), as well as reduce the resilience of kelp to disturbance events, such as wave action or grazing by consumers (Wernberg et al., 2010). Our results imply that the nutritional content of giant kelp may also decline significantly with warming elsewhere. This decline may be due to giant kelp's inability to store nitrogen reserves for longer than approximately three weeks (Gerard, 1982). In addition to short-term warming events, our findings suggest that decadal trends in the NPGO index may be associated with reductions in the nutritional quality of kelp tissue. Since 1950, the variance of the NPGO index has increased from ±2 to ±3 standard units (Di Lorenzo et al., 2008). If the variance of the NPGO index continues to amplify, our results suggest that the C:N values of giant kelp tissue will oscillate in response, magnifying the effect of more frequent warming events on both kelp abundance and nutritional quality. Greater amplification suggests longer time periods between oscillations, which, in the case of less frequent upwelling conditions, could lead to longer periods of nutritional decline and greater difficulty for kelp recovery. The response of primary consumers and higher trophic levels to variation in C:N values of kelp will likely vary depending on the timescales at which kelp nutritional quality changes and with the life history and demography of the consumer species.

As a foundation species, giant kelp provides physical structure and habitat to a diverse assemblage of reef-associated species (Steneck et al., 2002; Miller et al., 2018) and food resources to many herbivores and detritivores (Yorke et al., 2019). Sea urchins and

abalone, for example, depend on kelp as their main food source, and both are important components of the kelp forest food web (Dayton, 1985). Both taxa are targeted by commercial and recreational fisheries. In California, red urchins (*Strongylocentrotus franciscanu*s) are harvested for their roe in one of the state's most valuable fisheries (California Department of Fish and Wildlife, 2013). Urchin growth and gonad quality are dependent on food quality (McBride et al., 2004) and sea water temperature (Azad et al., 2011), which we found were negatively correlated in the Santa Barbara Channel (*Figure 3*). Similarly, growth rates of abalone are sensitive to water temperature and food quantity and quality (Vilchis et al., 2005).

Greater dietary protein content is directly linked to greater wet weight, gonad size, and test sizes of sea urchins (Hammer et al., 2012) as well as greater body weight and shell size of abalone (Naidoo et al., 2006). Our data show that giant kelp nitrogen content ranged from 0.66% to 4.36% of dry mass, which translates to a range in protein content of 3.3% to 21.8%, using the seaweed-specific conversion factor of 5 (Angell et al., 2016). Mean annual nitrogen content of giant kelp declined from roughly 2.5% to 2.0% of dry mass over the course of this study, corresponding to a 25% decline in protein content from 12.5% to 10%. This implies that sea urchins, abalone, and other consumers would need to ingest 25% more kelp to receive the same nutritional benefit.

As the nutritional quality of kelp declines with warming, the implications will extend beyond the kelp forest and its associated fisheries by impacting ecosystems subsidized by kelp production. Most annual kelp production becomes detritus (Krumhansl and Scheibling, 2012) that fuels the kelp forest food web and adjacent, recipient ecosystems (*Figure 5*). On sandy beaches, kelp wrack inputs influence the abundance and biomass of macroinvertebrate

kelp consumers, which support higher trophic levels, such as shorebirds (Dugan et al., 2003). Exported kelp is similarly important to deep water benthos, including urchins and other invertebrates (Filbee-Dexter and Scheibling, 2014) as well as deep-sea canyon communities (Vetter and Dayton, 1999).

In summary, our results suggest that giant kelp has experienced a nearly 50% decline in the nutritional quality of blade tissue (C:N) over the course of 17 years. Reductions in kelp nutritional quality, in addition to declines in kelp biomass, in response to increased sea surface temperatures have serious implications for kelp forest food webs and kelp-subsidized ecosystems. Long-term studies of marine ecosystems need to consider food quality in addition to primary production when projecting the responses of ecosystem structure and function to changing ocean climate.

Tables and Figures

Table 1: Published values of tissue C:N (as a function of dry sample mass) for 9 globally-distributed kelp genera from *in situ* as well as laboratory studies and covering all major ocean basins. Only C:N values measured from *in situ* samples or un-manipulated experimental treatments were included. See supplemental materials for full reference list. We present the total range of C:N values reported for each kelp species, and studies where C:N was measured over a period greater than 1 year (12 months) are indicated with an asterisk (*).

Genus	Species	C:N	Sources
Alaria	*crassifolia*	8.9	Johnston, 1971
A.	*esculenta*	23 - 30	Gordillo et al., 2006; Gordillo et al., 2015
A.	*marginata*	12.5 - 14.5	Pelletreau and Muller-Parker, 2002; McDonald and Bingham, 2010
Durvillaea	*antarctica*	30	Suárez-Jiménez et al., 2017
Ecklonia	*radiata*	17 - 44.1	Atkinson and Smith, 1983; Staehr and Wernberg, 2009; Falkenberg et al., 2013; Britton et al., 2016; Gladstone-Gallagher et al., 2016
E.	*maxima*	15 - 17.8	Probyn and McQuaid 1985
Laminaria	*angustata*	23.3	Johnston, 1971
L.	*dentiger*	21.7	Atkinson and Smith, 1983
L.	*digitata*	19.4 - 28.6	Mann, 1972; Schaal et al., 2010; Xia et al., 2016
L.	*groenlandica*	12.4 - 17	Harrison et al., 1986
L.	*hyperborea*	6 - 60	Sjøtun et al., 1996; Norderhaug et al., 2003; Leclerc et al., 2013

Table 1 cont.

Genus	Species	C:N	Sources
L.	*japonica*	10 - 50	Johnston, 1971; Mizuta et al., 1997
L.	*longicruris*	13.8 - 16.7	Mann, 1972
L.	*religiosa*	15.4	Johnston, 1971
L.	*saccharina*	7.1 - 30	Subandar et al., 1993; Henley and Dunton, 1995; Ahn et al., 1998; Gevaert et al., 2001*; Pelletreau and Muller-Parker, 2002; Gordillo et al., 2006
L.	*solidungula*	10 - 26	Dunton and Schell, 1986; Henley and Dunton, 1995; Gordillo et al., 2006
Lessonia	*nigrescens*	16.6	Reddin et al., 2015
Macrocystis	*pyrifera*	7.5 - 47.2	(This paper); Jackson, 1977; Wheeler and North, 1981*; Atkinson and Smith, 1983; Rosell and Srivastava, 1985*; van Tussenbroek 1989; Hurd et al., 1994; Hurd et al., 1996; Brown et al., 1997; Hurd et al., 2000; Pennings et al., 2000; Hepburn et al., 2006, 2007; Davenport and Anderson, 2007; Brown et al. 2014; Stephens and Hepburn, 2014, 2016; Fernández et al., 2015; Hamersley et al., 2015; Dobkowski et al., 2017; Suárez-Jiménez et al., 2017
Nereocystis	*luetkeana*	9.8 - 24	Atkinson and Smith, 1983; Rosell and Srivastava, 1985*; Ahn et al., 1998; Pennings et al., 2000; Pelletreau and Muller-Parker, 2002; Dethier et al., 2014; Dobkowski et al., 2017
Saccharina	*japonica*	7.1	Wang et al., 2013
S.	*latissima*	7 - 45	McDonald and Bingham, 2010; Handå et al., 2013; Olischläger et al., 2014; Gordillo et al., 2015
Undaria	*pinnatifida*	8.4 - 23.6	Johnston 1971; Yoshikawa et al., 2001; Dean and Hurd, 2007; Sfriso and Facca 2013; Suárez-Jiménez et al., 2017

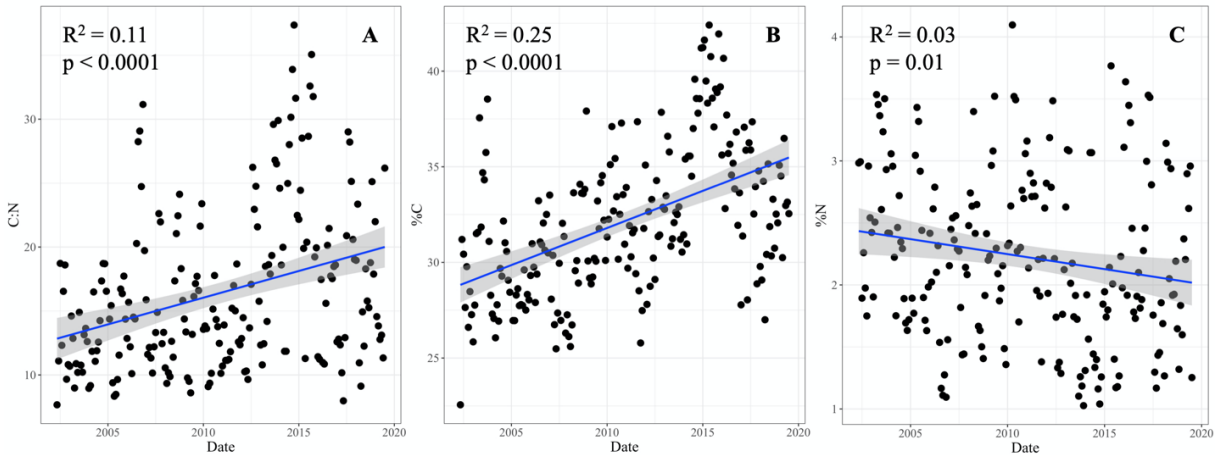

Figure 1: Mean monthly values of (A) C:N, (B) % carbon of dry sample mass, and (C) % nitrogen of dry sample mass of *Macrocystis pyrifera* blades collected from three sites (ABUR, AQUE, MOHK) from May 2002 to July 2019. Linear models are represented by blue lines with 95% confidence level intervals in grey.

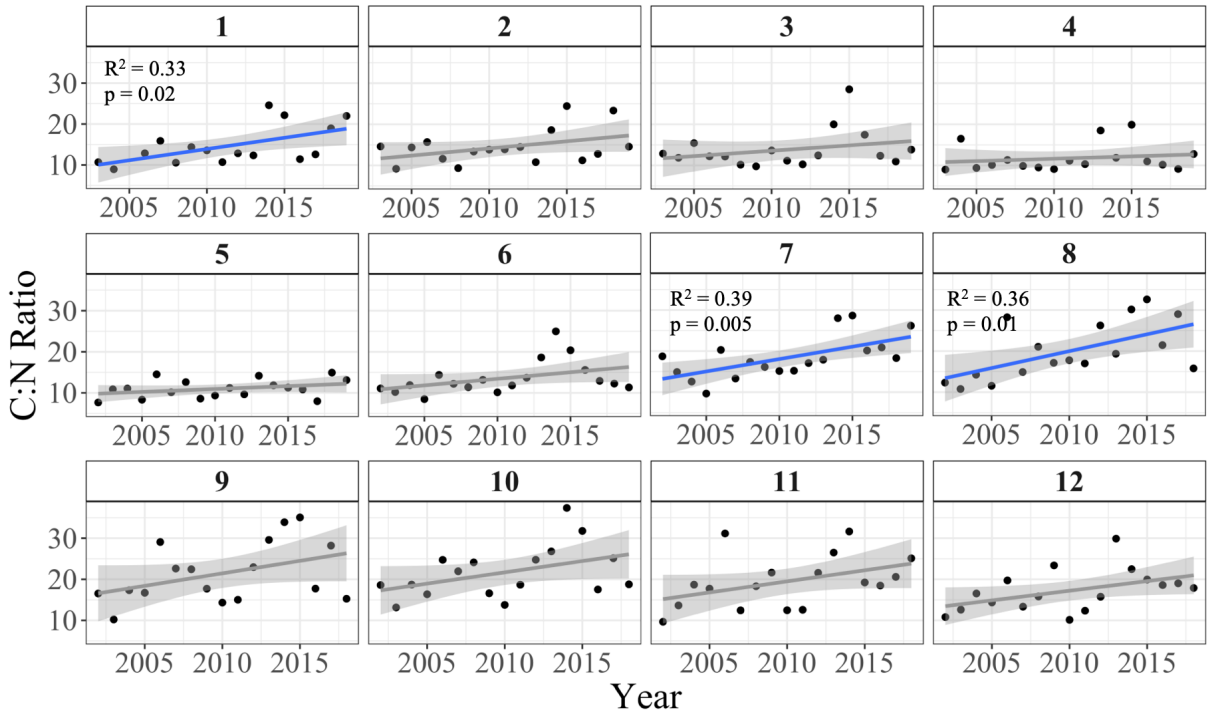

Figure 2: Mean values of C:N (as a function of dry sample mass) in giant kelp blades across all three sites paneled by month (1-12, January-December) across all years (2002-2019). Months for which there was a significant relationship through time are presented with linear model in blue, 95% confidence level interval in grey, and model statistics. Other months for which the relationship was not significant are shown in grey.

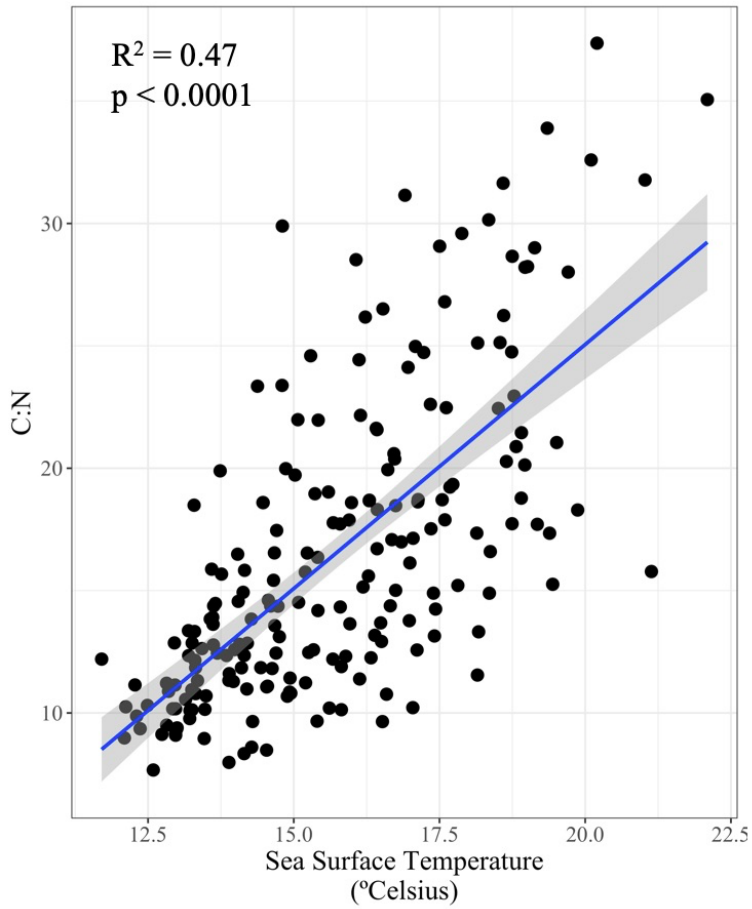

Figure 3: Mean monthly values of C:N (as a function of dry sample mass) versus mean monthly sea surface temperature from satellite-derived data. The blue line represents a linear regression with 95% confidence level intervals in grey.

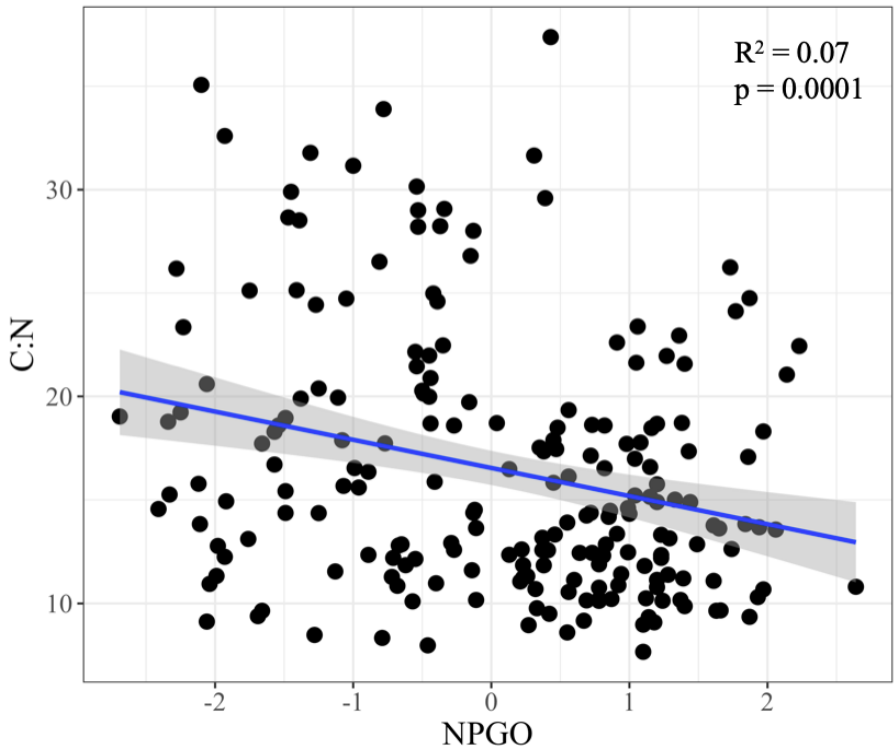

Figure 4: Mean monthly values of C:N (as a function of dry sample mass) in giant kelp blades plotted as a function of mean monthly NPGO values for the 17 year period (2002-2019). The blue line represents a linear regression with 95% confidence level intervals in grey.

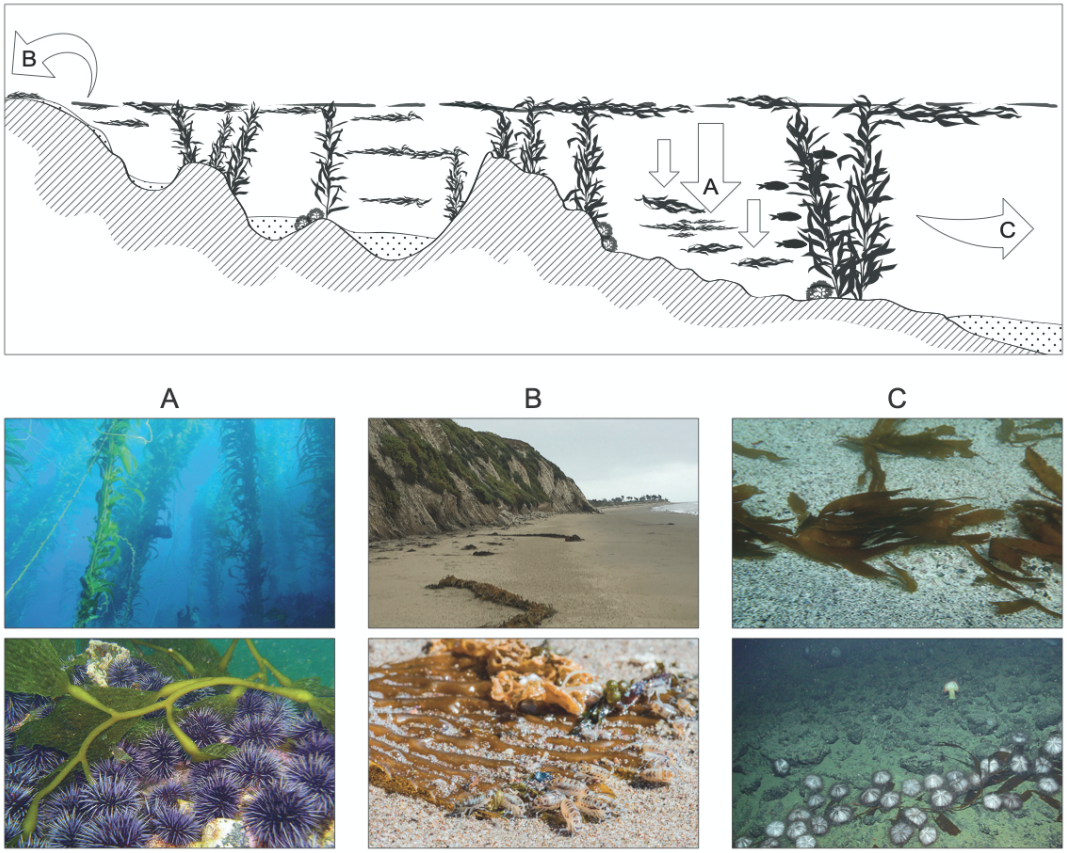

Figure 5: Conceptual diagram (top) of the trophic fate of giant kelp detritus in kelp forest (A), beach (B), and offshore canyon (C) ecosystems (adapted from Ebeling et al., 1980). Images of the ecosystems and associated consumers are below. (A) Purple sea urchins, *Strongylocentrotus purpuratus*, consume a kelp frond on the seafloor in a kelp forest. (B) Talitrid amphipods, or beachhoppers, consume kelp wrack cast up on a sandy beach (talitrid photo, Nicholas Schooler). (C) Fragile pink sea urchins, *Strongylocentrotus fragilis*, consume kelp on the seafloor in Monterey Canyon (kelp photo, Karen Filbee-Dexter; urchin photo, courtesy of Monterey Bay Aquarium Research Institute).

Appendix

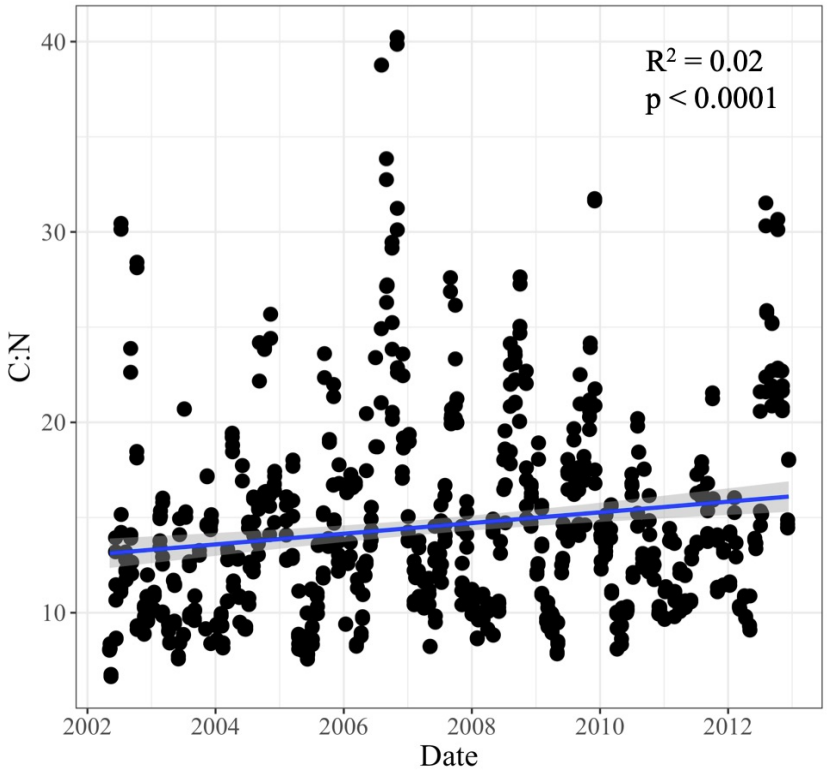

Appendix Figure 1: Mean monthly C:N content (as a function of dry sample mass) of *Macrocystis pyrifera* blades from May 2002 to December 2012, prior to the onset of the anomalous warming event known as the "Blob". Data combined from all sites sampled, and monthly means calculated by site. The blue line represents a linear regression with 95% confidence level intervals in grey.

References

Abraham, J. P., Baringer, M., Bindoff, N. L., Boyer, T., Cheng, L. J., Church, J. A., Conroy, J. L., Domingues, C. M., Fasullo, J. T., Gilson, J., Goni, G., Good, S. A., Gorman, J. M., Gouretski, V., Ishii, M., Johnson, G. C., Kizu, S., Lyman, J. M., Macdonald, A. M., Minkowycz, W. J., Moffitt, S. E., Palmer, M. D., Piola, A. R., Reseghetti, F., Schuckmann, K., Trenberth, K. E., Velicogna, I., Willis, J. K., 2013. A review of global ocean temperature observations: Implications for ocean heat content estimates and climate change. *Reviews of Geophysics* 51, 450–483. https://doi.org/10.1002/rog.20022

Ahn, O., Petrell, R. J., Harrison, P. J., 1998. Ammonium and nitrate uptake by Laminaria saccharina and Nereocystis luetkeana originating from a salmon sea cage farm. *Journal of Applied Phycology* 10, 333–340.

Angell, A. R., Mata, L., de Nys, R., Paul, N. A., 2016. The protein content of seaweeds: A universal nitrogen-to-protein conversion factor of five. *Journal of Applied Phycology* 28, 511–524. https://doi.org/10.1007/s10811-015-0650-1

Atkinson, M. J., Smith, S. V., 1983. C:N:P ratios of benthic marine plants. *Limnology and Oceanography* 28, 568–574.

Azad, A. K., Pearce, C. M., McKinley, R. S., 2011. Effects of diet and temperature on ingestion, absorption, assimilation, gonad yield, and gonad quality of the purple sea urchin (Strongylocentrotus purpuratus). *Aquaculture* 317, 187–196. https://doi.org/10.1016/j.aquaculture.2011.03.019

Bell, T. W., Cavanaugh, K. C., Reed, D. C., Siegel, D. A., 2015. Geographical variability in the controls of giant kelp biomass dynamics. *Journal of Biogeography* 42, 2010–2021. https://doi.org/10.1111/jbi.12550

Boada, J., Arthur, R., Alonso, D., Pagès, J. F., Pessarrodona, A., Oliva, S., Ceccherelli, G., Piazzi, L., Romero, J., Alcoverro, T., 2017. Immanent conditions determine imminent collapses: Nutrient regimes define the resilience of macroalgal communities. *Proceedings of the Royal Society B: Biological Sciences* 284, 20162814. https://doi.org/10.1098/rspb.2016.2814

Boyer, K. E., Fong, P., Armitage, A. R., Cohen, R. A., 2004. Elevated nutrient content of tropical macroalgae increases rates of herbivory in coral, seagrass, and mangrove habitats. *Coral Reefs* 23, 530–538. https://doi.org/10.1007/s00338-004-0421-y

Britton, D., Cornwall, C. E., Revill, A. T., Hurd, C. L., Johnson, C. R., 2016. Ocean acidification reverses the positive effects of seawater pH fluctuations on growth and photosynthesis of the habitat-forming kelp, Ecklonia radiata. *Scientific Reports* 6, 26036. https://doi.org/10.1038/srep26036

Brown, M. B., Edwards, M. S., Kim, K. Y., 2014. Effects of climate change on the physiology of giant kelp, Macrocystis pyrifera, and grazing by purple urchin, Strongylocentrotus purpuratus. *Algae* 29, 203-215. https://doi.org/10.4490/algae.2014.29.3.203

Brown, M. T., Nyman, M. A., Koegh, J. A., Chin, N. K. M., 1997. Seasonal growth of the giant kelp Macrocystis pyrifera in New Zealand. *Marine Biology* 129, 417-424.

Brzezinski, M., Reed, D., Harrer, S., Rassweiler, A., Melack, J., Goodridge, B., Dugan, J., 2013. Multiple sources and forms of nitrogen sustain year-round kelp growth on the

inner continental shelf of the Santa Barbara Channel. *Oceanography* 26, 114–123. https://doi.org/10.5670/oceanog.2013.53

California Department of Fish and Wildlife., 2013. *Status of the Fisheries Report: An Update Through 2011* [Marine Region].

Cavanaugh, K. C., Reed, D. C., Bell, T. W., Castorani, M. C. N., Beas-Luna, R., 2019. Spatial variability in the resistance and resilience of giant kelp in southern and Baja California to a multiyear heatwave. *Frontiers in Marine Science* 6, 413. https://doi.org/10.3389/fmars.2019.00413

Cavanaugh, K., Siegel, D., Reed, D., Dennison, P., 2011. Environmental controls of giant-kelp biomass in the Santa Barbara Channel, California. *Marine Ecology Progress Series* 429, 1–17. https://doi.org/10.3354/meps09141

Cebrian, J., 1999. Patterns in the fate of production in plant communities. *The American Naturalist* 154, 449–468.

Cebrian, J., Shurin, J. B., Borer, E. T., Cardinale, B. J., Ngai, J. T., Smith, M. D., Fagan, W. F., 2009. Producer nutritional quality controls ecosystem trophic structure. *PLoS ONE* 4, e4929. https://doi.org/10.1371/journal.pone.0004929

Cruz-Rivera, E., Hay, M. E., 2000. Can quantity replace quality? Food choice, compensatory feeding, and fitness of marine mesograzers. *Ecology* 81, 201–219. https://doi.org/10.1890/0012-9658(2000)081[0201:CQRQFC]2.0.CO;2

Davenport, A. C., Anderson, T. W., 2007. Positive indirect effects of reef fishes on kelp performance: the importance of mesograzers. *Ecology* 88, 1548-1561. https://doi.org/10.1890/06-0880

Dayton, P. K., 1985. Ecology of kelp communities. *Annual Review of Ecology and Systematics* 16, 215–245.

Dean, P. R., Hurd, C. L., 2007. Seasonal growth, erosion rates, and nitrogen and photosynthetic ecophysiology of Undaria pinnatifida (Heterokontophyta) in southern New Zealand. *Journal of Phycology* 43, 1138-1148. https://doi.org/10.1111/j.1529-8817.2007.00416.x

Dethier, M. N., Brown, A. S., Burgess, S., Eisenlord, M. E., Galloway, A. W. E., Kimber, J., Lowe, A. T., O'Neil, C. M., Raymond, W. W., Sosik, E. A., Duggins, D. O., 2014. Degrading detritus: Changes in food quality of aging kelp tissue varies with species. *Journal of Experimental Marine Biology and Ecology* 460, 72–79. https://doi.org/10.1016/j.jembe.2014.06.010

Di Lorenzo, E., Schneider, N., Cobb, K. M., Franks, P. J. S., Chhak, K., Miller, A. J., McWilliams, J. C., Bograd, S. J., Arango, H., Curchitser, E., Powell, T. M., Rivière, P., 2008. North Pacific Gyre Oscillation links ocean climate and ecosystem change. *Geophysical Research Letters* 35, L08607. https://doi.org/10.1029/2007GL032838

Di Lorenzo, E., Mantua, N., 2016. Multi-year persistence of the 2014/15 North Pacific marine heatwave. *Nature Climate Change* 6, 1042–1047. https://doi.org/10.1038/nclimate3082

Dobkowski, K. A., Kobelt, J., Brentin, S., Van Alstyne, K. L., Dethier, M. N., 2017. Picky Pugettia: A tale of two kelps. *Marine Biology* 164, 210. https://doi.org/10.1007/s00227-017-3244-4

Dugan, J. E., Hubbard, D. M., McCrary, M. D., Pierson, M. O., 2003. The response of macrofauna communities and shorebirds to macrophyte wrack subsidies on exposed

sandy beaches of southern California. *Estuarine, Coastal and Shelf Science* 58, 25–40. https://doi.org/10.1016/S0272-7714(03)00045-3

Dunton, K., Schell, D., 1986. Seasonal carbon budget and growth of Laminaria solidungula in the Alaskan high Arctic. *Marine Ecology Progress Series* 31, 57–66.

Ebeling, A. W., Larson, R. J., Alevizon, W. S., Bray, R. N., 1980. Annual variability of reef-fish assemblages in kelp forests off Santa Barbara, California. *Fishery Bulletin* 78, 361–377.

Falkenberg, L. J., Russell, B. D., Connell, S. D., 2012. Stability of strong species interactions resist the synergistic effects of local and global pollution in kelp forests. *PLoS ONE* 7, e33841. https://doi.org/10.1371/journal.pone.0033841

Falkenberg, L. J., Russell, B. D., Connell S. D., 2013. Contrasting resource limitations of marine primary producers: implications for competitive interactions under enriched CO2 and nutrient regimes. *Oecologia* 172, 575-583. https://doi.org/10.1007/s00442-012-2507-5

Fernández, P. A., Roleda, M. Y., Hurd, C. L., 2015. Effects of ocean acidification on the photosynthetic performance, carbonic anhydrase activity and growth of the giant kelp Macrocystis pyrifera. *Photosynthesis Research* 124, 293-304. https://doi.org/10.1007/s11120-015-0138-5

Filbee-Dexter, K., Scheibling, R., 2014. Detrital kelp subsidy supports high reproductive condition of deep-living sea urchins in a sedimentary basin. *Aquatic Biology* 23, 71–86. https://doi.org/10.3354/ab00607

Gerard, V. A., 1982. Growth and utilization of internal nitrogen reserves by the giant kelp Macrocystis pyrifera in a low-nitrogen environment. *Marine Biology* 66, 27–35.

Gevaert, F., Davoult, D., Creach, A., Kling, R., 2001. Carbon and nitrogen content of Laminaria saccharina in the eastern English Channel: biometrics and seasonal variations. *Journal of the Marine Biological Association of the United Kingdom* 81, 727–734. https://doi.org/10.1017/S0025315401004532

Gladstone-Gallagher, R. V., Lohrer, A. M., Lundquist, C. J., Pilditch, C. A., 2016. Effects of detrital subsidies on soft-sediment ecosystem function are transient and source dependent. *PLoS ONE* 11, e0154790. https://doi.org/10.1371/journal.pone.0154790

Gordillo, F. J. L., 2006. The response of nutrient assimilation and biochemical composition of Arctic seaweeds to a nutrient input in summer. *Journal of Experimental Botany* 57, 2661–2671. https://doi.org/10.1093/jxb/erl029

Gordillo, F. J. L., Aguilera, J., Wiencke, C., Jiménez, C., 2015. Ocean acidification modulates the response of two Arctic kelps to ultraviolet radiation. *Journal of Plant Physiology* 173, 41–50. https://doi.org/10.1016/j.jplph.2014.09.008

Hamersley, M. R., Sohm, J. A., Burns, J. A., Capone, D. G., 2015. Nitrogen fixation associated with the decomposition of the giant kelp Macrocystis pyrifera. *Aquatic Botany* 125, 57-63. https://doi.org/10.1016/j.aquabot.2015.05.003

Hammer, H. S., Powell, M. L., Jones, W. T., Gibbs, V. K., Lawrence, A. L., Lawrence, J. M., Watts, S. A., 2012. Effect of feed protein and carbohydrate levels on feed intake, growth, and gonad production of the sea urchin, Lytechinus variegatus. *Journal of the World Aquaculture Society* 43, 145–158. https://doi.org/10.1111/j.1749-7345.2012.00562.x

Handå, A., Forbord, S., Wang, X., Broch, O. J., Dahle, S. W., Størseth, T. R., Reitan, K. I., Olsen, Y., Skjermo, J., 2013. Seasonal- and depth-dependent growth of cultivated

kelp (Saccharina latissima) in close proximity to salmon (Salmo salar) aquaculture in Norway. *Aquaculture* 414–415, 191–201. https://doi.org/10.1016/j.aquaculture.2013.08.006

Hansen, J., Sato, M., Reudy, R., Lea, D. W., Medina-Elizade, M., 2006. Global temperature change. *Proceedings of the National Academy of Sciences of the United States of America* 103, 14288–14293. https://doi.org/10.1073/pnas.0606291103

Harley, C. D. G., Anderson, K. M., Demes, K. W., Jorve, J. P., Kordas, R. L., Coyle, T. A., Graham, M. H., 2012. Effects of climate change on global seaweed communities. *Journal of Phycology* 48, 1064–1078. https://doi.org/10.1111/j.1529-8817.2012.01224.x

Harley, C. D. G., Randall Hughes, A., Hultgren, K. M., Miner, B. G., Sorte, C. J. B., Thornber, C. S., Rodriguez, L. F., Tomanek, L., Williams, S. L., 2006. The impacts of climate change in coastal marine systems: Climate change in coastal marine systems. *Ecology Letters* 9, 228–241. https://doi.org/10.1111/j.1461-0248.2005.00871.x

Harrison, P. J., Druehl, L. D., Lloyd, K. E., Thompson, P. A., 1986. Nitrogen uptake kinetics in three year-classes of Laminaria groenlandica (Laminariales: Phaeophyta). *Marine Biology* 93, 29–35.

Hemmi, A., Jormalainen, V., 2002. Nutrient enhancement increases performance of a marine herbivore via quality of its food alga. *Ecology* 83, 1052–1064. https://doi.org/10.1890/0012-9658(2002)083[1052:NEIPOA]2.0.CO;2

Henley, W.J., Dunton, K.H., 1995. A seasonal comparison of carbon, nitrogen, and pigment content in Laminaria Solidungula and L. Saccharina (Phaeophyta) in the Alaskan Arctic. *Journal of Phycology* 31, 325–331.

Hepburn, C. D., Hurd, C. L., Frew, R. D., 2006. Colony structure and seasonal differences in light and nitrogen modify the impact of sessile epifauna on the giant kelp Macrocystis pyrifera (L.) C Agardh. *Hydrobiologia* 560, 373-384. https://doi.org/10.1007/s10750-005-1573-7

Hepburn, C. D., Holborow, J. D., Wing, S. R., Frew, R. D., Hurd, C.L., 2007. Exposure to waves enhances the growth rate and nitrogen status of the giant kelp Macrocystis pyrifera. *Marine Ecology Progress Series* 339, 99-108. https://doi.org/10.3354/meps339099

Hoegh-Guldberg, O., Jacob, D., Taylor, M., Bindi, M., Brown, S., Camilloni, I., Diedhiou, A., Djalante, R., Ebi, K. L., Engelbrecht, F., Guiot, J., Hijioka, Y., Mehrotra, S., Payne, A., Seneviratne, S. I., Thomas, A., Warren, R., Zhou, G., 2018. Impacts of 1.5°C of Global Warming on Natural and Human Systems. In: *Global Warming of 1.5°C. An IPCC Special Report on the impacts of global warming of 1.5°C above pre-industrial levels and related global greenhouse gas emission pathways, in the context of strengthening the global response to the threat of climate change, sustainable development, and efforts to eradicate poverty*. Masson-Delmotte, V., Zhai, P., Pörtner, H. O., Roberts, D., Skea, J., Shukla, P. R., Pirani, A., Moufouma-Okia, W., Péan, C., Pidcock, R., Connors, S., Matthews, J. B. R., Chen, Y., Zhou, X., Gomis, M. I., Lonnoy, E., Maycock, T., Tignor, M., Waterfield, T. (eds.)

Hurd, C. L., Durante, K. M., Chia, F. S., Harrison, P. J., 1994. Effect of bryozoan colonization on inorganic nitrogen acquisition by the kelps Agarum fimbriatum and Macrocystis integrifolia. *Marine Biology* 121, 167-173.

Hurd, C. L., Harrison, P. J., Druehl, L. D., 1996. Effect of seawater velocity on inorganic nitrogen uptake by morphologically distinct forms of Macrocystis integrifolia from wave-sheltered and exposed sites. *Marine Biology* 126, 205-514.

Hurd, C. L., Durante, K. M., Harrison, P. J., 2000. Influence of bryozoan colonization on the physiology of the kelp Macrocystis integrifolia (Laminariales, Phaeophyta) from nitrogen-rich and -poor sites in Barkley Sound, British Columbia, Canada. *Phycologia* 39, 435-440. https://doi.org/10.2216/i0031-8884-39-5-435.1

Jackson, G. A., 1977. Nutrients and production of giant kelp, Macrocystis pyrifera, off southern California. *Limnology and Oceanography* 22, 979-995.

Johnson, C. R., Banks, S. C., Barrett, N. S., Cazassus, F., Dunstan, P. K., Edgar, G. J., Frusher, S. D., Gardner, C., Haddon, M., Helidoniotis, F., Hill, K. L., Holbrook, N. J., Hosie, G. W., Last, P. R., Ling, S. D., Melbourne-Thomas, J., Miller, K., Pecl, G. T., Richardson, A. J., Ridgway, K., Rintoul, S. R., Ritz, D. A., Ross, D. J., Sanderson, J. C., Shepherd, S. A., Slotwinski, A., Swadling, K. M., Taw, N., 2011. Climate change cascades: Shifts in oceanography, species' ranges and subtidal marine community dynamics in eastern Tasmania. *Journal of Experimental Marine Biology and Ecology* 400, 17–32. https://doi.org/10.1016/j.jembe.2011.02.032

Johnston, H. W., 1971. A detailed chemical analysis of some edible Japanese seaweeds. *Proceedings of the 7th International Seaweed Symposium* 429–435.

JPL MUR MEaSUREs Project., 2015. GHRSST Level 4 MUR Global Foundation Sea Surface Temperature Analysis (Vers. 4.1). https://doi.org/10.5067/GHGMR-4FJ04

Krumhansl, K., Scheibling, R., 2012. Production and fate of kelp detritus. *Marine Ecology Progress Series* 467, 281–302. https://doi.org/10.3354/meps09940

Leclerc, J. C., Riera, P., Leroux, C., Leveque, L., Davoult, D., 2013. Temporal variation in organic matter supply in kelp forests: linking structure to trophic functioning. *Marine Ecology Progress Series* 494**,** 87-105. https://doi.org/10.3354/meps10564

Lotze, H. K., Tittensor, D. P., Bryndum-Buchholz, A., Eddy, T. D., Cheung, W. W. L., Galbraith, E. D., Barange, M., Barrier, N., Bianchi, D., Blanchard, J. L., Bopp, L., Büchner, M., Bulman, C. M., Carozza, D. A., Christensen, V., Coll, M., Dunne, J. P., Fulton, E. A., Jennings, S., Jones, M. C., Mackinson, S., Maury, O., Niiranen, S., Oliveros-Ramos, R., Roy, T., Fernandes, J. A., Schewe, J., Shin, Y., Silva, T. A. M., Steenbeek, J., Stock, C. A., Verley, P., Volkholz, J., Walker, N. D., Worm, B., 2019. Global ensemble projections reveal trophic amplification of ocean biomass declines with climate change. *Proceedings of the National Academy of Sciences of the United States of America* 116, 12907–12912. https://doi.org/10.1073/pnas.1900194116

Mann, K.H., 1972. Ecological energetics of the seaweed zone in a marine bay on the Atlantic coast of Canada. I. Zonation and biomass of seaweeds. *Marine Biology* 12, 1-10.

McBride, S. C., Price, R. J., Tom, P. D., Lawrence, J. M., Lawrence, A. L., 2004. Comparison of gonad quality factors: Color, hardness and resilience, of Strongylocentrotus franciscanus between sea urchins fed prepared feed or algal diets and sea urchins harvested from the Northern California fishery. *Aquaculture* 233, 405–422. https://doi.org/10.1016/j.aquaculture.2003.10.014

McDonald, P. S., Bingham, B. L., 2010. Comparing macroalgal food and habitat choice in sympatric, tube-building amphipods, Ampithoe lacertosa and Peramphithoe humeralis. *Marine Biology* 157, 1513–1524. https://doi.org/10.1007/s00227-010-1425-5

McPhee-Shaw, E. E., Siegel, D. A., Washburn, L., Brzezinski, M. A., Jones, J. L., Leydecker, A., Melack, J., 2007. Mechanisms for nutrient delivery to the inner shelf: Observations from the Santa Barbara Channel. *Limnology and Oceanography* 52, 1748–1766. https://doi.org/10.4319/lo.2007.52.5.1748

Miller, R. J., Lafferty, K. D., Lamy, T., Kui, L., Rassweiler, A., Reed, D. C., 2018. Giant kelp, Macrocystis pyrifera, increases faunal diversity through physical engineering. *Proceedings of the Royal Society B: Biological Sciences* 285, 20172571. https://doi.org/10.1098/rspb.2017.2571

Mizuta, H., Torii, K., Yamamoto, H., 1997. The relationship between nitrogen and carbon contents in the sporophytes of Laminaria japonica (Phaeophyceae). *Fisheries Science* 63, 553–556.

Naidoo, K., Maneveldt, G., Ruck, K., Bolton, J. J., 2006. A comparison of various seaweed-based diets and formulated feed on growth rate of abalone in a land-based aquaculture system. *Journal of Applied Phycology* 18, 437–443. https://doi.org/10.1007/s10811-006-9045-7

National Climatic Data Center., 2007. GHRSST Level 4 AVHRR_OI Global Blended Sea Surface Temperature Analysis (Ver. 1.0). https://doi.org/10.5067/GHAAO-4BC01

Norderhaug, K., Fredriksen, S., Nygaard, K., 2003. Trophic importance of Laminaria hyperborea to kelp forest consumers and the importance of bacterial degradation to food quality. *Marine Ecology Progress Series* 255, 135–144. https://doi.org/10.3354/meps255135

Olischläger, M., Iñiguez, C., Gordillo, F. J. L., Wiencke, C., 2014. Biochemical composition of temperate and Arctic populations of Saccharina latissima after exposure to

increased pCO2 and temperature reveals ecotypic variation. *Planta* 240, 1213–1224. https://doi.org/10.1007/s00425-014-2143-x

Pelletreau, K., Muller-Parker, G., 2002. Sulfuric acid in the phaeophyte alga Desmarestia munda deters feeding by the sea urchin Strongylocentrotus droebachiensis. *Marine Biology* 141, 1–9. https://doi.org/10.1007/s00227-002-0809-6

Pennings, S. C., Carefoot, T. H., Zimmer, M., Danko, J. P., Ziegler, A., 2000. Feeding preferences of supralittoral isopods and amphipods. *Canadian Journal of Zoology* 78, 1918-1929. https://doi.org/10.1139/cjz-78-11-1918

Pfister, C. A., Berry, H. D., Mumford, T., 2018. The dynamics of kelp forests in the northeast Pacific Ocean and the relationship with environmental drivers. *Journal of Ecology* 106, 1520–1533. https://doi.org/10.1111/1365-2745.12908

Phelps, C. M., Boyce, M. C., Huggett, M. J., 2017. Future climate change scenarios differentially affect three abundant algal species in southwestern Australia. *Marine Environmental Research* 126, 69–80. https://doi.org/10.1016/j.marenvres.2017.02.008

Probyn, T. A., McQuaid, C. D., 1985. In-situ measurements of nitrogenous nutrient uptake by kelp (Ecklonia maxima) and phytoplankton in a nitrate-rich upwelling environment. *Marine Biology* 88, 149-154.

R Core Team., 2016. *R: A Language and Environment for Statistical Computing*. R Foundation for Statistical Computing. https://www.R-project.org/

Raybaud, V., Beaugrand, G., Goberville, E., Delebecq, G., Destombe, C., Valero, M., Davoult, D., Morin, P., Gevaert, F., 2013. Decline in Kelp in West Europe and Climate. *PLoS ONE* 8, e66044. https://doi.org/10.1371/journal.pone.0066044

Reddin, C. J., Docmac, F., O'Connor, N. E., Bothwell, J. H., Harrod, C., 2015. Coastal upwelling drives intertidal assemblage structure and trophic ecology. *PLoS ONE* 10, e0130789. https://doi.org/10.1371/journal.pone.0130789

Reed, D., 2019. SBC LTER: Reef: Macrocystis pyrifera CHN content (carbon, hydrogen, nitrogen). *Environmental Data Initiative*. https://doi.org/10.6073/pasta/f2c945e3fb8559fa436dab9d9cce3491

Reed, D., Washburn, L., Rassweiler, A., Miller, R., Bell, T., Harrer, S., 2016. Extreme warming challenges sentinel status of kelp forests as indicators of climate change. *Nature Communications* 7, 13757. https://doi.org/10.1038/ncomms13757

Rogers-Bennett, L., Catton, C. A., 2019. Marine heat wave and multiple stressors tip bull kelp forest to sea urchin barrens. *Scientific Reports* 9, 15050. https://doi.org/10.1038/s41598-019-51114-y

Rosell, K. G., Srivastava, L., 1985. Seasonal variations in total nitrogen, carbon and amino acids in Macrocystis integrifolia and Nereocystis luetkeana (Phaeophyta). *Journal of Phycology* 21, 304–309.

Schaal, G., Riera, P., Leroux, C., 2010. Trophic ecology in a Northern Brittany (Batz Island, France) kelp (Laminaria digitata) forest, as investigated through stable isotopes and chemical assays. *Journal of Sea Research* 63, 24–35. https://doi.org/10.1016/j.seares.2009.09.002

Sfriso, A., Facca, C., 2013. Annual growth and environmental relationships of the invasive species Sargassum muticum and Undaria pinnatifida in the lagoon of Venice. *Estuarine, Coastal and Shelf Science* 129, 162-172. https://doi.org/10.1016/j.ecss.2013.05.031

Simonson, E., Metaxas, A., Scheibling, R., 2015. Kelp in hot water: II. Effects of warming seawater temperature on kelp quality as a food source and settlement substrate. *Marine Ecology Progress Series* 537, 105–119. https://doi.org/10.3354/meps11421

Sjøtun, K., Fredriksen, S., Rueness, J., 1996. Seasonal growth and carbon and nitrogen content in canopy and first-year plants of Laminaria hyperborea (Laminariales, Phaeophyceae). *Phycologia* 35, 1–8.

Smale, D. A., Wernberg, T., Oliver, E. C., Thomsen, M., Harvey, B. P., Straub, S. C., Burrows, M. T., Alexander, L. V., Benthuysen, J. A., Donat, M. G., Feng, M., 2019. Marine heatwaves threaten global biodiversity and the provision of ecosystem services. *Nature Climate Change* 9, 306–312. https://doi.org/10.1038/s41558-019-0412-1

Staehr, P. A., Wernberg, T., 2009. Physiological responses of Ecklonia radiata (Laminariales) to a latitudinal gradient in ocean temperature. *Journal of Phycology* 45, 91-99. https://doi.org/10.1111/j.1529-8817.2008.00635.x

Steneck, R. S., Graham, M. H., Bourque, B. J., Corbett, D., Erlandson, J. M., Estes, J. A., Tegner, M. J., 2002. Kelp forest ecosystems: Biodiversity, stability, resilience and future. *Environmental Conservation* 29. https://doi.org/10.1017/S0376892902000322

Stephens, T. A., Hepburn, C. D., 2014. Mass-transfer gradients across kelp beds influence Macrocystis pyrifera growth over small spatial scales. *Marine Ecology Progress Series* 515, 97-109. https://doi.org/10.3354/meps10974

Stephens, T. A., Hepburn, C. D., 2016. A kelp with integrity: Macrocystis pyrifera prioritises tissue maintenance in response to nitrogen fertilisation. *Oecologia* 182, 71-84. https://doi.org/10.1007/s00442-016-3641-2

Suárez-Jiménez, R., Hepburn, C. D., Hyndes, G. A., McLeod, R. J., Taylor, R. B., Hurd, C. L., 2017. Importance of the invasive macroalga Undaria pinnatifida as trophic subsidy for a beach consumer. *Marine Biology* 164, 113. https://doi.org/10.1007/s00227-017-3140-y

Subandar, A., Petrell, R. J., Harrison, P. J., 1993. Laminaria culture for reduction of dissolved inorganic nitrogen in salmon farm effluent. *Journal of Applied Phycology* 5**,** 455–463.

Thomsen, M. S., Mondardini, L., Alestra, T., Gerrity, S., Tait, L., South, P. M., Lilley, S. A., Schiel, D. R., 2019. Local extinction of bull kelp (Durvillaea spp.) due to a marine heatwave. *Frontiers in Marine Science* 6, 84. https://doi.org/10.3389/fmars.2019.00084

Van Alstyne, K. L., Pelletreau, K. N., Kirby, A., 2009. Nutritional preferences override chemical defenses in determining food choice by a generalist herbivore, Littorina sitkana. *Journal of Experimental Marine Biology and Ecology* 379, 85–91. https://doi.org/10.1016/j.jembe.2009.08.002

Van Tussenbroek, B. I., 1989. Seasonal growth and composition of fronds of Macrocystis pyrifera in the Falkland Islands. *Marine Biology* 100, 419-430.

Vetter, E. W., Dayton, P. K., 1999. Organic enrichment by macrophyte detritus, and abundance patterns of megafaunal populations in submarine canyons. *Marine Ecology Progress Series* 186, 137–148.

Vilchis, L. I., Tegner, M. J., Moore, J. D., Friedman, C. S., Riser, K. L., Robbins, T. T., Dayton, P. K., 2005. Ocean warming effects on growth, reproduction, and

survivorship of southern California abalone. *Ecological Applications* 15, 469–480. https://doi.org/10.1890/03-5326

Wang, Y., Xu, D., Fan, X., Zhang, X., Ye, N., Wang, W., Mao, Y., Mou, S., Cao, S., 2013. Variation of photosynthetic performance, nutrient uptake, and elemental composition of different generations and different thallus parts of Saccharina japonica. *Journal Applied Phycology* 25, 631–637. https://doi.org/10.1007/s10811-012-9897-y

Wernberg, T., Thomsen, M. S., Tuya, F., Kendrick, G. A., Staehr, P. A., Toohey, B. D., 2010. Decreasing resilience of kelp beds along a latitudinal temperature gradient: Potential implications for a warmer future. *Ecology Letters* 13, 685–694. https://doi.org/10.1111/j.1461-0248.2010.01466.x

Wheeler, P. A., North, W .J., 1981. Nitrogen supply, tissue composition and frond growth rates for Macrocystis pyrifera off the coast of southern California. *Marine Biology* 64, 59-69.

Wickham, H., Averick, M., Bryan, J., Chang, W., D'Agostino McGowan, L., François, R., Grolemund, G., Hayes, A., Henry, L., Hester, J., Kuhn, M., Lin Pedersen, T., Miller, E., Milton Bache, S., Müller, K., Ooms, J., Robinson, D., Paige Seidel, D., Spinu, V., Takahashi, K., Vaughan, D., Wilke, C., Woo, K., Yutani, H., 2019. Welcome to the Tidyverse. *Journal of Open Source Software* 4, 1686. https://doi.org/10.21105/joss.01686

Wilson, K. L., Kay, L. M., Schmidt, A. L., Lotze, H. K., 2015. Effects of increasing water temperatures on survival and growth of ecologically and economically important seaweeds in Atlantic Canada: Implications for climate change. *Marine Biology* 162, 2431–2444. https://doi.org/10.1007/s00227-015-2769-7

Xia, A., Jacob, A., Tabassum, M. R., Herrmann, C., Murphy, J. D., 2016. Production of hydrogen, ethanol and volatile fatty acids through co-fermentation of macro- and micro-algae. *Bioresource Technology* 205, 118–125. https://doi.org/10.1016/j.biortech.2016.01.025

Yorke, C. E., Page, H. M., Miller, R. J., 2019. Sea urchins mediate the availability of kelp detritus to benthic consumers. *Proceedings of the Royal Society B: Biological Sciences* 286, 1–8. https://doi.org/10.1098/rspb.2019.0846

Yoshikawa, T., Takeuchi, I., Furuya, K., 2001. Active erosion of Undaria pinnatifida Suringar (Laminariales, Phaeophyceae) mass-cultured in Otsuchi Bay in northeastern Japan. *Journal of Experimental Marine Biology and Ecology* 266, 51-65. https://doi.org/10.1016/S0022-0981(01)00346-X

Zimmerman, R. C., Kremer, J. N., 1984. Episodic nutrient supply to a kelp forest ecosystem in Southern California. *Journal of Marine Research* 42, 591–604.